

# Ridge-Regularized Largest Root Test For High-Dimensional General Linear Hypotheses

Haoran Li\*

*Auburn University*

July 9, 2025

## Abstract

A fundamental problem in multivariate analysis is testing general linear hypotheses for regression coefficients in a multivariate linear model. This framework encompasses a wide range of well-studied tasks, including MANOVA, joint significance testing of predictors, and the detection of trends or seasonal effects. Among classical approaches, Roy's largest root test is particularly effective for detecting concentrated signals, relying on the largest eigenvalue of an  $F$ -matrix constructed from residual covariance matrices. However, in high-dimensional settings, these matrices often become ill-conditioned or singular, rendering the test infeasible. To address this, we propose a ridge-regularized Roy's test that stabilizes the covariance estimation via a ridge term. We establish the asymptotic Tracy–Widom distribution of the largest eigenvalue of the regularized  $F$ -matrix under a high-dimensional regime, where both the dimension and hypotheses are comparable to the sample size, assuming only finite-moment conditions. A computationally efficient procedure is developed to estimate the associated centering and scaling parameters. We further analyze the power of the test under a class of low-rank alternatives and examine the influence of the regularization parameter. The method demonstrates strong performance in simulations and is applied to data from the Human Connectome Project to assess associations between volumetric brain measurements and behavioral variables.

**Keywords:** Ridge regularization, Tracy-Widom law, F-matrix, Random Matrix Theory.

---

\*Department of Mathematics and Statistics, Auburn University, 221 Parker Hall, Auburn, AL, 36849, hzl0152@auburn.edu

# 1 Introduction

In multivariate analysis, one of the fundamental inferential problems is to test a group of hypotheses jointly involving linear transformations of regression coefficients under a multivariate linear model. We consider a setting with  $p$ -variate responses and  $m$ -variate predictors, observed from independent subjects of size  $n_T$ . The relationship between the responses and predictors is modeled as

$$\mathbf{Y} = B\mathbf{X} + \Sigma_p^{1/2}\mathbf{Z},$$

where  $\mathbf{Y}$  is a  $p \times n_T$  response matrix,  $\mathbf{X}$  is a  $m \times n_T$  deterministic predictor matrix,  $B$  is a  $p \times m$  coefficient matrix, and  $\mathbf{Z}$  is a  $p \times n_T$  error matrix with i.i.d. entries of mean zero and variance one.  $\Sigma_p$  is the  $p \times p$  positive definite population covariance matrix, and  $\Sigma_p^{1/2}$  is its symmetric ‘‘square-root’’, satisfying  $(\Sigma_p^{1/2})^2 = \Sigma_p$ . The primary objective is to test linear hypotheses about the regression coefficients:

$$H_0 : BC = 0 \quad \text{vs.} \quad H_a : BC \neq 0,$$

where  $C$  is a  $m \times n_1$  constraint matrix, with each column specifying a linear constraint on the coefficients. Without loss of generality, we assume that  $\mathbf{X}$  and  $C$  are of full rank, and  $BC$  is estimable in the sense that the matrix  $C^T(\mathbf{X}\mathbf{X}^T)^{-1}C$  is positive definite.

With various choices of  $\mathbf{X}$  and  $C$ , this formulation is broadly applicable across various fields, encompassing many classical problems such as MANOVA, testing the joint significance of predictors, and detecting trends or seasonal patterns. When the sample size  $n_T$  is substantially larger than  $p$ ,  $m$  and  $n_1$ , the problem is well-studied. Anderson (1958) and Muirhead (2009) are among standard references.

Various classical inferential procedures rely on the eigen-analysis of an F-matrix of the form  $\mathbf{F} = \mathbf{W}_1\mathbf{W}_2^{-1}$  where

$$\begin{aligned} \mathbf{W}_1 &= \frac{1}{n_1}\mathbf{Y}\mathbf{X}^T(\mathbf{X}\mathbf{X}^T)^{-1}C\left[C^T(\mathbf{X}\mathbf{X}^T)^{-1}C\right]^{-1}C^T(\mathbf{X}\mathbf{X}^T)^{-1}\mathbf{X}\mathbf{Y}^T := \frac{1}{n_1}\mathbf{Y}P_1\mathbf{Y}^T, \\ \mathbf{W}_2 &= \frac{1}{n_2}\mathbf{Y}\left(I_{n_T} - \mathbf{X}^T(\mathbf{X}\mathbf{X}^T)^{-1}\mathbf{X}\right)\mathbf{Y}^T := \frac{1}{n_1}\mathbf{Y}P_2\mathbf{Y}^T, \end{aligned} \tag{1.1}$$

and  $n_1$  and  $n_2 = n_T - m$  are the respective degrees of freedom. The matrix  $\mathbf{W}_2$  is the residual covariance of the full model and serves as an estimator of  $\Sigma_p$ , while  $\mathbf{W}_1$  is the hypothesis sum-of-squares and cross-products matrix, scaled by  $n_1^{-1}$ . In a one-way MANOVA set-up,  $\mathbf{W}_1$  and  $\mathbf{W}_2$  reduce to the between-group and within-group sum-of-squares and cross-products matrices, each normalized by its associated degrees of freedom. Both matrices involve the projection of  $\mathbf{Y}$  onto two orthogonal subspaces via the projection matrices  $P_1$  and  $P_2$ , defined in (1.1), of rank  $n_1$  and  $n_2$ . Under the null hypothesis and assuming Gaussian errors,  $\mathbf{W}_1$  and  $\mathbf{W}_2$  are independent Wishart matrices:  $n_1\mathbf{W}_1 \sim \text{Wishart}(\Sigma_p, n_1)$  and  $n_2\mathbf{W}_2 \sim \text{Wishart}(\Sigma_p, n_2)$ . For this reason,  $\mathbf{F}$  is

often referred to as a double Wishart matrix.

To test the hypothesis, classical literature commonly employs two main types of techniques, both relying on the eigenvalues of  $\mathbf{F}$ . The first approach involves aggregating all eigenvalues of  $\mathbf{F}$  after applying a specific transformation, as in the classical likelihood ratio test statistic, also known as Wilk’s lambda. This method is useful for assessing the overall deviation from the null hypothesis.

In this paper, we focus on the second approach, known as Roy’s largest root test, which relies exclusively on the largest eigenvalue of  $\mathbf{F}$ , denoted by  $\ell_{\max}$ . This technique is particularly powerful for detecting concentrated alternatives, where the signal is primarily aligned with the leading eigen-direction. Specifically, the test rejects the null hypothesis  $H_0 : BC = 0$  if  $\ell_{\max} > \zeta_\alpha$  at a significance level  $\alpha$ , where  $\zeta_\alpha$  is the critical value corresponding to the  $(1 - \alpha) \times 100\%$  quantile of the distribution of  $\ell_{\max}$  under the null. Traditionally,  $\zeta_\alpha$  is approximated using the critical value of an  $F$  or  $\chi^2$  distribution after appropriate scaling; see Chapter 10 of Muirhead (2009) for details.

In contemporary statistical research, it is increasingly common for the dimension  $p$  to be at least comparable to, or even exceed, the sample size  $n_T$ . While Roy’s largest root test performs well when  $n_T$  are much larger than  $p$  and  $m$ , its reliability diminishes significantly in high-dimensional settings. In particular, when  $p > n_2$ , the singularity of  $\mathbf{W}_2$  renders the F-matrix ill-defined. Even when  $p$  is smaller than  $n_2$ , the presence of small eigenvalues in  $\mathbf{W}_2$  can cause instability in  $\mathbf{W}_2^{-1}$ , thereby compromising the power of the test. Addressing these issues is essential to ensure the robustness and validity of inferential procedures in high-dimensional regimes.

To correct the asymptotic null distribution of Roy’s largest root, Johnstone (2008) showed that, under normality, the largest root of  $\mathbf{F}$  converges to the Tracy–Widom distribution of type one after appropriate scaling, provided that  $p$ ,  $n_1$ , and  $n_2$  grow proportionally with  $p < n_2$ . This result was later extended to non-Gaussian settings by Han et al. (2016) and Han et al. (2018).

However, when  $p > n_2$ , existing remedy methods have primarily focused on problems corresponding to the case when  $n_1$  is small, such as two-sample mean tests and MANOVA. As summarized in Huang et al. (2022), these methods can be roughly grouped into three categories. The first category involves quadratic-form tests, which construct modified statistics by replacing  $\mathbf{W}_2^{-1}$  with regularized substitutes. For example, Bai and Saranadasa (1996) and Chen and Qin (2010) proposed replacing  $\mathbf{W}_2^{-1}$  with the identity matrix in two-sample mean tests. This idea was extended to MANOVA settings by Srivastava and Fujikoshi (2006), Yamada and Himeno (2015), and Hu et al. (2017). Chen et al. (2014) introduced a ridge regularization in the context of mean testing, further developed in Li et al. (2020b) and extended to MANOVA by Li et al. (2020a). The second category includes extreme-type tests, which typically rely on the maximum value among a sequence of test statistics. Notable examples include Cai et al. (2014), Xu et al. (2016), and Chang et al. (2017). The third category comprises projection-based tests, which reduce dimensionality by projecting the

high-dimensional observations onto a lower-dimensional subspace, followed by a classical likelihood ratio test. Prominent works include Lopes et al. (2011), Li and Li (2022), and Liu et al. (2024). Relatedly, He et al. (2021) proposed a screening-based approach that first reduces the response dimension and then applies the likelihood ratio test to the reduced data.

This paper aims to develop a high-dimensional largest root test that remains applicable when  $p$ ,  $n_1$  and  $n_2$  are comparable. To address the challenge posed by the singularity of  $\mathbf{W}_2$  when  $p > n_2$ , we introduce a ridge regularization framework. Specifically, inspired by the work of Li et al. (2020b), we propose a family of ridge-regularized F-matrices:

$$\mathbf{F}_\lambda = \mathbf{W}_1 \left( \mathbf{W}_2 + \lambda I_p \right)^{-1} = \left( \frac{1}{n_1} \Sigma_p^{1/2} \mathbf{Z} P_1 \mathbf{Z}^T \Sigma_p^{1/2} \right) \left( \frac{1}{n_2} \Sigma_p^{1/2} \mathbf{Z} P_2 \mathbf{Z}^T \Sigma_p^{1/2} + \lambda I_p \right)^{-1}, \quad (1.2)$$

where  $\lambda > 0$  is a regularization parameter. The largest eigenvalue of  $\mathbf{F}_\lambda$ , denoted by  $\ell_{\max}(\mathbf{F}_\lambda)$ , serves as the test statistic, designed to detect departures from the null hypothesis.

Importantly, the regularized F-matrix and its largest root are *rotation-invariant*, meaning they remain unchanged under arbitrary orthogonal transformations of the data. This invariance arises from the fact that the regularized matrix  $\mathbf{W}_2 + \lambda I_p$  preserves the eigen-structure of  $\mathbf{W}_2$ . This property is particularly advantageous in settings where additional structural knowledge, such as sparsity, is limited. It ensures that the test's performance does not depend on the specific coordinate system in which the data are observed. Consequently, the test remains robust across different data representations, making it broadly applicable in various high-dimensional scenarios.

In this paper, we focus on the regime where  $p$ ,  $n_1$ , and  $n_2$  are all comparable (see **C1** in Section 2). Under this regime, we establish the asymptotic Tracy-Widom distribution of  $\ell_{\max}(\mathbf{F}_\lambda)$  under the null hypothesis after appropriate scaling. We propose consistent estimators for the scaling parameters, which rely exclusively on the eigenvalues of  $\mathbf{W}_2$ . Finally, we conduct a power analysis of the proposed test under a class of low-rank alternatives and examine the influence of the regularization parameter  $\lambda$ .

The main contributions of this work are as follows. First, we extend the existing analysis of high dimensional general linear hypotheses to the regime where  $n_1$  is comparable to  $n_2$  while also allowing  $p$  exceed  $n_2$ . Second, although the regularization scheme is not new—being inspired by classical ridge regularization and Li et al. (2020a)—to the best of our knowledge, this is the first study to examine largest root-type tests under statistical regularization. Third, from an *Random Matrix Theory* (RMT) perspective, this work is the first to establish the asymptotic Tracy-Widom distribution for the extreme eigenvalue of a regularized random matrix. Fourth, we propose an estimation procedure for the complicated parameters involved in the asymptotic Tracy-Widom distribution of extreme eigenvalues of a random matrix. These types of parameters frequently appear in the

RMT literature, yet their estimation has remained challenging.

The paper is organized as follows. Section 2 introduces the asymptotic Tracy–Widom distribution for the ridge-regularized largest root test statistic, following a brief review of necessary preliminaries from random matrix theory. Section 3 presents the estimation procedure for the scaling parameters, which relies solely on the eigenvalues of  $\mathbf{W}_2$ , and establishes the consistency of the proposed method. A power analysis under a class of low-rank alternatives is conducted in Section 4. Section 5 reports the results of simulation studies. In Section 6, we demonstrate the application of the proposed procedure to data from the *Human Connectome Project*. Section 7 concludes with a summary of the main findings and a discussion of future research directions. Technical details and proofs of the main results are provided in the Supplementary Material.

## 2 Asymptotic theory

After giving necessary preliminaries on Random Matrix Theory, the asymptotic theory of the proposed ridge-regularized largest root is presented in this section. First of all, note that  $\mathbf{F}_\lambda$  is asymmetric, making it technically more convenient to analyze a symmetric dual matrix of the form  $\tilde{\mathbf{F}}_\lambda = U_1^T \mathbf{Z}^T \mathbf{G}_\lambda^{-1} \mathbf{Z} U_1$ , where

$$\mathbf{G}_\lambda = \mathbf{Z} U_2 U_2^T \mathbf{Z}^T + \lambda \Sigma_p^{-1}.$$

Here,  $U_1$  and  $U_2$  are  $p \times n_1$  and  $p \times n_2$  scaled orthogonal matrices satisfying  $U_1 U_1^T = n_1^{-1} P_1$  and  $U_2 U_2^T = n_2^{-1} P_2$ . It is straightforward to see that  $\tilde{\mathbf{F}}_\lambda$  shares the same nonzero eigenvalues as  $\mathbf{F}_\lambda$ . Thus, for technical convenience, we focus our analysis on  $\tilde{\mathbf{F}}_\lambda$ .

**Definition 2.1** (Empirical Spectral Distribution). *For any  $p \times p$  matrix  $A$  with real-valued eigenvalues, denote  $\ell_j(A)$  to be the  $j$ -th largest eigenvalue of  $A$  and specifically  $\ell_{\max}(A) = \ell_1(A)$  and  $\ell_{\min}(A) = \ell_p(A)$ . Define the Empirical Spectral Distribution (ESD)  $F^A$  of  $A$  by*

$$F^A(\tau) = \frac{1}{p} \sum_{j=1}^p \delta_{\ell_j(A)}(\tau),$$

where  $\delta_x(y) = 1$  if  $x \leq y$  and 0 otherwise.

The following basic assumptions are employed.

**C1** (High-dimensional regime) We assume  $p, n_T, n_1, n_2$  grow to infinity simultaneously in the sense that  $p/n_T \rightarrow \gamma_T$ ,  $p/n_1 \rightarrow \gamma_1$ ,  $p/n_2 \rightarrow \gamma_2$ , where  $\gamma_T, \gamma_1, \gamma_2 \in (0, \infty)$  are constants. Moreover, we assume the convergence rate is such that  $p^{2/3}|p/n_1 - \gamma_1| \rightarrow 0$  and  $p^{2/3}|p/n_2 - \gamma_2| \rightarrow 0$ .

**C2** (Moments conditions)  $\mathbb{E}|z_{ij}|^k < \infty$  for any  $k \geq 2$ .

**C3** (Boundedness of spectrum)  $\liminf_{p \rightarrow \infty} \ell_{\min}(\Sigma_p) > 0$  and  $\limsup_{p \rightarrow \infty} \ell_{\max}(\Sigma_p) < \infty$ .

**C4** (Asymptotic stability of population ESD) There exists a deterministic distribution  $F^{\Sigma_\infty}$  with compact support in  $(0, \infty)$ , such that

$$p^{2/3} \mathcal{D}_W(F^{\Sigma_p}, F^{\Sigma_\infty}) \rightarrow 0, \quad \text{as } p \rightarrow \infty,$$

where  $\mathcal{D}_W(F_1, F_2)$  denotes the *Wasserstein distance* between distributions  $F_1$  and  $F_2$ , defined as

$$\mathcal{D}_W(F_1, F_2) = \sup_f \left\{ \left| \int f dF_1 - \int f dF_2 \right| : f \text{ is 1-Lipschitz} \right\}.$$

**C5** (Asymptotic stability of edge eigenvalues) Denote the rightmost edge point of the support of  $F^{\Sigma_\infty}$  to be  $\sigma_{\max}$ . That is,  $\sigma_{\max} = \inf\{x \in \mathbb{R} : F^{\Sigma_\infty}(x) = 1\}$ . We assume

$$n^{2/3} |\ell_{\max}(\Sigma_p) - \sigma_{\max}| \rightarrow 0.$$

Additionally, if  $\sigma_{\max}$  is a point of discontinuity of  $F^{\Sigma_\infty}$ , we assume  $F^{\Sigma_p}(\{\ell_{\max}(\Sigma_p)\}) \rightarrow F^{\Sigma_\infty}(\{\sigma_{\max}\})$ .

**C6** (Regular edge) We assume  $F^{\Sigma_\infty}$  is regular near  $\sigma_{\max}$  in the sense of Definition 2.2 (see Section 2.2).

**C1** defines the asymptotic regime where dimensionality  $p$ , the sample size  $n_T$ , degrees of freedom  $n_1$ , and  $n_2$  grow proportionately. As stated in **C2**, our asymptotic results only require moment conditions. **C3** is a standard assumption in the RMT literature, ensuring that eigenvalue bounds are obtainable. **C4** ensures that the bulk spectrum of  $\Sigma_p$  characterized by its ESD stabilizes at a deterministic limit as  $p$  increases. While **C4** offers limited insight into the edge eigenvalue, **C5** ensures that the largest eigenvalue of  $\Sigma_p$  also stabilizes at the rightmost support edge of  $F^{\Sigma_\infty}$ . The details of **C6** are given in Section 2.2.

It is worth mentioning that **C5** excludes the possibility that a fixed number of eigenvalues of  $\Sigma_p$  remain outside the support of  $F^{\Sigma_\infty}$ . This situation arises in classical factor models. While we conjecture that our analysis can be extended to a class of factor models, such a generalization is beyond the scope of this work. Instead, to assess the performance of the proposed method when these assumptions are violated, we include a factor model setting in our numerical study in Section 5.

## 2.1 Preliminary results

In this section, we present key preliminary results in RMT, focusing on the asymptotic Marčenko-Pastur law for the ESD of  $\mathbf{G}_\lambda$  and the matrix

$$\widetilde{\mathbf{W}}_2 = U_2^T \mathbf{Z}^T \Sigma_p \mathbf{Z} U_2.$$

The matrix  $\widetilde{\mathbf{W}}_2$  is the companion matrix of  $\mathbf{W}_2$  in the sense that  $\widetilde{\mathbf{W}}_2$  shares the same nonzero eigenvalues as  $\mathbf{W}_2$ , differing only by  $|p - n_2|$  additional zeros in their spectra. Consequently, the ESD of  $\widetilde{\mathbf{W}}_2$  and  $\mathbf{W}_2$  can be easily reconstructed from one another. For mathematical convenience, we focus on the asymptotics of  $F^{\widetilde{\mathbf{W}}_2}$  rather than  $F^{\mathbf{W}_2}$  in the subsequent analysis, as it results in cleaner and more tractable expressions. Results in this section are based on Silverstein and Bai (1995) and Bai and Silverstein (2004).

Recall that the *Stieltjes transform*  $\varphi(\cdot)$  of any function  $F$  of bounded variation on  $\mathbb{R}$  is defined as:

$$\varphi(z) = \int_{-\infty}^{\infty} \frac{dF(x)}{x - z}, \quad z \in \mathbb{C}^+ := \{E + i\eta : \eta > 0\}.$$

Note that  $\varphi$  is a mapping from  $\mathbb{C}^+$  to  $\mathbb{C}^+$ . The Stieltjes transform plays a role in RMT analogous to that of the Fourier transform in classical probability theory. It allows for the reconstruction of a distribution function via an inversion formula and facilitates the study of probability measure convergence through the convergence of its Stieltjes transform. For further details, see Bai and Silverstein (2010).

Given a compactly supported probability measure  $F$  and any  $\gamma > 0$ , the renowned Marčenko-Pastur equation in RMT defined on  $z \in \mathbb{C}^+$  is expressed as

$$z = -\frac{1}{\varphi} + \gamma \int \frac{\tau dF(\tau)}{\tau\varphi + 1}. \quad (2.1)$$

**Lemma 2.1.** *Under the conditions on  $F$  and  $\gamma$ , for any  $z \in \mathbb{C}^+$ , there exists a unique solution  $\varphi \equiv \varphi(z) \in \mathbb{C}^+$  to Eq. (2.1). The function  $\varphi(z)$  is the Stieltjes transform of a probability measure with bounded support in  $[0, \infty)$ .*

Unfortunately, except in extreme cases where  $F$  has a simple structure, there is no explicit closed-form solution for  $\varphi_{\gamma, F}(z)$  or the associated probability distribution. For further details of Marčenko-Pastur equation, see Chapter 3 of Bai and Silverstein (2010).

**Lemma 2.2** (Marčenko-Pastur Theorem). *Assume that conditions C1–C4 hold. As  $p \rightarrow \infty$ , the ESD  $F^{\widetilde{\mathbf{W}}_2}$  converges pointwise almost surely to  $\mathcal{W}$  at all points of continuity of  $\mathcal{W}$ , where  $\mathcal{W}$  is the probability measure associated with  $\varphi_{\gamma_2, F^{\Sigma_\infty}}$ .*

Moreover, for any  $z \in \mathbb{C}^+$ , let  $\hat{\varphi}(z)$  be the Stieltjes transform of  $F^{\widetilde{\mathbf{W}}_2}$ . That is,

$$\hat{\varphi}(z) = \int \frac{dF^{\widetilde{\mathbf{W}}_2}(\tau)}{\tau - z} = \frac{1}{n_2} \sum_{j=1}^{n_2} \frac{1}{\ell_j(\widetilde{\mathbf{W}}_2) - z}.$$

For any closed and bounded region  $\mathcal{Z} \subset \mathbb{C}^+$  and any fixed  $k \in \mathbb{N}$ , we have

$$\sup_{z \in \mathcal{Z}} p^{2/3} |\hat{\varphi}^{(k)}(z) - \varphi^{(k)}(z)| \xrightarrow{P} 0.$$

Following immediately from Lemma 2.1, the Marčenko-Pastur equation (2.1) holds approximately at  $\hat{\varphi}(z)$  in the sense that

$$z + \frac{1}{\hat{\varphi}(z)} - \frac{p}{n_2} \int \frac{\tau dF^{\Sigma_\infty}(\tau)}{\tau \hat{\varphi}(z) + 1} \xrightarrow{P} 0, \quad (2.2)$$

uniformly for  $z \in \mathcal{Z}$ . This result serves as the foundation for the estimation method proposed in Section 3.

Next, we analyze the limiting ESD of  $\mathbf{G}_\lambda$ . For any fixed  $\lambda > 0$ , consider the following equation defined for  $z \in \mathbb{C}^+$

$$\phi = \int \frac{\tau dF^{\Sigma_\infty}(\tau)}{\tau \{ [1 + \gamma_2 \phi]^{-1} - z \} + \lambda}. \quad (2.3)$$

**Lemma 2.3.** *Let  $F^{\Sigma_\infty}$  be any compactly supported probability measure that is non-degenerate to zero. For any given  $z \in \mathbb{C}^+$ , there exists a unique solution  $\phi \equiv \phi(z) \in \mathbb{C}^+$  to Eq. (2.3). The function  $\phi(z)$  is the Stieltjes transform of a probability measure with bounded support in  $(0, \infty)$ , henceforth denoted by  $\mathcal{G}_\lambda$ .*

**Theorem 2.1** (Generalized Marčenko-Pastur Theorem of  $\mathbf{G}_\lambda$ ). *Suppose C1–C4 hold. Fix  $\lambda > 0$ . As  $p \rightarrow \infty$ , the ESD  $F^{\mathbf{G}_\lambda}$  of  $\mathbf{G}_\lambda$  converges pointwise almost surely to  $\mathcal{G}_\lambda$  at all points of continuity of  $\mathcal{G}_\lambda$ .*

While Eq. (2.3) plays a fundamental role in the subsequent analysis, we present an equivalent reformulation that is more convenient to work with in certain cases. For any  $z \in \mathbb{C}^+$ , define

$$h = h(z) = z - [1 + \gamma_2 \phi(z)]^{-1}.$$

Then, Eq. (2.3) can be rewritten as

$$z = h + \left( 1 + \gamma_2 \int \frac{\tau dF^{\Sigma_\infty}(\tau)}{\lambda - \tau h} \right)^{-1}. \quad (2.4)$$

By Lemma 2.3, it follows that for any  $z \in \mathbb{C}^+$ , there exists a unique solution  $h \in \mathbb{C}^+$  to Eq. (2.4).

Lastly, we consider the extension of  $\phi(z)$  to the real line.

**Lemma 2.4.** *Under the conditions of Lemma 2.3, the measure  $\mathcal{G}_\lambda$  is compactly supported in  $(0, \infty)$ . Denote the leftmost edge of the support of  $\mathcal{G}_\lambda$  by  $\rho \equiv \rho_\lambda$ , i.e.,  $\rho = \sup\{x \in \mathbb{R} : \mathcal{G}_\lambda(x) = 0\}$ . The following results hold:*

(i) *We have  $\rho > 0$ , and for any  $x \in [0, \rho)$ ,*

$$\lim_{z \in \mathbb{C}^+ \rightarrow x} \phi(z) := s(x) \quad \text{exists and is real-valued.}$$

Moreover, the following relationship holds:

$$s(x) = \int \frac{d\mathcal{G}_\lambda(\tau)}{\tau - x}, \quad x \in [0, \rho). \quad (2.5)$$

(ii) From Eq (2.5),  $s(x)$  is analytic on  $[0, \rho)$ , and its  $k$ th derivative satisfies  $s^{(k)}(x) > 0$  for any  $k \in \mathbb{N}$  and  $x \in [0, \rho)$ . This implies that  $s^{(k)}(x)$  is monotonically increasing on  $[0, \rho)$  for all  $k$ .

## 2.2 Asymptotic Tracy-Widom distribution

In this section, we present the asymptotic Tracy-Widom distribution for the proposed ridge-regularized largest root statistic  $\ell_{\max}(\mathbf{F}_\lambda)$  (or equivalently  $\ell_{\max}(\tilde{\mathbf{F}}_\lambda)$ ) after appropriate scaling. All quantities introduced in this section may depend on  $(\gamma_1, \gamma_2, F^{\Sigma_\infty}, \lambda)$ . To simplify notation and reduce complexity, we omit these arguments when there is no risk of ambiguity.

We first impose an edge regularity condition on  $F^{\Sigma_\infty}$ . Recall that  $\sigma_{\max}$  is the rightmost edge point of the support of  $F^{\Sigma_\infty}$ . For  $h \in (-\infty, \lambda/\sigma_{\max})$ , define

$$x(h) = h + \left[ 1 + \gamma_2 \int \frac{\tau dF^{\Sigma_\infty}(\tau)}{\lambda - \tau h} \right]^{-1}. \quad (2.6)$$

It can be viewed as an extension of Eq. (2.4) when  $h \in \mathbb{C}^+$  approaches the real line.

**Definition 2.2.** We say that  $F^{\Sigma_\infty}$  is regular near  $\sigma_{\max}$  if any of the following holds:

- (i)  $F^{\Sigma_\infty}$  is discontinuous at  $\sigma_{\max}$  and  $\omega_{\max}\gamma_2 \neq 1$ , where  $\omega_{\max} = F^{\Sigma_\infty}(\{\sigma_{\max}\})$ .
- (ii)  $F^{\Sigma_\infty}$  is continuous at  $\sigma_{\max}$ , and there exists  $h_0 < \lambda/\sigma_{\max}$  such that  $x'(h_0) = 0$ .

We claim that the regularity conditions are mild in the sense that  $F^{\Sigma_p}$  is discrete for any finite  $p$ , and any continuous probability measure can be well-approximated by a discrete one. Under this condition,  $\mathcal{G}_\lambda$  is *well-behaved* near  $\rho$  in the following sense: either  $\rho$  is a discrete point of  $\mathcal{G}_\lambda$ , or the density  $f_{\mathcal{G}}$  of  $\mathcal{G}_\lambda$  exhibits a *square-root behavior* near  $\rho$ . The former case occurs when  $\omega_{\max}\gamma_2 > 1$ ; otherwise, the latter applies. Specifically, in the latter case, there exist positive constants  $C_1, C_2$ , and  $\epsilon$  such that

$$C_1\sqrt{x - \rho} \leq f_{\mathcal{G}}(x) \leq C_2\sqrt{x - \rho}, \quad \text{for } x \in (\rho, \rho + \epsilon).$$

Similar regularity conditions are widely used in the RMT literature when studying the Tracy-Widom fluctuations of extreme eigenvalues, albeit in various forms. For example, see Definition 2.7 of Knowles and Yin (2017), Condition (1) of El Karoui (2007), and Condition (2.12) of Lee and Schnelli (2016). Furthermore,

the square-root behavior near the edge of the spectrum is broadly observed across various random matrix models. This behavior is closely associated with Tracy-Widom fluctuations and plays a critical role in their characterization.

The following lemma follows from the behavior of  $\mathcal{G}_\lambda$  near  $\rho$ .

**Lemma 2.5.** *Suppose the conditions in Lemma 2.4 hold, and further assume that  $F^{\Sigma_\infty}$  is regular near  $\sigma_{\max}$ . Then,  $s'(x) \rightarrow \infty$  as  $x \uparrow \rho$ .*

Our main theorem is presented as follows.

**Theorem 2.2.** *Suppose that **C1–C6** hold. For any fixed  $\lambda > 0$ , as  $p \rightarrow \infty$ , the asymptotic distribution of the largest eigenvalue of  $\mathbf{F}_\lambda$  (or equivalently  $\tilde{\mathbf{F}}_\lambda$ ) is given by*

$$\frac{p^{2/3}}{\Theta_2(\lambda)} \left( \ell_{\max}(\mathbf{F}_\lambda) - \Theta_1(\lambda) \right) \Longrightarrow \text{TW}_1, \quad (2.7)$$

where  $\text{TW}_1$  denotes the Tracy-Widom distribution of type 1, and  $\Longrightarrow$  indicates convergence in distribution. The centering and scaling parameters  $\Theta_1(\lambda)$  and  $\Theta_2(\lambda)$  are determined as follows. Define  $\beta = \beta(\lambda)$  to be the unique solution in  $(0, \rho)$  to

$$\beta^2 s'(\beta) = \frac{1}{\gamma_1}. \quad (2.8)$$

By Lemma 2.5, such a solution  $\beta$  exists and is unique. Then,

$$\Theta_1(\lambda) = \frac{1}{\beta} \left[ 1 + \gamma_1 \beta s(\beta) \right], \quad (2.9)$$

$$\Theta_2(\lambda) = \left[ \frac{\gamma_1^3}{2} s''(\beta) + \frac{\gamma_1^2}{\beta^3} \right]^{1/3}. \quad (2.10)$$

**Remark 2.1.** *For detailed information on Tracy-Widom distributions, we refer readers to Tracy and Widom (1994), Tracy and Widom (1996), and Johnstone (2008). Available software for working with Tracy-Widom laws includes the R package **RMTstat** (Johnstone et al., 2022) and the MATLAB package **RMLab** (Dieng, 2006).*

**Remark 2.2.** *Unlike the  $O(p)$  scaling observed in classical extreme value theory for i.i.d. random variables with appropriate tail behavior, the normalized largest eigenvalue of  $\mathbf{F}_\lambda$  fluctuates on the  $O(p^{2/3})$  scale. An analogous scaling has been established for the largest eigenvalue of various random matrices, such as those in the Jacobi orthogonal ensemble (Johnstone, 2008). This  $O(p^{2/3})$  fluctuation reflects the repulsion between eigenvalues, causing them to be more regularly spaced than i.i.d. random variables.*

**Remark 2.3.** *When  $\lambda = 0$  and  $\gamma_2 < 1$ , the matrix  $\mathbf{F}_0$  reduces to the classical F-matrix. Han et al. (2018) established the asymptotic Tracy-Widom distribution for the largest eigenvalue of an F-matrix in that setting.*

Theorem 2.2 can be viewed as a generalization of Han et al. (2018) to  $\lambda > 0$  and an arbitrary covariance matrix  $\Sigma_p$ .

**Remark 2.4.** Theorem 2.2 can be generalized to the joint asymptotic distribution of the first  $k$  largest eigenvalues of  $\mathbf{F}_\lambda$ . Specifically, under **C1–C6**, for any fixed integer  $k$  and  $\lambda > 0$ , we have

$$\begin{aligned} & \lim_{p \rightarrow \infty} \mathbb{P} \left( \frac{p^{2/3}}{\Theta_2(\lambda)} \left( \ell_1(\mathbf{F}_\lambda) - \Theta_1(\lambda) \right) \leq t_1, \dots, \frac{p^{2/3}}{\Theta_2(\lambda)} \left( \ell_k(\mathbf{F}_\lambda) - \Theta_1(\lambda) \right) \leq t_k \right) \\ &= \lim_{p \rightarrow \infty} \mathbb{P} \left( \frac{p^{2/3}}{\gamma_1^{2/3}} \left( \ell_1^{\text{GOE}} - 2 \right) \leq t_1, \dots, \frac{p^{2/3}}{\gamma_1^{2/3}} \left( \ell_k^{\text{GOE}} - 2 \right) \leq t_k \right), \end{aligned} \quad (2.11)$$

for any  $t_1, \dots, t_k \in \mathbb{R}$ . Here,  $\ell_k^{\text{GOE}}$  denotes the  $k$ -th largest eigenvalue of a  $p \times p$  matrix from the Gaussian Orthogonal Ensemble (GOE).

### 3 Estimation

In this section, we develop an estimation procedure for the centering and scaling parameters  $\Theta_1(\lambda)$  and  $\Theta_2(\lambda)$ . The proposed estimators leverage the eigenvalues of  $\mathbf{W}_2$  and are designed to be computationally efficient while maintaining robustness in high-dimensional settings. This section is organized as follows. Section 3.1 introduces a reformulation of the problem as an optimization task. The proposed algorithm is described in detail in Section 3.2. In Section 3.3, we establish the consistency of the proposed estimators. Additional implementation details and practical considerations are provided in Section S.1 of the Supplementary Material.

Throughout this section, for notational simplicity, the dependence on the regularization parameter  $\lambda$  is suppressed, as  $\lambda$  is treated as fixed. The parameters  $\gamma_1$  and  $\gamma_2$  are estimated as  $\hat{\gamma}_1 = p/n_1$  and  $\hat{\gamma}_2 = p/n_2$ , respectively, without further elaboration.

#### 3.1 Problem formulation

The estimation of  $\Theta_1$  and  $\Theta_2$  necessitates the precise estimation of the edge  $\rho$  and the function  $s(x)$  along with its derivatives on the interval  $[0, \rho)$ . Although  $s(x)$  is formally defined as the extension of the Stieltjes transform  $\phi(z)$  from  $\mathbb{C}^+$  to the real line as in Lemma 2.4, this definition provides limited practical utility due to the absence of an explicit analytical expression. In this section, we rigorously demonstrate that both  $\rho$  and  $s(x)$  can be characterized by Eq. (2.6), thereby establishing a foundation for their accurate estimation.

**Lemma 3.1.** Assume that  $F^{\Sigma_\infty}$  is regular near  $\sigma_{\max}$  as defined in Definition 2.2. If there exists  $h_0 < \lambda/\sigma_{\max}$  such that  $x'(h_0) = 0$ , then the edge  $\rho$  is given by  $\rho = x(h_0) > \lambda/\sigma_{\max}$ ; otherwise,  $\rho = \lambda/\sigma_{\max}$ .

**Corollary 3.1.** Consider the case where  $\sigma_{\max}$  is a point of discontinuity of  $F^{\Sigma_\infty}$ , and recall that  $\omega_{\max} = F^{\Sigma_\infty}(\{\sigma_{\max}\})$ . The edge  $\rho$  is determined as follows:

- (i) If  $\gamma_2\omega_{\max} < 1$ , there exists  $h_0 < \lambda/\sigma_{\max}$  such that  $x'(h_0) = 0$ . In this case,  $\rho = x(h_0) > \lambda/\sigma_{\max}$ , and  $\rho$  is a point of continuity of  $\mathcal{G}_\lambda$ .
- (ii) If  $\gamma_2\omega_{\max} > 1$ , we have  $x'(h) > 0$  for any  $h \in (0, \lambda/\sigma_{\max})$ . We have  $\rho = \lambda/\sigma_{\max}$ , and  $\rho$  is a point of discontinuity of  $\mathcal{G}_\lambda$ .

Define the auxiliary functions on  $h \in (-\infty, \lambda/\sigma_{\max})$  as

$$\mathcal{H}_j(h) = \int \frac{\tau^j dF^{\Sigma_\infty}(\tau)}{(\lambda - \tau h)^j}, \quad j = 1, 2, 3.$$

With the definition,  $x(h) = h + [1 + \gamma_2\mathcal{H}_1(h)]^{-1}$  and  $x'(h) = 1 - \gamma_2[1 + \gamma_2\mathcal{H}_1(h)]^{-2}\mathcal{H}_2(h)$ .

**Theorem 3.1.** Assume that  $F^{\Sigma_\infty}$  is regular near  $\sigma_{\max}$  as defined in Definition 2.2. Fix any  $x_0 \in [0, \rho)$ . Then,  $s(x_0)$  is determined as

$$s(x_0) = \frac{1}{\gamma_2} \left( \frac{1}{x_0 - h_0} - 1 \right),$$

where  $h_0$  is the unique solution in  $(-\infty, \lambda/\sigma_{\max})$  to

$$\begin{cases} x_0 = h_0 + [1 + \gamma_2\mathcal{H}_1(h_0)]^{-1}, \\ 1 - \gamma_2[1 + \gamma_2\mathcal{H}_1(h_0)]^{-2}\mathcal{H}_2(h_0) > 0. \end{cases} \quad (3.1)$$

Furthermore, the derivatives  $s'(x_0)$  and  $s''(x_0)$  are determined as:

$$\begin{aligned} g(x_0) &= x_0 - \frac{1}{1 + \gamma_2 s(x_0)}, \\ \zeta(x_0) &= \frac{\gamma_2}{(1 + \gamma_2 s(x_0))^2}, \\ s'(x_0) &= \mathcal{H}_2(g(x_0)) (\zeta(x_0)s'(x_0) + 1), \\ s''(x_0) &= 2 (\zeta(x_0)s'(x_0) + 1)^2 \mathcal{H}_3(g(x_0)) + \mathcal{H}_2(g(x_0)) \left[ \frac{-2(\gamma_2 s'(x_0))^2}{(1 + \gamma_2 s(x_0))^3} + \zeta(x_0)s''(x_0) \right]. \end{aligned} \quad (3.2)$$

It is worth noting that the third equation in (3.2) is linear in  $s'(x_0)$ , given  $s(x_0)$  and  $\mathcal{H}_2(\cdot)$ . Similarly, the last equation in (3.2) is linear in  $s''(x_0)$ , given  $s(x_0)$ ,  $s'(x_0)$ ,  $\mathcal{H}_2(\cdot)$ , and  $\mathcal{H}_3(\cdot)$ .

The following lemma is useful for the numerical computation of  $s(x_0)$ .

**Lemma 3.2.** Under the conditions of Theorem 3.1, the derivative  $x'(h) = 1 - \gamma_2[1 + \gamma_2\mathcal{H}_1(h)]^{-2}\mathcal{H}_2(h)$  is monotonically decreasing on  $(-\infty, \lambda/\sigma_{\max})$ .

This result implies that  $x(h)$  is either strictly increasing on  $(-\infty, \lambda/\sigma_{\max})$  or exhibits a single concave-down peak within this interval. If  $x_0 = h + [1 + \gamma_2 \mathcal{H}_1(h)]^{-1}$  has two distinct roots, Eq. (3.1) indicates that  $h_0$  corresponds to the smaller root.

Through the results in Theorem 3.1, we can transform the problem of estimating  $s(x)$ ,  $s'(x)$ , and  $s''(x)$  into the task of estimating  $\mathcal{H}_j(h)$  for  $j = 1, 2, 3$  over  $h \in (-\infty, \lambda/\sigma_{\max})$ . To this end, we revisit Lemma 2.2 and Eq. (2.2), which together suggest that:

$$\begin{aligned}\mathcal{H}_1(-\lambda\hat{\varphi}(z)) &= \int \frac{\tau dF^{\Sigma_\infty}(\tau)}{\lambda + \tau\lambda\hat{\varphi}(z)} \approx \frac{z}{\lambda\hat{\gamma}_2} + \frac{1}{\lambda\hat{\gamma}_2\hat{\varphi}(z)}, \\ \mathcal{H}_2(-\lambda\hat{\varphi}(z)) &= \int \frac{\tau^2 dF^{\Sigma_\infty}(\tau)}{(\lambda + \tau\lambda\hat{\varphi}(z))^2} \approx \frac{1}{\lambda^2\hat{\gamma}_2\hat{\varphi}^2(z)} - \frac{1}{\lambda^2\hat{\gamma}_2\hat{\varphi}'(z)}.\end{aligned}$$

Here, we are extending the definition of  $\mathcal{H}_j(h)$  to the complex domain. The second result is obtained by differentiating both sides of Eq. (2.2). Notably,  $\hat{\varphi}(z)$  solely relies on the eigenvalues of  $\mathbf{W}_2$  as

$$\hat{\varphi}(z) = \frac{1}{n_2} \sum_{j=1}^{n_2} \frac{1}{\ell_j(\mathbf{W}_2) - z}, \quad \text{with } \ell_j(\mathbf{W}_2) = 0 \text{ if } j > p.$$

This observation motivates the following strategy for estimating  $\mathcal{H}_j(y)$  for  $j = 1, 2, 3$ .

For general  $F^{\Sigma_\infty}$ , it can be approximated by a weighted sum of point masses, expressed as:

$$F^{\Sigma_\infty}(\tau) \simeq \sum_{k=1}^K w_k \delta_{\sigma_k}(\tau),$$

where  $\{\sigma_k\}_{k=1}^K$  is a grid of points chosen to densely cover the support of  $F^{\Sigma_\infty}$ , and  $w_k$  are weights satisfying  $w_k \geq 0$  and  $\sum_{k=1}^K w_k = 1$ . The grid  $\{\sigma_k\}_{k=1}^K$  is user-selected and fixed throughout the estimation procedure, while the weights  $w_k$  are model parameters. This approach was introduced in El Karoui (2008) and later generalized in Ledoit and Wolf (2012). The recommended choice of the grid  $\{\sigma_k\}_{k=1}^K$  is discussed in Section S.1. Accordingly, the integrals can be approximated as:

$$\mathcal{H}_j(h) = \int \frac{\tau^j dF^{\Sigma_\infty}(\tau)}{(\lambda - \tau h)^j} \simeq \sum_{k=1}^K \frac{w_k \sigma_k^j}{(\lambda - \sigma_k h)^j} := \tilde{\mathcal{H}}_j(h, w_1, \dots, w_K).$$

For  $z \in \mathbb{C}^+$ , define:

$$\hat{Q}_1(z) = \frac{z}{\lambda\hat{\gamma}_2} + \frac{1}{\lambda\hat{\gamma}_2\hat{\varphi}(z)}, \quad \text{and} \quad \hat{Q}_2(z) = \frac{1}{\lambda^2\hat{\gamma}_2\hat{\varphi}^2(z)} - \frac{1}{\lambda^2\hat{\gamma}_2\hat{\varphi}'(z)}.$$

Consider a grid of points  $z$  in  $\mathbb{C}^+$ , denoted by  $\{z_i\}_{i=1}^I$ . The recommended choice of  $\{z_i\}_{i=1}^I$  is provided in Section S.1 of the Supplementary Material. We select the weights  $w_k$  such that  $\hat{Q}_j(z_i)$  approximately matches

$\tilde{\mathcal{H}}_j(-\lambda\hat{\varphi}(z_i), w_1, \dots, w_K)$  for all  $i = 1, 2, \dots, I$ , and  $j = 1, 2$ . Further details are presented in the following sections.

### 3.2 The algorithm

Given the grids  $\{\sigma_k\}_{k=1}^K$  and  $\{z_i\}_{i=1}^I$ , define the loss function as

$$L_\infty(w_1, \dots, w_K) = \max_{i=1, \dots, I} \max_{j=1, 2} \{|\Re(e_{ij})|, |\Im(e_{ij})|\}, \text{ where}$$

$$e_{ij} = \frac{\hat{Q}_j(z_i) - \tilde{\mathcal{H}}_j(-\lambda\hat{\varphi}(z_i), w_1, \dots, w_K)}{|\hat{Q}_j(z_i)|}, \quad i = 1, \dots, I; j = 1, 2.$$

---

#### Algorithm 1 Linear Programming Formulation for Selecting Weights

---

**Input:** A grid of masses  $\sigma_1, \dots, \sigma_K$ ; a grid of points  $z_1, \dots, z_I$ ; eigenvalues  $\ell_j$ 's of  $\mathbf{W}_2$ ; regularization parameter  $\lambda$ .

**Calculation:** Compute

$$e_{ij} = \frac{\hat{Q}_j(z_i)}{|\hat{Q}_j(z_i)|} - \frac{1}{|\hat{Q}_j(z_i)|} \sum_{k=1}^K \frac{\sigma_k^j w_k}{(\sigma_k \lambda \hat{\varphi}(z_i) + \lambda)^j}, \quad i = 1, \dots, I; j = 1, 2,$$

**Optimization:** Find the optimal  $(w_1, \dots, w_K, \theta)$  through the linear programming

$$\begin{aligned} & \text{minimize} && \theta \\ & \theta, w_1, \dots, w_K \\ & \text{subject to} && -\theta \leq \Re(e_{ij}) \leq \theta, \quad \forall i = 1, \dots, I; j = 1, 2, \\ & && -\theta \leq \Im(e_{ij}) \leq \theta, \quad \forall i = 1, \dots, I; j = 1, 2, \\ & && w_k \geq 0, \quad \forall k = 1, \dots, K, \\ & && \text{and } w_1 + w_2 + \dots + w_K = 1. \end{aligned}$$

**Truncation:** To mitigate the effect of floating-point errors, truncate the optimal weight  $w_k$  to  $w_k \times \mathbb{1}(w_k > K^{-1}10^{-d})$  and rescale the truncated weights to be of sum one. The recommended choice of  $d$  is  $d = 2$ .

**Output:** All positive weights  $\hat{w}_1, \dots, \hat{w}_B$ , the associated masses  $\hat{\sigma}_1, \dots, \hat{\sigma}_B$  and loss  $\theta$ .

---

We choose the weights as

$$(w_1^*, \dots, w_K^*) = \arg \min_{w_j \geq 0, \sum w_j = 1} L_\infty(w_1, \dots, w_K).$$

The main motivation for choosing the  $L_\infty$  type loss is that given the point masses  $\{\sigma_k\}_{k=1}^K$ , the optimization can be formulated into a linear programming problem as presented in Algorithm 1.

Suppose the optimal positive weights given by Algorithm 1 are  $\hat{w}_1, \dots, \hat{w}_B$  and the associated point masses are  $\hat{\sigma}_1 > \hat{\sigma}_2 > \dots > \hat{\sigma}_B$ . We estimate  $\mathcal{H}_j(h)$  by

$$\hat{\mathcal{H}}_j(h) = \sum_{k=1}^B \frac{\hat{w}_k \hat{\sigma}_k^j}{(\lambda - \hat{\sigma}_k h)^j}, \quad j = 1, 2, 3, \quad 0 < h < \lambda / \hat{\sigma}_1.$$

Given  $\hat{\mathcal{H}}_j(\cdot)$ ,  $j = 1, 2, 3$ , the estimation of  $s(x)$  and its derivatives over the domain  $[0, \rho)$  can be performed efficiently by leveraging its inherent smoothness. First of all, following Corollary 3.1, the estimator  $\hat{\rho}$  of  $\rho$  is obtained in Algorithm 2. Secondly, note that (3.2) defines an ordinary differential equation (ODE) system. We propose to estimate  $s(x)$ ,  $s'(x)$ ,  $s''(x)$  by solving this ODE, as detailed in Algorithm 3.

---

**Algorithm 2** Estimation of  $\rho$

---

**Input:**  $\lambda$ ,  $\hat{\mathcal{H}}_1(\cdot)$ ,  $\hat{\mathcal{H}}_2(\cdot)$ , largest point-mass  $\hat{\sigma}_1$ , the associated weight  $\hat{w}_1$ ;

**Case 1:** If  $\hat{\gamma}_2 \hat{w}_1 \geq 1$ ,  $\hat{\rho} = \lambda / \hat{\sigma}_1$ ;

**Case 2:** Otherwise, solve for the unique root  $\hat{h}$  in  $(-\infty, \lambda / \hat{\sigma}_1)$  to

$$\frac{\hat{\gamma}_2 \hat{\mathcal{H}}_2(\hat{h})}{(1 + \hat{\gamma}_2 \hat{\mathcal{H}}_1(\hat{h}))^2} = 1.$$

The function on the left-hand side is monotonically increasing on  $(-\infty, \lambda / \hat{\sigma}_1)$ . The equation can be solved using Newton's method with an initial value pre-selected through grid search. Then,  $\hat{\rho} = \hat{h} + [1 + \hat{\gamma}_2 \hat{\mathcal{H}}_1(-\hat{h})]^{-1}$ .

**Output:** Estimated edge  $\hat{\rho}$ .

---

Following Algorithm 2 and Algorithm 3, we estimate  $\beta$  by  $\hat{\beta}$ , which is the unique solution on  $(0, \hat{\rho})$  to  $\beta^2 \hat{s}'(\beta) = 1 / \hat{\gamma}_1$ . Then,  $\Theta_1$  and  $\Theta_2$  are estimated as:

$$\hat{\Theta}_1 = \frac{1}{\hat{\beta}} \left[ 1 + \hat{\gamma}_1 \hat{\beta} \hat{s}(\hat{\beta}) \right] \quad \text{and} \quad \hat{\Theta}_2 = \left[ \frac{\hat{\gamma}_1^3}{2} \hat{s}''(\hat{\beta}) + \frac{\hat{\gamma}_1^2}{\hat{\beta}^3} \right]^{1/3}. \quad (3.3)$$

---

**Algorithm 3** ODE Formulation For Estimation of  $s(x)$ ,  $s'(x)$ , and  $s''(x)$

---

**Input:**  $\hat{\rho}$ ,  $\hat{\mathcal{H}}_1(\cdot)$ ,  $\hat{\mathcal{H}}_2(\cdot)$ ,  $\hat{\mathcal{H}}_3(\cdot)$ ;

**Initial:** Find  $s$  as the unique solution to  $\hat{\mathcal{H}}_1\left(\frac{-1}{1 + \hat{\gamma}_2 s}\right) = s$  and  $\hat{\gamma}_2 \hat{\mathcal{H}}_2\left(\frac{-1}{1 + \hat{\gamma}_2 s}\right) < (1 + \hat{\gamma}_2 s)^2$ .

**ODE:** On  $x \in [0, \hat{\rho})$ , solve the following ODE with the initial  $\hat{s}(0) = s$ :

$$\begin{aligned} \hat{s}'(x) &= \frac{\hat{\mathcal{H}}_2(\hat{g}(x))}{1 - \hat{\mathcal{H}}_2(\hat{g}(x)) \hat{\zeta}(x)}, \\ \hat{s}''(x) &= \frac{2[\hat{\zeta}(x) \hat{s}'(x) + 1]^2 \hat{\mathcal{H}}_3(\hat{g}(x)) - 2[1 + \hat{\gamma}_2 \hat{s}(x)]^{-3} \hat{\mathcal{H}}_2(\hat{g}(x)) (\hat{\gamma}_2 \hat{s}'(x))^2}{1 - \hat{\zeta}(x) \hat{\mathcal{H}}_2(\hat{g}(x))}, \\ \hat{g}(x) &= x - \frac{1}{1 + \hat{\gamma}_2 \hat{s}(x)}, \quad \text{and} \quad \hat{\zeta}(x) = \frac{\hat{\gamma}_2}{(1 + \hat{\gamma}_2 \hat{s}(x))^2}. \end{aligned}$$

**Output:** Estimated functions:  $\hat{s}(x)$ ,  $\hat{s}'(x)$ ,  $\hat{s}''(x)$  on  $[0, \hat{\rho})$ .

---

In Algorithm 1, the choice of the  $L_\infty$  type loss function leads to a linear programming problem. Alternative convex loss functions, such as the  $L_2$ -norm, can also be considered, transforming the optimization into a general convex problem. However, our numerical studies indicate that the  $L_2$ -loss provides no significant advantage over the  $L_\infty$ -loss. Given that linear programming is computationally more efficient, we recommend the use of

the  $L_\infty$ -loss. A detailed comparison between different loss functions is beyond the scope of the current work.

Additional constraints can be incorporated into Algorithm 1 to further enhance precision. For instance, to improve the accuracy of  $\hat{\mathcal{H}}_3(y)$ , we may want to ensure that the second-order derivative of  $\hat{Q}_1(z)$  matches those of  $\tilde{\mathcal{H}}_1(-\lambda\hat{\varphi}(z))$ . Since the derivatives are also linear in the weights  $w_k$ , it is straightforward to regularize the problem and add such constraints. Our numerical studies suggest that when  $\hat{\gamma}_2$  is relatively small (e.g.,  $\hat{\gamma}_2 \leq 1$ ), incorporating constraints on the second-order derivative of  $\tilde{\mathcal{H}}_1(-\lambda\hat{\varphi}(z))$  can slightly improve the estimation accuracy of  $\hat{\Theta}_1$  and  $\hat{\Theta}_2$ . However, when  $\hat{\gamma}_2$  is relatively large (e.g.,  $\hat{\gamma}_2 \geq 5$ ), such constraints tend to reduce estimation precision. This is mainly because the accuracy of  $\hat{\varphi}''(z)$ , which serve as the estimator of  $\varphi''(z)$ , diminishes when  $p$  becomes much larger than  $n_2$ .

Algorithm 1 is inspired by El Karoui (2008) and Ledoit and Wolf (2012), but it diverges in the choice of basis functions and the design of the loss function. While El Karoui (2008) and Ledoit and Wolf (2012) prioritize achieving smoothness in the estimator of  $F^{\Sigma_\infty}$  by employing a combination of smooth basis functions and point masses, our focus is fundamentally different. In the context of estimating  $s(x)$ , the smoothness of  $F^{\Sigma_\infty}$  is not a primary concern. Consequently, we adopt a simpler approach by approximating  $F^{\Sigma_\infty}$  solely using a mixture of point masses. Our numerical experiments indicate that this method performs comparably to, if not better than, the smooth basis approach, provided the grid of  $\sigma_k$  points is sufficiently dense. This finding suggests that the additional complexity introduced by smooth basis functions offers no substantial benefit in this specific setting. As a result, we focus exclusively on point-mass mixture models in our estimation procedure. In addition, the loss functions used by El Karoui (2008) and Ledoit and Wolf (2012) control only the discrepancy between  $\hat{Q}_1$  and  $\tilde{\mathcal{H}}_1$ . In contrast, our method explicitly penalizes the discrepancy between  $\hat{Q}_2$  and  $\tilde{\mathcal{H}}_2$ , as accurate estimation of  $\mathcal{H}_2$  is of direct interest.

### 3.3 Consistency

In this section, we show the consistency of the proposed estimation procedure.

**Definition 3.1.** For a grid of complex values  $J = \{t_1, t_2, t_3, \dots\}$ , define the corresponding grid size as  $\text{size}(J) = \sup_k |t_k - t_{k-1}|$ .

**Definition 3.2.** A grid  $R$  of real numbers is said to cover a compact interval  $[a, b]$  if there exists at least one  $t_k \in R$  with  $t_k \leq a$  and at least another  $t_{k'} \in R$  with  $t_{k'} \geq b$ . A sequence of grids  $\{R_m, m = 1, 2, 3, \dots\}$  is said to eventually cover a compact interval  $[a, b]$  if for every  $\epsilon > 0$  there exists  $M$  such that  $R_m$  covers the compact interval  $[a + \epsilon, b - \epsilon]$  for all  $m \geq M$ .

**Theorem 3.2.** Suppose that **C1–C6** hold. Assume that  $R_p = \{\sigma_{p1}, \sigma_{p2}, \dots\}$ , for  $p = 1, 2, \dots$ , is a sequence of grids on the real line that eventually covers  $[0, \sigma_{\max}]$ , with  $\text{size}(R_p) = o(p^{-2/3})$ . Suppose that

$J_p = \{z_{p1}, z_{p2}, \dots\}$ , for  $p = 1, 2, \dots$ , is a sequence of grids.

(i) Let  $\hat{F}_p$  denote the estimated measure obtained from Algorithm 1 using the inputs  $\{\sigma_k\} = R_p$  and  $\{z_i\} = J_p$ .

If  $J_p$  is such that for some  $\nu > 0$ ,

$$\sup_{z \in D(\nu)} \inf_{y \in J_p} |z - \varphi(y)| = o(p^{-2/3}), \quad (3.4)$$

where  $D(\nu)$  is the closed half-disk in  $\mathbb{C}^+$  centered at 0 with radius  $\nu$ . Then, there exists a constant  $C$  such that for any  $T \geq 3$

$$\mathcal{D}_W(\hat{F}_p, F^{\Sigma_\infty}) \leq \frac{C(1+\nu)}{\nu^2} p^{-2/3} \exp(T) \delta_p + \frac{C}{T},$$

where  $\delta_p$  is such that  $\delta_p \xrightarrow{P} 0$ , as  $p \rightarrow \infty$ .

(ii) Let  $h_\beta$  be the solution to Eq. (3.1) when  $x_0 = \beta$ . If  $J_p$  is such that there exists  $\varepsilon > 0$  such that  $\{\varphi(y), y \in J_p\}$  eventually covers  $[-h_\beta/\lambda - \varepsilon, -h_\beta/\lambda + \varepsilon]$ . Then, the proposed estimators  $\hat{\Theta}_1$  and  $\hat{\Theta}_2$ , obtained using the inputs  $\{\sigma_k\} = R_p$  and  $\{z_i\} = J_p$ , satisfy:

$$p^{2/3} |\hat{\Theta}_1 - \Theta_1| \xrightarrow{P} 0 \quad \text{and} \quad |\hat{\Theta}_2 - \Theta_2| \xrightarrow{P} 0.$$

**Lemma 3.3.** For any  $\gamma_1, \gamma_2, \lambda$ , and  $F^{\Sigma_\infty}$  satisfying **C1–C6**, there exists  $\nu > 0$  and a sequence of grids  $\{J_p\}$  such that Condition (3.4) is satisfied.

Theorem 3.2 establishes two fundamental results. First, it provides a Berry-Esseen type bound on the Wasserstein distance between the estimated population empirical spectral distribution (ESD) and its limiting counterpart. Second, it demonstrates that the proposed estimator achieves  $o_P(p^{-2/3})$  consistency, provided that  $\{\varphi(y), y \in J_p\}$  is dense around  $-h_\beta/\lambda$ . We can find a sequence of  $J_p$  satisfying the condition when  $\beta$  is not excessively close to  $\rho$ . The positioning of  $\beta$  is influenced by the parameters  $\gamma_1$  and  $\gamma_2$ . Specifically,  $\beta$  approaches 0, as  $\gamma_1$  grows. Reversely, for small  $\gamma_1$ ,  $\beta$  is close to  $\rho$ .

**Lemma 3.4.** Fix any  $\gamma_2, \lambda$ , and  $F^{\Sigma_\infty}$  satisfying **C1–C6**. There exists  $\gamma_1^{(0)}$  such that for any  $\gamma_1 > \gamma_1^{(0)}$ , we can find a sequence of grids  $\{J_p\}$  such that the condition in (ii) of Theorem 3.2 is satisfied.

Lemma 3.4 indicates that the condition in (ii) of Theorem 3.2 can be satisfied when  $\gamma_1$  is large. This scenario corresponds to the regime where  $n_2$  is large and  $n_1$  is relatively small compared to  $p$ . The numerical simulation results reported in Table 5.1 and Table 5.2 support these findings, showing that the estimation precision decreases as  $p/n_2$  increases or as  $p/n_1$  decreases under the given simulation settings. Nonetheless, the overall estimation precision remains well-controlled within a reasonable range for all settings under consideration.

## 4 Power analysis under low-rank alternatives

In this section, we investigate the power of the proposed family of tests under a class of low-rank alternatives, with particular focus on the impact of the regularization parameter  $\lambda$  on power. We begin with a deterministic alternative framework, commonly used in the literature to study asymptotic power. We then adopt a Bayesian perspective by introducing a class of priors on the alternatives that encode structural assumptions. Within this framework, we also provide a data-driven strategy for selecting  $\lambda$ .

### 4.1 Deterministic alternatives

Consider a sequence of rank-one deterministic alternatives as follows.

**DA** Under  $H_a : BC \neq 0$ , assume that  $BC$  satisfies

$$\frac{1}{n_1} BC(C^T(XX^T)^{-1}C)^{-1}C^TB^T = p^s d_p q_p q_p^T, \quad (4.1)$$

where  $s > 0$  is a constant controlling the signal magnitude;  $d_p$  is a sequence of positive scalars such that  $d_p \rightarrow d > 0$ ; and  $q_p \in \mathbb{R}^p$  is a sequence of unit vectors representing the direction in which the signal resides.

**Lemma 4.1.** *Suppose that **C1-C6** hold and  $BC$  is as in **DA**. For any fixed  $\lambda > 0$ , we have as  $p \rightarrow \infty$ ,*

$$\frac{1}{p^s} \ell_{\max}(\mathbf{F}_\lambda) = d_p q_p^T (\lambda \varphi(-\lambda) \Sigma_p + \lambda I_p)^{-1} q_p + o_P(1).$$

Given the estimators  $\hat{\Theta}_1(\lambda)$  and  $\hat{\Theta}_2(\lambda)$  of  $\Theta_1(\lambda)$  and  $\Theta_2(\lambda)$ , respectively, define the standardized test statistic as

$$\tilde{\ell}(\lambda) = \frac{p^{2/3}}{\hat{\Theta}_2(\lambda)} \{\ell_{\max}(\mathbf{F}_\lambda) - \hat{\Theta}_1(\lambda)\}.$$

**Corollary 4.1.** *Suppose that **C1-C6** hold and  $BC$  is as in **DA**. Fix  $\lambda > 0$ . If  $\hat{\Theta}_1(\lambda) - \Theta_1(\lambda) \xrightarrow{P} 0$  and  $\hat{\Theta}_2(\lambda) - \Theta_2(\lambda) \xrightarrow{P} 0$ , then the power of the test is such that, as  $p \rightarrow \infty$ ,*

$$\mathbb{P}\left(\tilde{\ell}(\lambda) > \text{TW}_1(1 - \alpha) \mid BC\right) \rightarrow 1,$$

where  $\text{TW}_1(1 - \alpha)$  denotes the  $(1 - \alpha)$ -quantile of the Tracy-Widom distribution of type one.

## 4.2 Probabilistic alternatives

While deterministic alternatives offer valuable insight, they can be somewhat restrictive for a systematic investigation of the power properties of the test. To address this limitation, we consider probabilistic alternatives in the form of a sequence of prior distributions on  $BC$ . This approach offers greater flexibility, allowing structural information about the regression coefficient matrix  $B$  and the constraint matrix  $C$  to be incorporated naturally through the choice of prior distributions. Such a probabilistic approach has been previously proposed and explored in Li et al. (2020b) and Li et al. (2020a).

**PA** Assume that under  $H_a$ ,  $BC$  is such that

$$\frac{1}{n_1} BC(C^T(XX^T)^{-1}C)^{-1}C^TB^T = p^{s+1}D^{1/2}\nu\nu^TD^{1/2}, \quad (4.2)$$

where  $s > 0$  is a constant controlling the signal magnitude;  $D$  is the  $p \times p$  symmetric covariance matrix satisfying  $\|D\|_2 < \infty$ ; and  $\nu$  is a random vector with independent entries having mean zero, variance one and finite fourth moments.

Under the **PA** model, the signal is aligned with the eigen-direction defined by the random vector  $D^{1/2}\nu$ . Structural information can be incorporated through appropriate choices of the covariance matrix  $D$  and the distribution of  $\nu$ . For instance,  $D$  may encode community-based structure or stationary auto-covariance patterns. The vector  $\nu$  can be selected to control signal sparsity: a Gaussian prior yields a dense signal across all coordinates, while a Bernoulli prior induces sparsity by concentrating the signal on a subset of coordinates.

**Lemma 4.2.** *Suppose that C1-C6 hold and  $BC$  is as in PA. For any fixed  $\lambda > 0$ , we have as  $p \rightarrow \infty$ ,*

$$\frac{1}{p^s} \ell_{\max}(\mathbf{F}_\lambda) = \frac{1}{p} \text{tr} \left[ (\lambda \varphi(-\lambda) \Sigma_p + \lambda I_p)^{-1} D \right] + o_P(1).$$

**Corollary 4.2.** *Suppose that C1-C6 hold and  $BC$  is as in PA. Fix  $\lambda > 0$ . If  $\hat{\Theta}_1(\lambda) - \Theta_1(\lambda) \xrightarrow{P} 0$  and  $\hat{\Theta}_2(\lambda) - \Theta_2(\lambda) \xrightarrow{P} 0$ , then the power of the test is such that, as  $p \rightarrow \infty$ ,*

$$\mathbb{P} \left( \tilde{\ell}(\lambda) > \text{TW}_1(1 - \alpha) \mid BC \right) \xrightarrow{\mathbb{P}_{BC}} 1,$$

where  $\xrightarrow{\mathbb{P}_{BC}}$  denotes convergence in probability with respect to the prior measure of  $BC$ .

Lemma 4.2 shows that, under the rank-one alternative as in **PA**, the power of the proposed test is primarily governed—up to a scaling factor—by the term

$$\Xi(\lambda) = \xi(\lambda)/\Theta_2(\lambda)$$

where

$$\xi(\lambda) = p^{-1} \text{tr} \left[ (\lambda \varphi(-\lambda) \Sigma_p + \lambda I_p)^{-1} D \right]. \quad (4.3)$$

We interpret  $\Xi(\lambda)$  as the scaled asymptotic signal-to-noise ratio.

An estimator of  $\Xi(\lambda)$  is desired for investigating how the regularization parameter  $\lambda$  influences the power of the proposed test and for guiding the selection of  $\lambda$  in practice. If the large matrix  $D$  can be fully specified, we can estimate  $\xi(\lambda)$  consistently by

$$\hat{\xi}(\lambda) = \frac{1}{p} \text{tr} [(\mathbf{W}_2 + \lambda I_p)^{-1} D]. \quad (4.4)$$

This situation typically arises when additional structural information about the data is available. For example, if it is reasonable to assume a stationary autocovariance structure,  $D$  can be taken as a Toeplitz matrix with  $(i, j)$ -th entry  $a^{|i-j|}$  for some  $a > 0$ . However, when no additional information is available, specifying a high dimensional positive definite matrix  $D$  can be challenging. In this paper, we take a different approach. Motivated by Li et al. (2020a), we consider a polynomial alternative framework, by which we mean the following model:  $BC$  satisfies **PA** with  $D$  given as a matrix polynomial of  $\Sigma_p$ , namely

$$D = \sum_{i=0}^r \pi_i \Sigma_p^i, \quad (4.5)$$

for pre-specified coefficients  $\pi_0, \pi_1, \dots, \pi_r$  such that  $D$  is positive definite. Since any arbitrary smooth function can be approximated by polynomials, this formulation is quite useful and fairly general. Moreover, the choice of  $D$  as a matrix polynomial in  $\Sigma_p$  also allows for an easier interpretation of the signal structure under the alternative. Note that unless  $\Sigma_p = I_p$ , such a prior implies a certain distribution of the rank-one alternative in the spectral coordinate system. Specifically, larger values of  $\pi_i$  for high powers  $i$  imply that the signal has larger contribution from the leading eigenvectors of  $\Sigma_p$ .

Under **PA** and the polynomial alternatives Eq. (4.5),  $\xi(\lambda)$  can be consistently estimated by

$$\hat{\xi}(\lambda) = \sum_{i=0}^r \pi_i \Upsilon_i(\lambda) \quad (4.6)$$

with  $\Upsilon(\lambda)$  satisfying the recursive formula

$$\Upsilon_{i+1}(\lambda) = \frac{1}{\lambda \hat{\varphi}(-\lambda)} \left\{ \mathfrak{M}_i - \lambda \Upsilon_i(\lambda) \right\}, \quad i = 0, 1, 2, \dots,$$

and  $\Upsilon_0(\lambda) = (n_1/p)(\hat{\varphi}(-\lambda) - (1 - p/n_1)/\lambda)$ , where  $\mathfrak{M}_i$  is a consistent estimator of the  $i$ th population spectral moment  $\int \tau^i dF^{\Sigma_\infty}(\tau)$ , given in Lemma 1 of Bai et al. (2010). The formula is deduced in Li et al. (2020a)

using Lemma 3 of Ledoit and P ech e (2011). In this paper, we restrict to the case  $r = 2$  which requires only  $\mathfrak{M}_0 = 1$  and  $\mathfrak{M}_1 = p^{-1}\text{tr}(\mathbf{W}_2)$ . There are several considerations that guides this choice of  $r$ . First, for  $r = 2$ , all quantities involved in estimating  $\hat{\xi}(\lambda)$  can be computed explicitly without requiring knowledge of higher order moments of the observations. Also, the corresponding estimating equations are more stable as they do not involve higher order spectral moments. Secondly, the choice of  $r = 2$  yields a significant, yet nontrivial, concentration of the prior covariance in the directions of the leading eigenvectors of  $\Sigma_p$ . Finally, the choice  $r = 2$  leads to a quadratic polynomial, which accommodates both convex and concave shapes. For extensions to  $r > 2$ , we refer to Lemma 1 of Bai et al. (2010) for the construction of  $\mathfrak{M}_i$  for  $i \geq 2$ .

### 4.3 Effect of the regularization parameter

It is of great interest to study how the regularization parameter  $\lambda$  affect the power of the proposed test. Under **PA** and the polynomial alternatives Eq. (4.5), we restrict our attention to how  $\Xi(\lambda)$  depends on  $\lambda$ . However, a direct analysis remains challenging due to the implicit dependence of  $\Theta_2(\lambda)$  on  $\lambda$ . Therefore, we investigate this question numerically by considering representative models.

First, we consider a three-point mixture model for  $F^{\Sigma_p}$  given by

$$A\delta_1 + \frac{1-A}{2}\delta_5 + \frac{1-A}{2}\delta_{15},$$

where  $0 < A < 1$ . In other words,  $\Sigma_p$  has three distinct eigenvalues 1, 5, and 15 with ratio  $A$ ,  $(1-A)/2$  and  $(1-A)/2$ , respectively. For convenience,  $\Sigma_p$  is further scaled to ensure  $\text{tr}(\Sigma_p) = p$ . We consider three canonical settings for  $D$ , namely,  $D = I_p$ ,  $\Sigma_p$ , and  $\Sigma_p^2$ . We explore three settings of  $\gamma_1$  and  $\gamma_2$ , namely  $\gamma_1, \gamma_2 \in \{0.5, 1, 2\}$ . We plot the scaled signal-to-noise ratio  $\Xi(\lambda)$  against  $\lambda$ . The case when  $\gamma_1 = 0.5$  is displayed in Figure 4.1 and Figure 4.2, for two cases of  $A$ , namely  $A = 0.5$  and  $A = 0.9$ . The cases when  $\gamma_1 = 1$  and 2 are displayed in Section S.2 of the Supplementary Material.

The figures indicate that the effect of  $\lambda$  on  $\Xi(\lambda)$  is approximately consistent across different settings of  $\gamma_1$  and  $\gamma_2$ . When  $\Sigma_p$  has a relatively small fraction of leading eigenvalues—corresponding to the case  $A = 0.9$ —a relatively small value of  $\lambda$  is preferred. When  $D$  is aligned with the leading eigen-directions of  $\Sigma_p$  (i.e.,  $D = \Sigma_p$  or  $\Sigma_p^2$ ), a larger value of  $\lambda$  is preferred.

### 4.4 Data-driven selection of $\lambda$

Given a sequence of alternatives as in **PA**, our strategy is to choose  $\lambda$  by maximizing the scaled asymptotic signal-to-noise ratio  $\Xi(\lambda) = \xi(\lambda)/\Theta_2(\lambda)$ . To implement this strategy, a consistent estimator of  $\Xi(\lambda)$  is required. First, the estimator of  $\Theta_2(\lambda)$  is given in Section 3. Recall the two scenarios under **PA** in which  $\xi(\lambda)$  can be

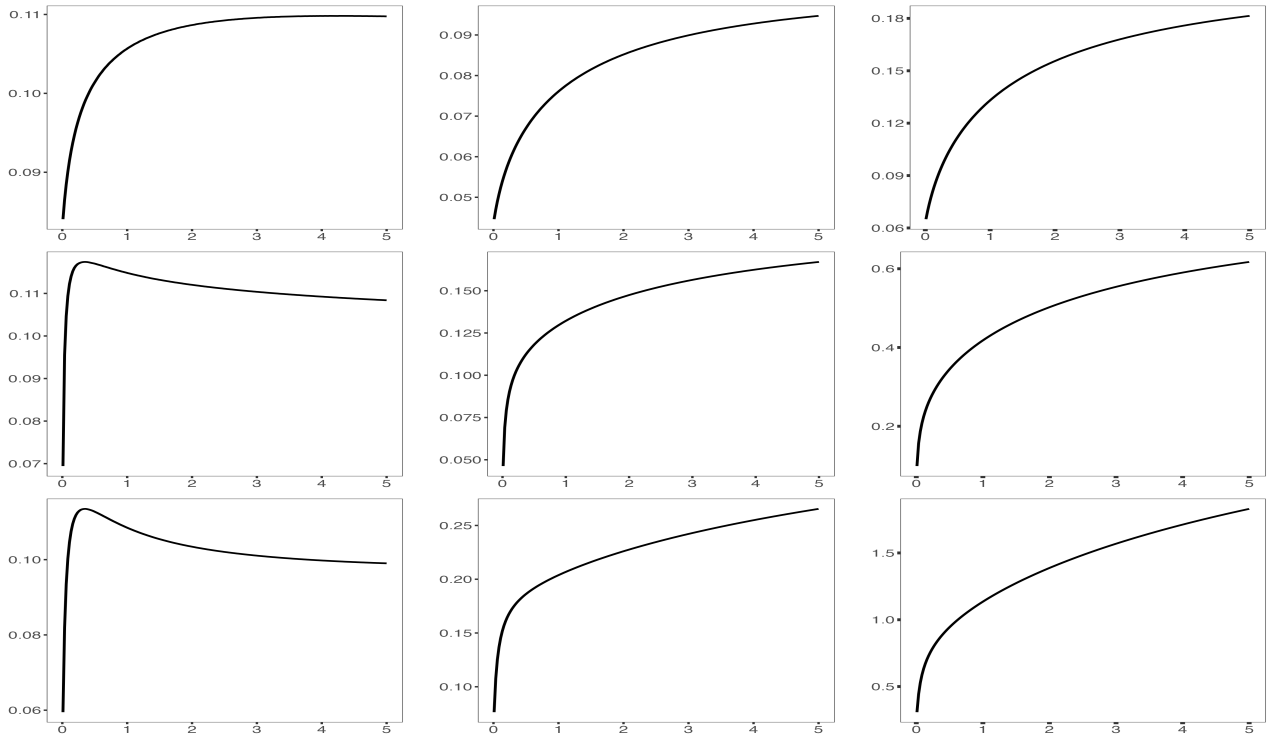


Figure 4.1:  $\Xi(\lambda)$  against  $\lambda$  when  $A = 0.5$  and  $\gamma_1 = 0.5$ . Columns (left-to-right):  $D = I_p, \Sigma_p, \Sigma_p^2$ ; Rows (top-to-bottom):  $\gamma_2 = 0.5, 1, 2$ .

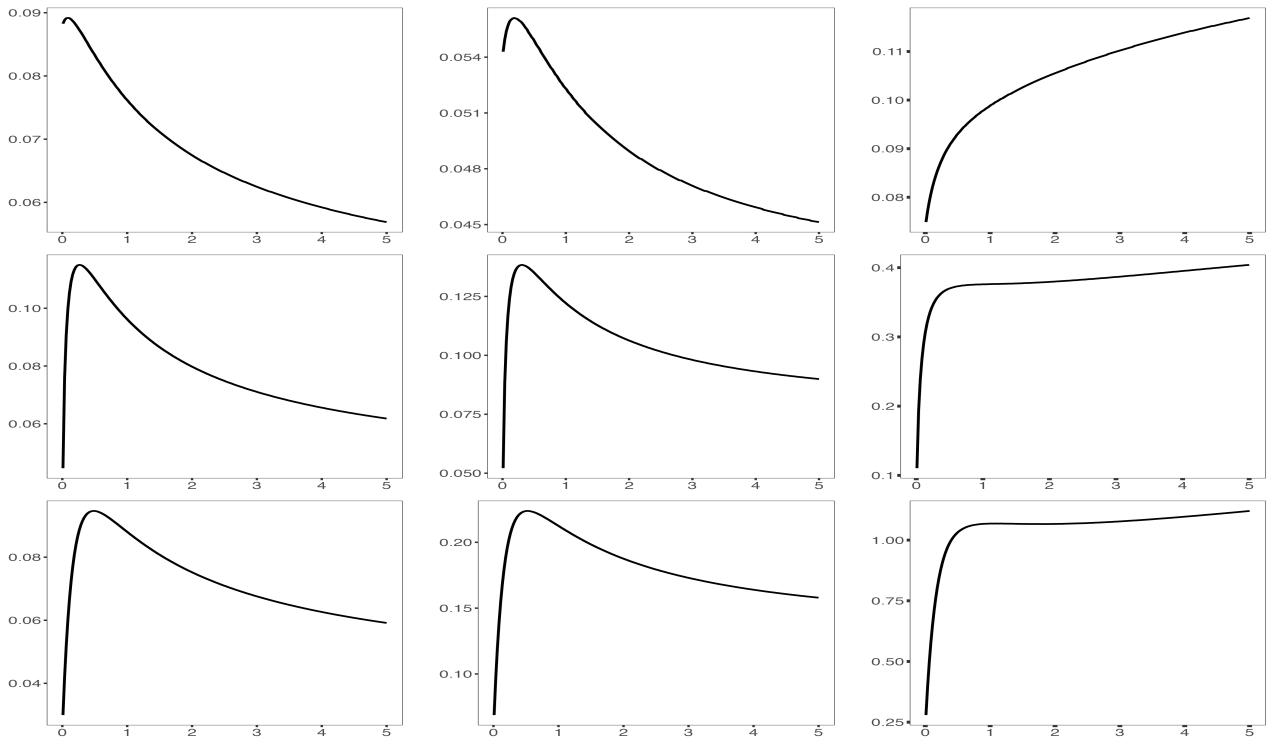


Figure 4.2:  $\Xi(\lambda)$  against  $\lambda$  when  $A = 0.9$  and  $\gamma_1 = 0.5$ . Columns (left-to-right):  $D = I_p, \Sigma_p, \Sigma_p^2$ ; Rows (top-to-bottom):  $\gamma_2 = 0.5, 1, 2$ .

estimated, as introduced in Section 4.2:

- (i) If  $D$  can be fully specified,  $\xi(\lambda)$  is estimated by  $\hat{\xi}(\lambda)$  as in Eq. (4.4).
- (ii) If  $D$  is specified as a polynomial of  $\Sigma_p$  with prior weights  $(\pi_0, \pi_1, \pi_2)$ ,  $\xi(\lambda)$  is estimated as in Eq. (4.6).

In practice, the data-driven selection of the regularization parameter  $\lambda$  is performed by

$$\hat{\lambda}_{\text{opt}} = \arg \max_{\lambda \in [\underline{\lambda}, \bar{\lambda}]} \frac{\hat{\xi}(\lambda)}{\hat{\Theta}_2(\lambda)},$$

where  $[\underline{\lambda}, \bar{\lambda}]$  are user-specified lower and upper bounds. A suggested choice is  $\underline{\lambda} = p^{-1}\text{tr}(\mathbf{W}_2)/50$  and  $\bar{\lambda} = 5p^{-1}\text{tr}(\mathbf{W}_2)$ .

A potential concern arises from the “double-dipping” problem, as we use the same dataset both to select  $\lambda$  and to conduct the test. While Theorem 2.2 indicates that the proposed test statistic with a fixed  $\lambda$  follows an asymptotic Tracy–Widom distribution after appropriate scaling, the data-driven selection of  $\lambda$  introduces additional variation that may alter the asymptotic behavior. However, our simulation studies in Section 5 suggest that this additional variation is limited, and the difference between the distribution of  $\ell_{\max}(\mathbf{F}(\hat{\lambda}_{\text{opt}}))$  and  $\ell_{\max}(\mathbf{F}(\lambda_{\text{opt}}))$  is negligible, where  $\lambda_{\text{opt}}$  is the maximizer of the true limiting  $\Xi(\lambda)$  in  $[\underline{\lambda}, \bar{\lambda}]$ . The reason is that  $\hat{\lambda}_{\text{opt}}$  converges quickly to  $\lambda_{\text{opt}}$  as  $p$  becomes large, since  $\hat{\xi}(\lambda)$  and  $\hat{\Theta}_2(\lambda)$  are consistent estimators. To alleviate the effect of “double-dipping”, an additional data-splitting technique can be applied, where a subset of the data is used for selecting  $\lambda$ , and the remaining data is used to conduct the test.

## 5 Simulation studies

In this section, we evaluate the performance of the proposed ridge-regularized F-matrix framework and the associated estimation methods through Monte Carlo experiments.

### 5.1 Simulation settings and competing methods

The study considers the following configurations:

- (i) The entries of the error matrix  $\mathbf{Z}$  are drawn from normal, t-distributions with 4 degrees of freedom, or Poisson distributions. However, as the results are consistent across these settings, only those for normal errors are reported in the manuscript.
- (ii) With  $n_2 = 500$ , the dimension  $p$  is set to 250, 1000, or 2500, corresponding to  $\hat{\gamma}_2 = 0.5, 2, \text{ and } 5$ .
- (iii) Three cases of  $n_1$  are considered:  $n_1 \in \{100, 250, 500\}$ .

(iv) The eigenvalues  $\tau_j$  of  $\Sigma_p$  are set according to three models:

- (a) *Poly-Decay*:  $\tau_j = 0.01 + (0.1 + p - j)^6$ ,  $j = 1, \dots, p$ , representing polynomial decay.
- (b) *Toeplitz*:  $\Sigma_p$  is a Toeplitz matrix with  $(i, j)$ -th entry  $0.3^{|i-j|}$ , for  $i, j = 1, \dots, p$ .
- (c) *Factor-model*: For  $j \geq 6$ , the eigenvalues  $\tau_j$  match those from the *Poly-Decay* model. The first five eigenvalues are spikes:  $\tau_j = (2.2 - 0.2j)\tau_6$ , for  $j = 1, \dots, 5$ .

All models are further normalized so that  $\text{tr}(\Sigma_p) = p$ . The eigenvector matrix of  $\Sigma_p$  is randomly generated from the Haar distribution on the group of orthogonal matrices.

(v)  $X$  is a  $n_1 \times (n_1 + n_2)$  matrix whose entries are iid  $N(0, 1)$ . The coefficient matrix  $B$  ( $p \times n_1$ ) is assumed to be of low rank with its first column drawn from  $N(0, \zeta^2)$  and all other columns set to zero. The parameter  $\zeta$  controls the signal strength. We test  $H_0 : B = 0$  against  $H_a : B \neq 0$ . That is,  $C = I_{n_1}$ .

The proposed method is compared to representative existing approaches in the literature. As discussed in the Introduction, most relevant methods fall into three broad categories. Since extreme-type tests—such as those by Cai et al. (2014) and Chang et al. (2017)—are not readily applicable to general linear hypotheses, we focus our comparisons on quadratic-form and projection-based tests. For the quadratic-form category, we consider the ridge-regularized likelihood ratio test proposed by Li et al. (2020a), which applies the same ridge regularization but aggregates all eigenvalues of  $\mathbf{F}_\lambda$  using a  $\log(1 + x)$  transformation. Specifically, we adopt the composite procedure recommended in Algorithm 4.2 of Li et al. (2020a), referred to as Ridge-LRT. To benchmark against projection-based methods, we note that most existing projection tests assume  $n_1 \ll p$  and are not directly applicable to the general linear hypothesis setting considered here. Therefore, we construct a baseline procedure, referred to as Proj-LRT, by projecting the observations onto random subspaces of dimension  $\min(n_1, n_2, p)/2$ , followed by applying the likelihood ratio test to the projected data. A composite test is formed by taking the supremum of the test statistics over 20 such projections, with projection matrices generated according to the Haar measure.

Notably, the *Factor-model* represents a setting in which Condition **C5** is violated. Across all simulation settings, the estimators  $\hat{\Theta}_1(\lambda)$  and  $\hat{\Theta}_2(\lambda)$  are computed using Algorithms 1, 2, and 3, implemented with the recommended configurations detailed in Section S.1.

## 5.2 Estimation precision

We begin by evaluating the numerical performance of the proposed estimation method. Figure 5.1 displays the estimated curves  $\hat{s}(x)$ ,  $\hat{s}'(x)$ , and  $\hat{s}''(x)$  under a representative setting. Two additional examples are provided in Section S.3.1 of the Supplementary Material (Figure S.3.1 and S.3.2); other results are omitted due to similar patterns.

The figures demonstrate that the overall estimation accuracy is high, though it declines as  $x$  approaches  $\rho_\lambda$ . This indicates that the estimators  $\hat{\Theta}_1$  and  $\hat{\Theta}_2$  remain accurate unless  $\beta$  is near  $\rho$ . Since  $\beta$  satisfies  $\beta^2 s'(\beta) = 1/\gamma_1$ , it only approaches  $\rho$  when  $\gamma_1$  is small—that is, when  $n_1 \gg p$ . This setting lies outside the high-dimensional regime assumed in **C1**, where  $n_1$  and  $p$  are of the same order.

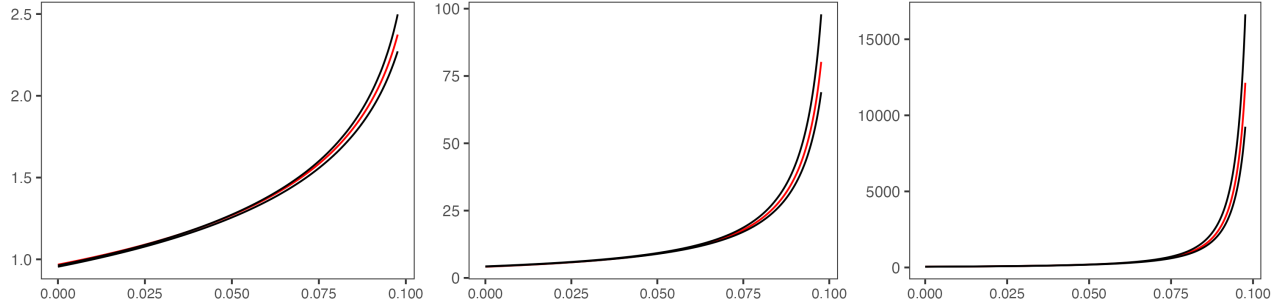


Figure 5.1: The estimated  $s(x)$ ,  $s'(x)$  and  $s''(x)$  (from left to right) when  $\Sigma_p$  is *Poly-Decay*,  $\hat{\gamma}_2 = 5$ ,  $\lambda = 0.5$ . Red: the true functions; Black: 5% and 95% pointwise percentile bands of the estimated functions.

$\Sigma_p$	$\hat{\gamma}_2$	$\lambda$	$n_1 = 500$	$n_1 = 250$	$n_1 = 100$
Poly-Decay	0.5	0.5	0.06 (0.04)	0.05 (0.04)	0.04 (0.03)
		1.0	0.08 (0.06)	0.06 (0.05)	0.05 (0.04)
		1.5	0.10 (0.07)	0.08 (0.06)	0.06 (0.05)
	2.0	0.5	0.10 (0.07)	0.09 (0.06)	0.08 (0.06)
		1.0	0.11 (0.08)	0.09 (0.07)	0.08 (0.06)
		1.5	0.11 (0.09)	0.09 (0.07)	0.07 (0.06)
	5.0	0.5	0.14 (0.10)	0.13 (0.10)	0.13 (0.09)
		1.0	0.14 (0.10)	0.12 (0.09)	0.12 (0.08)
		1.5	0.14 (0.11)	0.12 (0.09)	0.11 (0.08)
Toeplitz	0.5	0.5	0.11 (0.08)	0.09 (0.07)	0.08 (0.06)
		1.0	0.15 (0.11)	0.11 (0.08)	0.08 (0.06)
		1.5	0.19 (0.15)	0.14 (0.11)	0.10 (0.07)
	2.0	0.5	0.16 (0.12)	0.13 (0.09)	0.11 (0.09)
		1.0	0.19 (0.14)	0.13 (0.10)	0.10 (0.08)
		1.5	0.21 (0.16)	0.14 (0.11)	0.10 (0.08)
	5.0	0.5	0.26 (0.19)	0.35 (0.17)	0.15 (0.11)
		1.0	0.24 (0.18)	0.19 (0.13)	0.12 (0.09)
		1.5	0.29 (0.20)	0.18 (0.13)	0.12 (0.09)
Factor	0.5	0.5	0.06 (0.05)	0.06 (0.04)	0.06 (0.04)
		1.0	0.07 (0.06)	0.07 (0.05)	0.05 (0.04)
		1.5	0.09 (0.06)	0.07 (0.06)	0.06 (0.05)
	2.0	0.5	0.10 (0.08)	0.09 (0.07)	0.08 (0.06)
		1.0	0.10 (0.07)	0.09 (0.07)	0.08 (0.06)
		1.5	0.10 (0.08)	0.09 (0.07)	0.08 (0.06)
	5.0	0.5	0.13 (0.10)	0.12 (0.09)	0.13 (0.09)
		1.0	0.13 (0.10)	0.12 (0.09)	0.11 (0.08)
		1.5	0.14 (0.10)	0.12 (0.09)	0.11 (0.08)

Table 5.1: Mean (standard deviation) of  $p^{2/3}|\hat{\Theta}_1 - \Theta_1|/\Theta_2$  under different settings.

Table 5.1 reports the scaled estimation error between  $\hat{\Theta}_1$  and  $\Theta_1$ , while Table 5.2 reports the corresponding error for  $\hat{\Theta}_2$ . Estimation accuracy generally decreases as  $p/n_2$  increases or  $p/n_1$  decreases, but remains within a reasonable range across settings. The choice of  $\lambda$  has little impact on the accuracy. Figure S.3.3 in the Supplementary Material displays the density curves of the estimation errors between  $\hat{\Theta}_1$  and  $\Theta_1$  under a representative setting, showing approximately bell-shaped empirical distributions.

$\Sigma_p$	$\hat{\gamma}_2$	$\lambda$	$n_1 = 500$	$n_1 = 250$	$n_1 = 100$	
Poly-Decay	0.5	0.5	0.14 (0.10)	0.11 (0.09)	0.09 (0.07)	
		1.0	0.18 (0.14)	0.15 (0.11)	0.12 (0.09)	
		1.5	0.27 (0.21)	0.19 (0.15)	0.14 (0.11)	
	2.0	0.5	0.31 (0.23)	0.26 (0.21)	0.23 (0.18)	
		1.0	0.36 (0.28)	0.28 (0.20)	0.25 (0.19)	
		1.5	0.46 (0.36)	0.32 (0.25)	0.25 (0.19)	
	5.0	0.5	0.83 (0.61)	0.52 (0.40)	0.40 (0.31)	
		1.0	0.90 (0.68)	0.61 (0.46)	0.42 (0.33)	
		1.5	1.05 (0.77)	0.70 (0.53)	0.46 (0.35)	
	Toeplitz	0.5	0.5	0.18 (0.13)	0.13 (0.10)	0.10 (0.08)
			1.0	0.35 (0.27)	0.21 (0.16)	0.14 (0.10)
			1.5	0.59 (0.44)	0.31 (0.23)	0.18 (0.14)
2.0		0.5	0.66 (0.48)	0.36 (0.27)	0.29 (0.22)	
		1.0	0.89 (0.69)	0.45 (0.34)	0.31 (0.23)	
		1.5	1.19 (0.93)	0.55 (0.41)	0.35 (0.25)	
5.0		0.5	4.00 (2.32)	2.65 (0.64)	1.16 (0.46)	
		1.0	5.67 (3.43)	1.16 (0.81)	0.42 (0.33)	
		1.5	5.01 (3.41)	0.96 (0.72)	0.52 (0.39)	
Factor		0.50	0.50	0.15 (0.12)	0.19 (0.10)	0.14 (0.10)
			1.0	0.37 (0.18)	0.21 (0.16)	0.15 (0.11)
			1.5	0.35 (0.27)	0.34 (0.21)	0.21 (0.15)
	2.0	0.5	0.34 (0.25)	0.25 (0.19)	0.27 (0.19)	
		1.0	0.38 (0.28)	0.32 (0.23)	0.25 (0.19)	
		1.5	0.45 (0.34)	0.32 (0.24)	0.29 (0.22)	
	5.0	0.5	0.74 (0.55)	0.48 (0.37)	0.37 (0.28)	
		1.0	0.85 (0.63)	0.59 (0.44)	0.44 (0.33)	
		1.5	1.05 (0.77)	0.61 (0.46)	0.46 (0.35)	

Table 5.2: Mean (standard deviation) of  $p^{2/3}|\hat{\Theta}_2 - \Theta_2|/\Theta_2$  under different settings.

### 5.3 Empirical null distribution

In this section, we examine the empirical distribution of the ridge-regularized largest root under the null hypothesis. We consider five choices for the regularization parameter  $\lambda$ : fixed values  $\lambda = 0.5, 1$ , and  $1.5$ , as well as two data-driven values selected as the empirical optima when  $D = I_p$  and  $D = \Sigma_p$ , respectively. The latter two are denoted as  $\hat{\lambda}_{I_p}$  and  $\hat{\lambda}_{\Sigma_p}$ , respectively.

Figure 5.2 presents the empirical density of the regularized largest root  $\ell_{\max}(\mathbf{F}_\lambda)$  for  $\lambda = \hat{\lambda}_{\Sigma_p}$ . Results for other values of  $\lambda$  are provided in Section S.3.2 of the Supplementary Material. Densities are shown under two

standardizations: using the true values of  $\Theta_1(\lambda)$  and  $\Theta_2(\lambda)$ , and using their estimates  $\hat{\Theta}_1(\lambda)$  and  $\hat{\Theta}_2(\lambda)$ . In both cases, the empirical distributions closely match the Tracy–Widom law of type 1, confirming the validity of the asymptotic theory and the accuracy of the proposed estimators. This pattern holds across all five choices of  $\lambda$ , whether fixed or data-driven.

Table 5.3 reports the empirical sizes at the asymptotic 5% level for the decision rule  $\tilde{\ell}(\lambda) > \text{TW}_1(0.95)$ , where  $\tilde{\ell}(\lambda)$  is the normalized largest root based on  $\hat{\Theta}_1$  and  $\hat{\Theta}_2$ . The results indicate that empirical sizes are consistently close to the nominal level, generally falling within the range of 3%–6.5%. The sizes remain stable across different choices of  $\lambda$ ,  $\hat{\gamma}_1$ ,  $\hat{\gamma}_2$ , and covariance structures, demonstrating the robustness of the proposed test under the null.

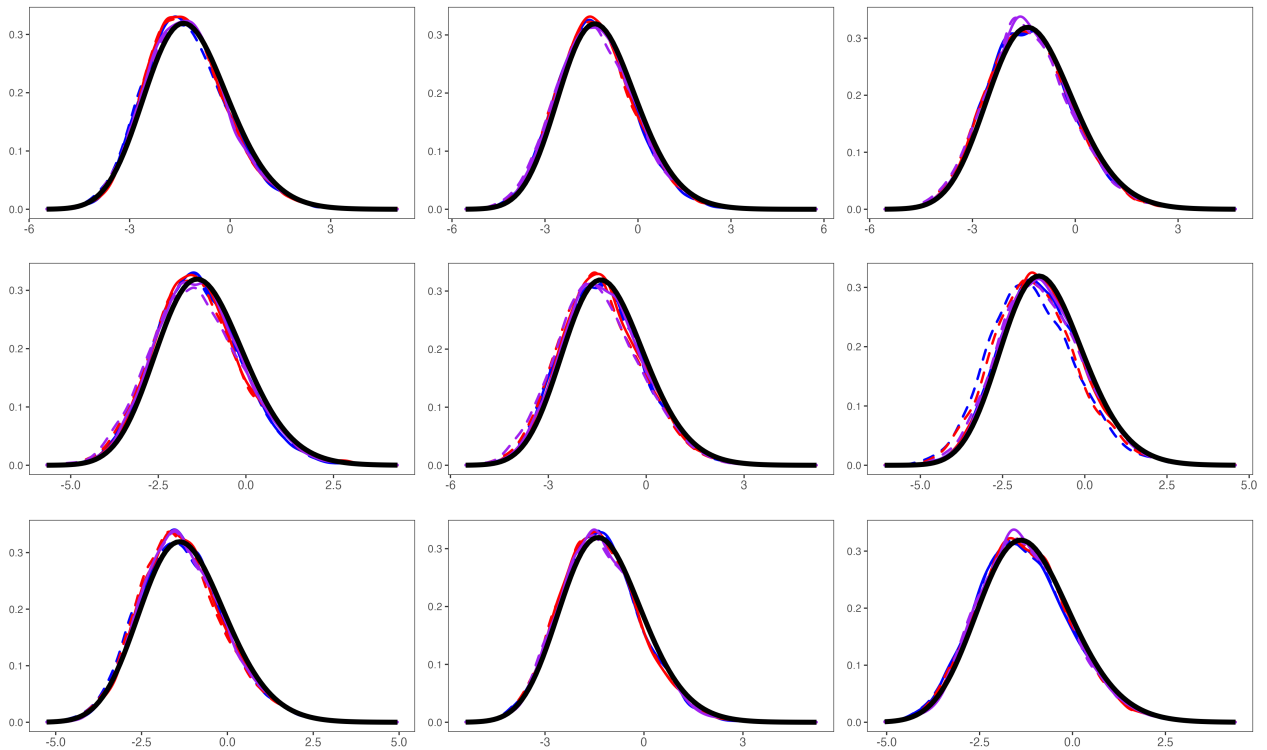


Figure 5.2: Empirical density of  $\ell_{\max}(\mathbf{F}_\lambda)$  with  $\lambda = \hat{\lambda}_{\Sigma_p}$ . Solid lines use true parameters for normalization; dashed lines use estimated ones. Colors indicate  $n_1$ : blue = 100, red = 250, purple = 500. Columns (left to right) correspond to  $\hat{\gamma}_2 = 0.5, 2, \text{ and } 5$ ; rows (top to bottom) correspond to  $\Sigma_p$  models: Poly-Decay, Toeplitz, and Factor. Black line: PDF of  $\text{TW}_1$  (baseline).

## 5.4 Empirical power

In this section, we evaluate the empirical power of the proposed tests and compare them with Ridge-LRT and Proj-LRT. Figure 5.3 presents power curves against the signal strength parameter  $\zeta$  under the Poly-Decay setting; results for other settings are provided in Section S.3.3 of the Supplementary Material. To ensure a fair

Size $\times 100\%$ , $n_2 = 500$			$\hat{\gamma}_2 = 0.5$			$\hat{\gamma}_2 = 2$			$\hat{\gamma}_2 = 5$		
$\Sigma$	$\lambda$	$n_1 =$	100	250	500	100	250	500	100	250	500
Poly-Decay	0.5		4.78	3.86	3.86	5.42	5.14	4.66	5.14	5.14	5.44
	1		4.52	3.76	3.92	5.24	4.60	4.16	4.74	4.80	5.16
	1.5		4.44	3.66	3.90	4.88	4.52	4.10	4.52	4.54	5.06
	$\hat{\lambda}_{I_p}$		5.04	4.34	4.26	6.30	6.40	5.20	5.02	5.62	6.20
	$\hat{\lambda}_{\Sigma_p}$		4.82	4.32	4.26	4.34	4.34	3.88	4.08	3.98	4.40
Toeplitz	0.5		4.48	5.16	4.16	4.38	4.28	5.00	3.62	3.30	4.10
	1		4.12	4.84	3.92	3.90	3.88	4.66	3.92	3.22	3.68
	1.5		4.08	4.56	3.92	3.86	4.10	4.54	4.16	3.40	3.50
	$\hat{\lambda}_{I_p}$		4.58	4.62	3.72	3.90	3.76	4.48	4.26	3.88	3.16
	$\hat{\lambda}_{\Sigma_p}$		4.38	4.48	3.56	3.94	3.80	4.48	4.32	3.88	3.16
Factor	0.5		4.46	4.54	4.44	5.38	4.96	4.96	5.12	5.66	5.10
	1		4.06	3.96	4.08	4.94	4.60	4.78	4.82	5.56	4.92
	1.5		4.10	4.06	3.88	4.28	4.50	4.34	4.72	5.22	4.92
	$\hat{\lambda}_{I_p}$		4.26	4.28	4.46	6.10	6.48	6.50	5.24	5.90	5.84
	$\hat{\lambda}_{\Sigma_p}$		4.74	4.28	4.52	3.98	4.26	3.60	3.86	4.00	4.40

Table 5.3: Empirical sizes of empirically normalized  $\ell_{\max}(\mathbf{F}_\lambda)$  at asymptotic level 5% under different settings.

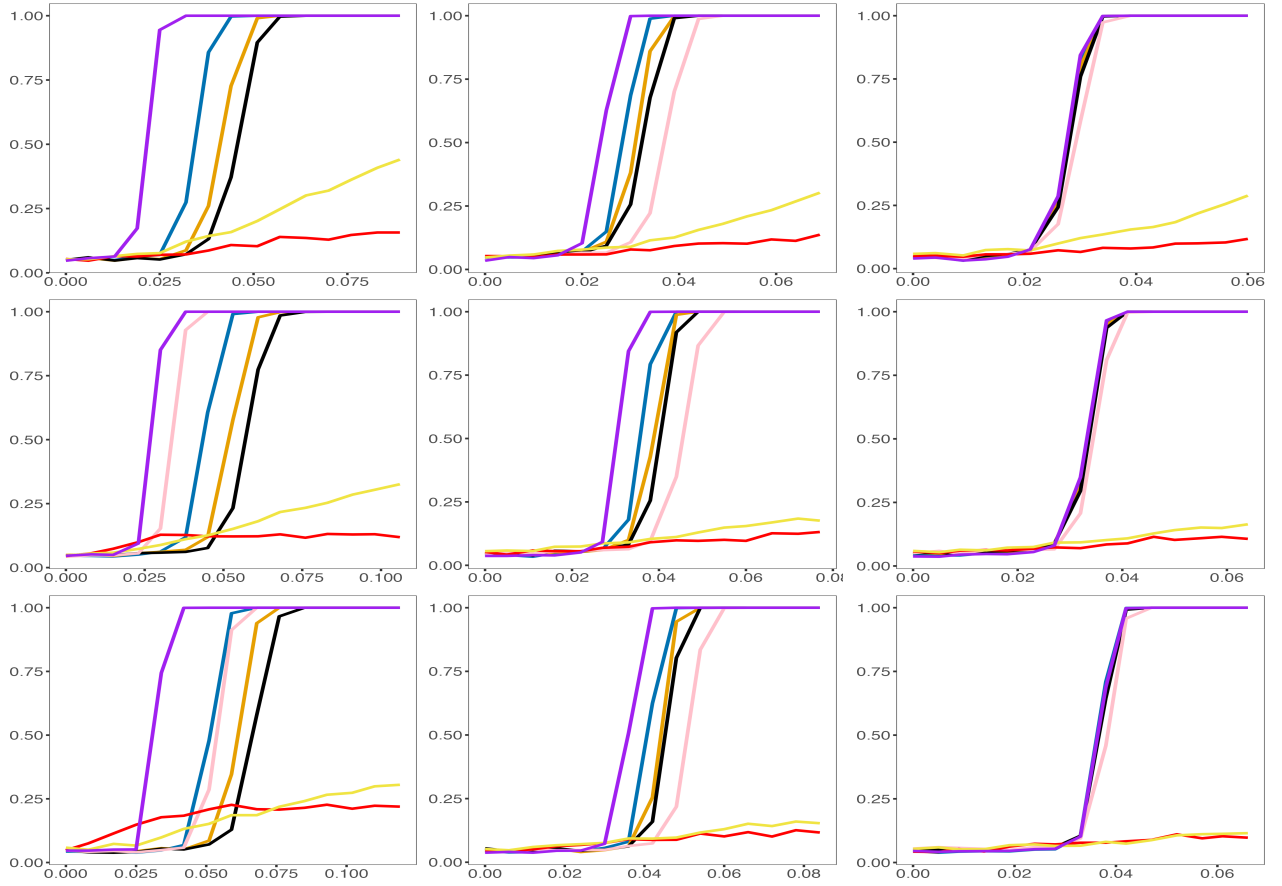


Figure 5.3: Size-adjusted empirical power when  $\Sigma$  is Poly-Decay. Columns (left to right):  $\hat{\gamma}_2 = 0.5, 2, 5$ . Rows (top to bottom):  $n_1 = 100, 250, 500$ . Blue:  $\lambda = 0.5$ ; Orange:  $\lambda = 1$ ; Black:  $\lambda = 1.5$ ; Purple:  $\lambda = \hat{\lambda}_{I_p}$ ; Pink:  $\lambda = \hat{\lambda}_{\Sigma_p}$ ; Red: Proj-LRT; Yellow: Ridge-LRT.

comparison, all power curves are adjusted using size-corrected cutoffs derived from each test’s empirical null distribution via simulation. Results based on asymptotic cutoffs are similar and therefore omitted for brevity.

The proposed methods demonstrate substantially higher power than Ridge-LRT and Proj-LRT across all simulation settings, highlighting their effectiveness in detecting concentrated alternatives. Notably, the empirical power curves of the proposed tests exhibit a sharp “jump” as  $\zeta$  increases, reflecting the transition from an undetectable regime—where the signal is overwhelmed by noise—to one where the signal becomes identifiable. In contrast, Ridge-LRT and Proj-LRT show a more gradual increase in power with growing signal strength.

Under the alternative model in Setting (v), the matrix  $BC$  can be viewed as a generalization of the **PA** model (4.5) with  $D = I_p$ . Accordingly,  $\lambda = \hat{\lambda}_{I_p}$  corresponds to the data-driven optimal regularization parameter under the correctly specified prior, while  $\hat{\lambda}_{\Sigma_p}$  reflects the case of prior misspecification. When  $p$  is small and the eigenvalues of  $\Sigma_p$  are dispersed (e.g., Poly-Decay and Factor models), the proposed test with  $\lambda = \hat{\lambda}_{I_p}$  consistently achieves the highest power among all choices. As  $p$  increases, or when the eigenvalues of  $\Sigma_p$  are more concentrated—as in the Toeplitz model—the performances under different  $\lambda$  values become comparable. Overall, the proposed test is not overly sensitive to the choice of  $\lambda$ .

Lastly, the power of the proposed methods remains stable across varying  $n_1$ , whereas increasing  $n_1$  leads to a noticeable decline in power for Proj-LRT and Ridge-LRT. This underscores the advantage of the proposed methods in settings involving the simultaneous testing of many linear hypotheses.

## 6 Real data analysis

The Human Connectome Project (HCP), funded by the National Institutes of Health (NIH), aims to map the neural pathways that underlie human brain function and behavior. A consortium led by Washington University in St. Louis and the University of Minnesota has collected extensive neuroimaging and behavioral data from  $n_T = 1,113$  healthy young adults aged 22 to 35. This dataset facilitates detailed analyses of brain circuits and their relationships to behavior and genetics. Among the publicly available data are cerebral volumetric measurements and various behavioral evaluation scores. In this section, we utilize the proposed tests to investigate the associations between cerebral measurements and behavioral variables using the HCP dataset.

The behavioral evaluation scores in the HCP dataset encompass several domains, including cognition, emotion, sensation, and motor functions. The cognition domain assesses various cognitive abilities such as episodic memory, cognitive flexibility, and attention control. The emotion domain includes measures of psychological well-being, social relationships, stress, and self-efficacy. The sensation domain comprises tests related to audi-

tion, olfaction, taste, and vision. The motor domain evaluates aspects like cardiovascular endurance, manual dexterity, grip strength, and gait speed. After a pre-screening process to filter out highly correlated variables, we selected  $p = 127$  representative behavioral variables to study their associations with cerebral measurements.

Cerebral measurements were obtained for 68 cortical surface regions, assessing surface area, cortical thickness, and gray matter volume. These regions are distributed across 14 cerebral lobes symmetrically located in both hemispheres, resulting in a total of 204 cortical surface variables (68 regions  $\times$  3 measurement types). Additionally, each voxel in the brain’s subcortical structures was assigned one of 44 labels, with the volume of each labeled region measured, yielding 44 subcortical variables. Four labels were excluded from the analysis due to a high proportion of missing values.

Available demographics information includes the age and gender of subjects. Specifically, the subjects are divided into four age groups, namely 22–25, 26–30, 31–35, and 36+. The data set is roughly balanced with respect to gender as the 1113 subjects consist of 606 females and 507 males.

Specifically, we consider the following multivariate regression model:

$$Y_i = \beta_0 + \beta_1^T \mathbf{L}_{1i} + \cdots + \beta_{14}^T \mathbf{L}_{14,i} + \beta_{15}^T \mathbf{SC}_i + \beta_{16}^T \mathbf{D}_i + \Sigma_p^{1/2} Z_i. \quad (6.1)$$

where (i)  $Y_i$  is the vector of 127 behavioral scores of subject  $i$ ; (ii)  $\mathbf{L}_{ji}$  ( $j = 1, \dots, 14$ ) represents the cerebral measurements vector of the surface regions belonging to lobe  $j$  for subject  $i$ , with dimensions varying from 3 to 33 depending on the lobe. The variables are of 3 types: surface area, cortical thickness and gray matter volume; (iii)  $\mathbf{SC}_i$  contains the volume measurements of 40 subcortical regions of subject  $i$ ; (iv)  $\mathbf{D}_i$  are age and gender group dummy variables of subject  $i$ . This model allows us to assess the associations between various cerebral measurements and behavioral outcomes while accounting for demographic variables. The dimension of the explanatory variables (including the intercept) is  $m = 249$ , the dimension of response  $Y_i$  is  $p = 127$  and the sample size is  $n_T = 1113$ . We are interested in testing the joint significance of all variables associated with each cerebral lobe. Namely, we test  $H_0 : \beta_j = 0$  against  $H_a : \beta_j \neq 0$ , for each  $j = 1, \dots, 14$ . The proposed test procedure is applied with five choices of  $\lambda$ :  $0.5\bar{\tau}$ ,  $\bar{\tau}$ ,  $1.5\bar{\tau}$ , the data-driven choice of  $\lambda$  described in Section 4.4 with  $D = I_p$  and when  $D = \Sigma_p$ . The latter two are referred to as  $\hat{\lambda}_{I_p}$  and  $\hat{\lambda}_{\Sigma_p}$ , respectively. Here,  $\bar{\tau}$  is the average of eigenvalues of  $\mathbf{W}_2$ . The p-values are reported in Table 6.1

Among the significant coefficients at 90% level detected by the proposed tests with at least one choice of  $\lambda$  are left medial temporal lobe, right frontal lobe and left parietal lobe. Similar results are reported in the literature, for example Li et al. (2024). The left medial temporal lobe, encompassing structures such as the hippocampus and parahippocampal gyrus, plays a pivotal role in memory formation and retrieval. Damage to the lobe has been associated with impairments in verbal memory tasks, indicating its importance in processing

Lobe name	$\lambda = 0.5\bar{\tau}$	$\lambda = \bar{\tau}$	$\lambda = 1.5\bar{\tau}$	$\lambda = \hat{\lambda}_{I_p}$	$\lambda = \hat{\lambda}_{\Sigma_p}$
Left Temporal Lobe Medial Aspect	0.070	0.020	0.009	0.070	0.070
Right Temporal Lobe Medial Aspect	0.435	0.565	0.637	0.435	0.435
Left Temporal Lobe Lateral Aspect	0.723	0.766	0.760	0.723	0.723
Right Temporal Lobe Lateral Aspect	0.085	0.035	0.022	0.085	0.085
Left Frontal Lobe	0.658	0.585	0.579	0.658	0.658
Right Frontal Lobe	0.010	0.001	0.001	0.010	0.010
Left Parietal Lobe	0.108	0.056	0.045	0.108	0.108
Right Parietal Lobe	0.365	0.337	0.338	0.365	0.365
Left Occipital Lobe	0.786	0.759	0.725	0.786	0.786
Right Occipital Lobe	0.204	0.357	0.357	0.204	0.204
Left Cingulate Cortex	0.252	0.252	0.285	0.252	0.252
Right Cingulate Cortex	0.153	0.094	0.086	0.153	0.153
Left Insula	0.164	0.210	0.266	0.164	0.164
Right Insula	0.185	0.244	0.291	0.185	0.185

Table 6.1: P-values: Joint significance tests of 14 lobes.

verbal material. Functional connectivity within the lobe is crucial for cognitive functions like episodic memory.

The frontal lobes, located directly behind the forehead, are the largest lobes in the human brain and are essential for voluntary movement, expressive language, and higher-level executive functions. These executive functions encompass a range of cognitive abilities, including planning, organizing, initiating, self-monitoring, and controlling responses to achieve specific goals. Damage to the frontal lobe can result in impairments in these areas, affecting one’s ability to perform tasks that require these skills.

The parietal lobe, situated behind the frontal lobe, plays a pivotal role in integrating sensory information from various parts of the body. It is responsible for processing touch, temperature, pressure, and pain sensations. Additionally, the left parietal lobe is involved in controlling skilled motor actions and is associated with numerical processing and language functions. Damage to this area can lead to difficulties in these domains, affecting one’s ability to perform tasks that require these skills.

## 7 Discussion

In this paper, we proposed a powerful and computationally efficient largest-root test for high-dimensional general linear hypotheses, based on a ridge-regularized  $F$ -matrix. Leveraging tools from Random Matrix Theory, we established that, under the null hypothesis, the largest eigenvalue follows an asymptotic Tracy–Widom distribution after appropriate scaling, in regimes where the dimension is comparable to the effective sample size and the number of hypotheses. We developed a consistent and efficient procedure for estimating the scaling parameters, relying solely on the empirical eigenvalues of the test matrices and without requiring structural assumptions. The power of the test and the influence of the regularization parameter were analyzed under a class of rank-one alternatives. Extensive simulation studies demonstrate that the proposed test maintains

well-controlled type I error rates and exhibits strong power across diverse settings. Furthermore, the method is robust to variations in covariance structure and data distributions, underscoring its practical utility in high-dimensional hypothesis testing.

Several promising research directions can be pursued to extend the current work. From a technical standpoint, our analysis assumes regular stability properties for the leading eigenvalues of the population covariance matrix. This excludes important models such as classical factor models, where a finite number of eigenvalues are well-separated from the bulk. Nevertheless, simulation results suggest that the proposed methodology may still perform well in such settings. Establishing rigorous theoretical guarantees under factor models is a valuable direction for future research. Another avenue is the integration of the proposed test with variable screening techniques to enable application in ultra-high-dimensional regimes, where  $p$  grows substantially faster than the sample sizes. By reducing dimensionality prior to testing, such an approach could improve computational efficiency while preserving statistical power.

## Supplementary Material

The Supplementary Material includes implementation details for Algorithms 1, 2, and 3, additional simulation results, and detailed proofs of the technical results presented in the paper.

## References

- Alex Bloemendal, László Erdős, Antti Knowles, Horng-Tzer Yau, and Jun Yin (2014). Isotropic local laws for sample covariance and generalized Wigner matrices. *Electronic Journal of Probability*, 19(33):1–53.
- Anderson, T. W. (1958). *An introduction to multivariate statistical analysis*, volume 2. Wiley New York.
- Bai, Z., Chen, J., and Yao, J. (2010). On estimation of the population spectral distribution from a high-dimensional sample covariance matrix. *Australian & New Zealand Journal of Statistics*, 52(4):423–437.
- Bai, Z. and Saranadasa, H. (1996). Effect of high dimension: by an example of a two sample problem. *Statistica Sinica*, 6:311–329.
- Bai, Z. and Silverstein, J. W. (1998). No eigenvalues outside the support of the limiting spectral distribution of large-dimensional sample covariance matrices. *The Annals of Probability*, 26(1):316–345.
- Bai, Z. and Silverstein, J. W. (2004). CLT for linear spectral statistics of large-dimensional sample covariance matrices. *The Annals of Probability*, 32(1A):553–605.
- Bai, Z. and Silverstein, J. W. (2010). *Spectral Analysis of Large Dimensional Random Matrices*. Springer.

- Bao, Z., Pan, G., and Wang, Z. (2015). Universality for the largest eigenvalue of sample covariance matrices with general population. *The Annals of Statistics*, 43(1):382–421.
- Bao, Z., Pan, G., and Zhou, W. (2014). Local density of the spectrum on the edge for sample covariance matrices with general population. *Manuscript (preprint)*. Available as PDF from NTU and NUS.
- Bobkov, S. G. (2016). Proximity of probability distributions in terms of Fourier–Stieltjes transforms. *Russian Mathematical Surveys*, 71(6):1021.
- Cai, T. T., Liu, W., and Xia, Y. (2014). Two-sample test of high dimensional means under dependence. *Journal of the Royal Statistical Society: Series B (Statistical Methodology)*, 76(2):349–372.
- Chang, J., Zheng, C., Zhou, W., and Zhou, W. (2017). Simulation-based hypothesis testing of high dimensional means under covariance heterogeneity. *Biometrics*, 73(4):1300–1310.
- Chen, S. X., Li, J., and Zhong, P.-S. (2014). Two-sample tests for high dimensional means with thresholding and data transformation. *arXiv preprint arXiv:1410.2848*.
- Chen, S. X. and Qin, Y.-L. (2010). A two-sample test for high-dimensional data with applications to gene-set testing. *The Annals of Statistics*, 38(2):808–835.
- Dieng, M. (2006). A MATLAB package for computing Tracy–Widom distribution and simulating random matrices. *RMLab. 2006*.
- El Karoui, N. (2007). Tracy–Widom limit for the largest eigenvalue of a large class of complex sample covariance matrices. *The Annals of Probability*, 35(2):663–714.
- El Karoui, N. (2008). Spectrum estimation for large dimensional covariance matrices using random matrix theory. *The Annals of Statistics*, 36(6):2757–2790.
- El Karoui, N. and Kösters, H. (2011). Geometric sensitivity of random matrix results: consequences for shrinkage estimators of covariance and related statistical methods. *arXiv preprint arXiv:1105.1404*.
- Erdős, L., Yau, H.-T., and Yin, J. (2012). Rigidity of eigenvalues of generalized Wigner matrices. *Advances in Mathematics*, 229(3):1435–1515.
- Erdős, L., Knowles, A., Yau, H.-T., and Yin, J. (2013). The local semicircle law for a general class of random matrices. *Electronic Journal of Probability*, 18:1–58.
- Han, X., Pan, G., and Yang, Q. (2018). A unified matrix model including both CCA and F matrices in multivariate analysis: the largest eigenvalue and its applications. *Bernoulli*, 24(4B):3447–3468.

- Han, X., Pan, G., and Zhang, B. (2016). The Tracy–Widom law for the largest eigenvalue of F type matrices. *The Annals of Statistics*, 44(4):1564–1592.
- He, Y., Jiang, T., Wen, J., and Xu, G. (2021). Likelihood ratio test in multivariate linear regression: From low to high dimension. *Statistica Sinica*, 31(3):1215–1238.
- Hu, J., Bai, Z., Wang, C., and Wang, W. (2017). On testing the equality of high dimensional mean vectors with unequal covariance matrices. *Annals of the Institute of Statistical Mathematics*, 69(2):365–387.
- Huang, Y., Li, C., Li, R., and Yang, S. (2022). An overview of tests on high-dimensional means. *Journal of multivariate analysis*, 188:104813.
- Johnstone, I. M. (2008). Multivariate analysis and jacobi ensembles: Largest eigenvalue, Tracy–Widom limits and rates of convergence. *Annals of statistics*, 36(6):2638.
- Johnstone, I. M., Ma, Z., Perry, P. O., and Shahram, M. (2022). *RMTstat: Distributions, Statistics and Tests derived from Random Matrix Theory*. R package version 0.3.1.
- Knowles, A. and Yin, J. (2017). Anisotropic local laws for random matrices. *Probability Theory and Related Fields*, 169:257–352.
- Ledoit, O. and Péché, S. (2011). Eigenvectors of some large sample covariance matrix ensembles. *Probability Theory and Related Fields*, 151(1):233–264.
- Ledoit, O. and Wolf, M. (2012). Nonlinear shrinkage estimation of large-dimensional covariance matrices. *The Annals of Statistics*, 40(2):1024–1060.
- Lee, J. O. and Schnelli, K. (2016). Tracy–Widom distribution for the largest eigenvalue of real sample covariance matrices with general population. *The Annals of Applied Probability*, 26(6):3786–3839.
- Li, H. (2024). Analysis of the limiting spectral distribution of large random matrices of the Marčenko–Pastur type. *Random Matrices: Theory and Applications*, 0(0):2550007.
- Li, H., Aue, A., and Paul, D. (2020a). High-dimensional general linear hypothesis tests via non-linear spectral shrinkage. *Bernoulli*, 26(4):2541–2571.
- Li, H., Aue, A., Paul, D., and Peng, J. (2024). Testing general linear hypotheses under a high-dimensional multivariate regression model with spiked noise covariance. *Journal of the American Statistical Association*, 119(548):2799–2810.
- Li, H., Aue, A., Paul, D., Peng, J., and Wang, P. (2020b). An adaptable generalization of Hotelling’s  $T^2$  test in high dimension. *The Annals of Statistics*, 48(3):1815–1847.

- Li, R. and Li, C. (2022). Linear hypothesis testing in linear models with high-dimensional responses. *Journal of the American Statistical Association*, 117(540):1738–1750.
- Liu, W., Yu, X., Zhong, W., and Li, R. (2024). Projection test for mean vector in high dimensions. *Journal of the American Statistical Association*, 119(545):744–756.
- Lopes, M., Jacob, L., and Wainwright, M. J. (2011). A more powerful two-sample test in high dimensions using random projection. In *Advances in Neural Information Processing Systems*, pages 1206–1214.
- Muirhead, R. J. (2009). *Aspects of multivariate statistical theory*, volume 197. John Wiley & Sons.
- Pillai, N. S. and Yin, J. (2014). Universality of covariance matrices. *Annals of Applied Probability*, 24(3):935–1001.
- Silverstein, J. W. and Bai, Z. (1995). On the empirical distribution of eigenvalues of a class of large dimensional random matrices. *Journal of Multivariate analysis*, 54(2):175–192.
- Silverstein, J. W. and Choi, S.-I. (1995). Analysis of the limiting spectral distribution of large dimensional random matrices. *Journal of Multivariate Analysis*, 54(2):295–309.
- Srivastava, M. S. and Fujikoshi, Y. (2006). Multivariate analysis of variance with fewer observations than the dimension. *Journal of Multivariate Analysis*, 97(9):1927–1940.
- Tracy, C. A. and Widom, H. (1994). Level-spacing distributions and the Airy kernel. *Communications in Mathematical Physics*, 159(1):151–174.
- Tracy, C. A. and Widom, H. (1996). On orthogonal and symplectic matrix ensembles. *Communications in Mathematical Physics*, 177(3):727–754.
- Xu, G., Lin, L., Wei, P., and Pan, W. (2016). An adaptive two-sample test for high-dimensional means. *Biometrika*, 103(3):609–624.
- Yamada, T. and Himeno, T. (2015). Testing homogeneity of mean vectors under heteroscedasticity in high-dimension. *Journal of Multivariate Analysis*, 139:7–27.

**Supplementary Material to**  
**“Ridge-regularized Largest Root Test for High-Dimensional**  
**General Linear Hypotheses”**

Haoran Li

Department of Mathematics and Statistics  
Auburn University

This Supplementary Material is organized as follows.

Section S.1 provides additional implementation details of the estimation algorithms.

Section S.2 shows additional results from the numerical study in Section 4.

Section S.3 presents supplementary results from the simulation studies.

Section S.4 introduces essential notations, definitions, and tools used in the proofs.

Section S.5 establishes key properties of the matrix  $\mathbf{G}_\lambda = \mathbf{Z}U_2U_2^T\mathbf{Z}^T + \lambda\Sigma_p^{-1}$  under Gaussianity.

Section S.6 establishes the proof of the main Theorem 2.2.

Section S.7 establishes the proof of Theorem 3.2, Lemma 3.3, and Lemma 3.4.

Section S.8 shows the proof of Lemma 4.1, Corollary 4.1, Lemma 4.2 and Corollary 4.2.

Section S.9 shows the proof of other technical results.

## S.1 Implementation details of Algorithm 1, Algorithm 2, and Algorithm 3

*Implementation details for Algorithm 1.* The recommended choice of the grid  $\{\sigma_k\}_{k=1}^K$  is equally spaced on  $[\tilde{\ell}_{n_2}, \tilde{\ell}_1]$ , with  $K \approx 500$ . The choice of  $K$  strikes a balance between computational efficiency and estimation accuracy. The recommended choice of  $\{z_i\}_{i=1}^I$  is such that  $\Re(\hat{\varphi}(z_i))$  are evenly spaced on  $[\hat{\varphi}(1.05\tilde{\ell}_1), \hat{\varphi}(-\lambda)]$ , and  $\Im(\hat{\varphi}(z_i)) = 10^{-2} \times \tilde{\ell}_1^{-1}$ . We can first select  $\hat{\varphi}(z_i)$  and numerically find the corresponding  $z_i$  using optimization methods like Newton-Raphson. While more points improve accuracy, we recommend setting  $I \approx 500$  to balance computational efficiency and estimation precision. Traditional linear programming solvers can be used for implementation. In our simulation, we utilize the R package `Rglpk`, which implements the GNU Linear Programming Kit. With the recommended settings, the problem can be efficiently handled on a typical PC ( $\leq 10$  seconds).

*Implementation details for Algorithm 3.* The proposed ODE requires high accuracy on the initial condition  $\hat{s}(0)$ . We propose using Newton-Raphson method to find  $\hat{s}(0)$ , starting from the initial point  $1/(\lambda\hat{\gamma}_2\hat{\varphi}(-\lambda)) - 1/\hat{\gamma}_2$ . The ODE can then be solved by traditional numerical methods such as the fourth-order Runge-Kutta method (RK4). In our simulation studies, the R package `deSolve` is used for implementation.

## S.2 Power analysis: additional details

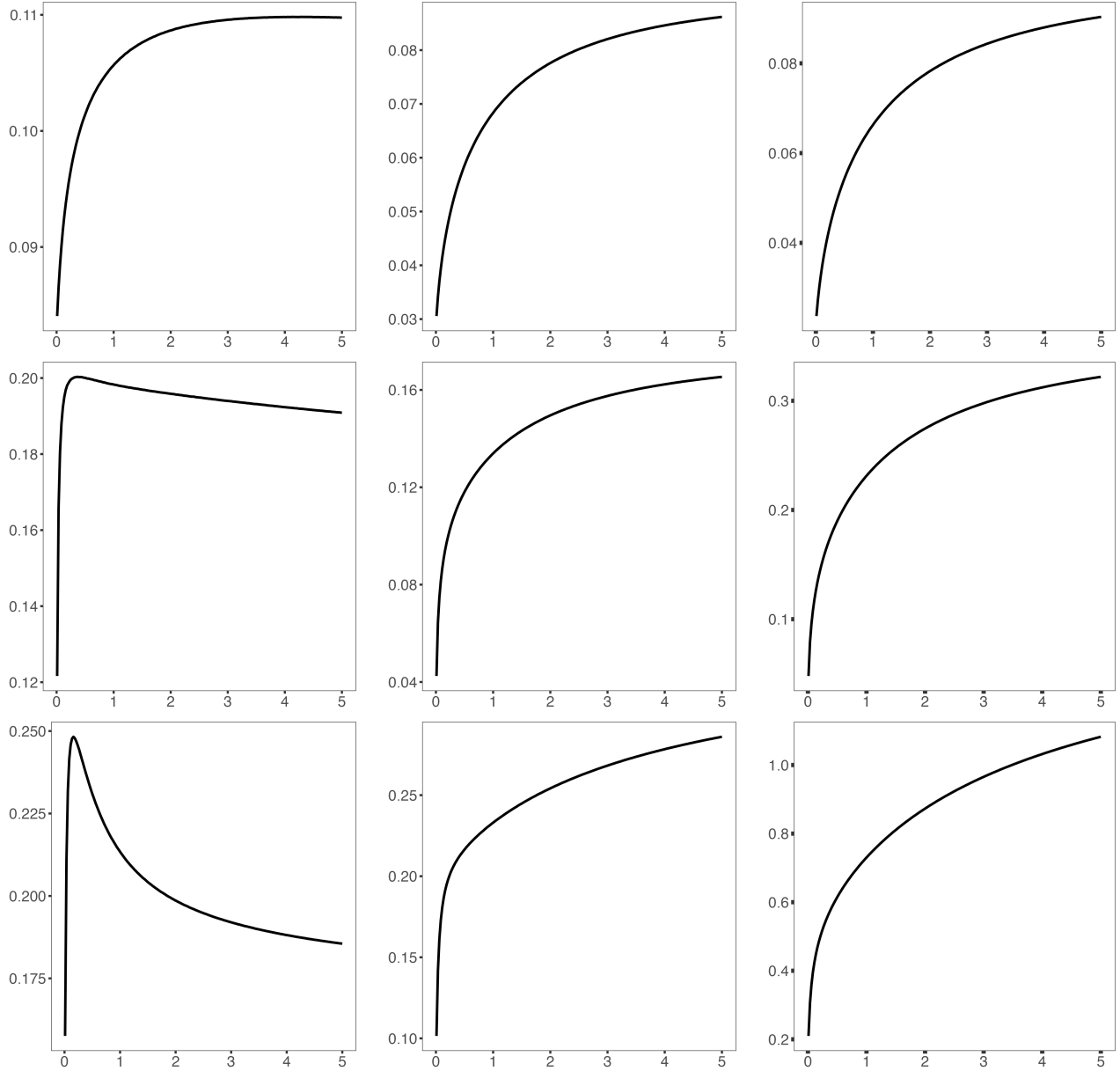


Figure S.2.1:  $\Xi(\lambda)$  against  $\lambda$  when  $A = 0.5$  and  $\gamma_1 = 1$ . Columns (left-to-right):  $D = I_p, \Sigma_p, \Sigma_p^2$ ; Rows (top-to-bottom):  $\gamma_2 = 0.5, 1, 2$ .

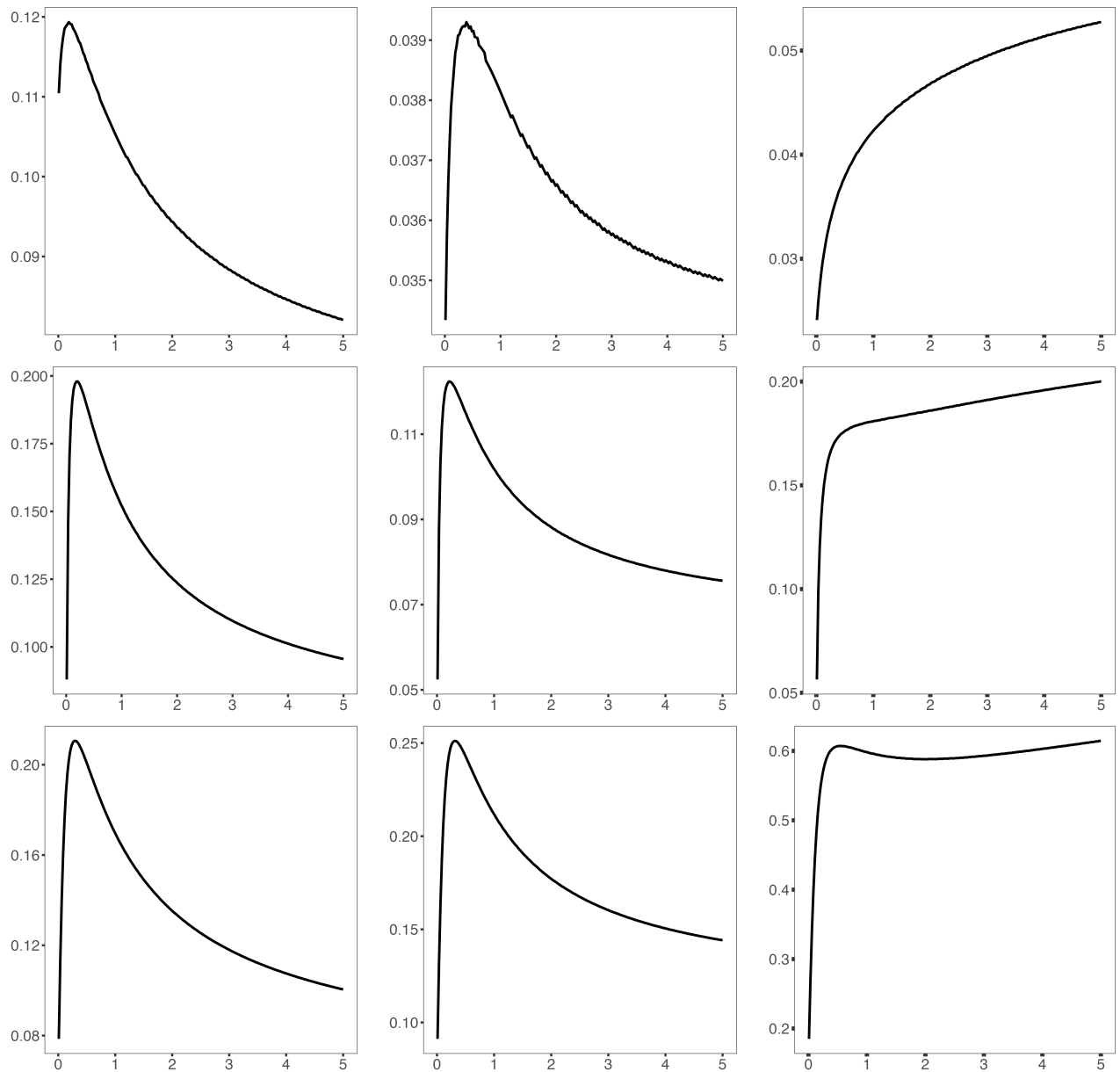


Figure S.2.2:  $\Xi(\lambda)$  against  $\lambda$  when  $A = 0.9$  and  $\gamma_1 = 1$ . Columns (left-to-right):  $D = I_p, \Sigma_p, \Sigma_p^2$ ; Rows (top-to-bottom):  $\gamma_2 = 0.5, 1, 2$ .

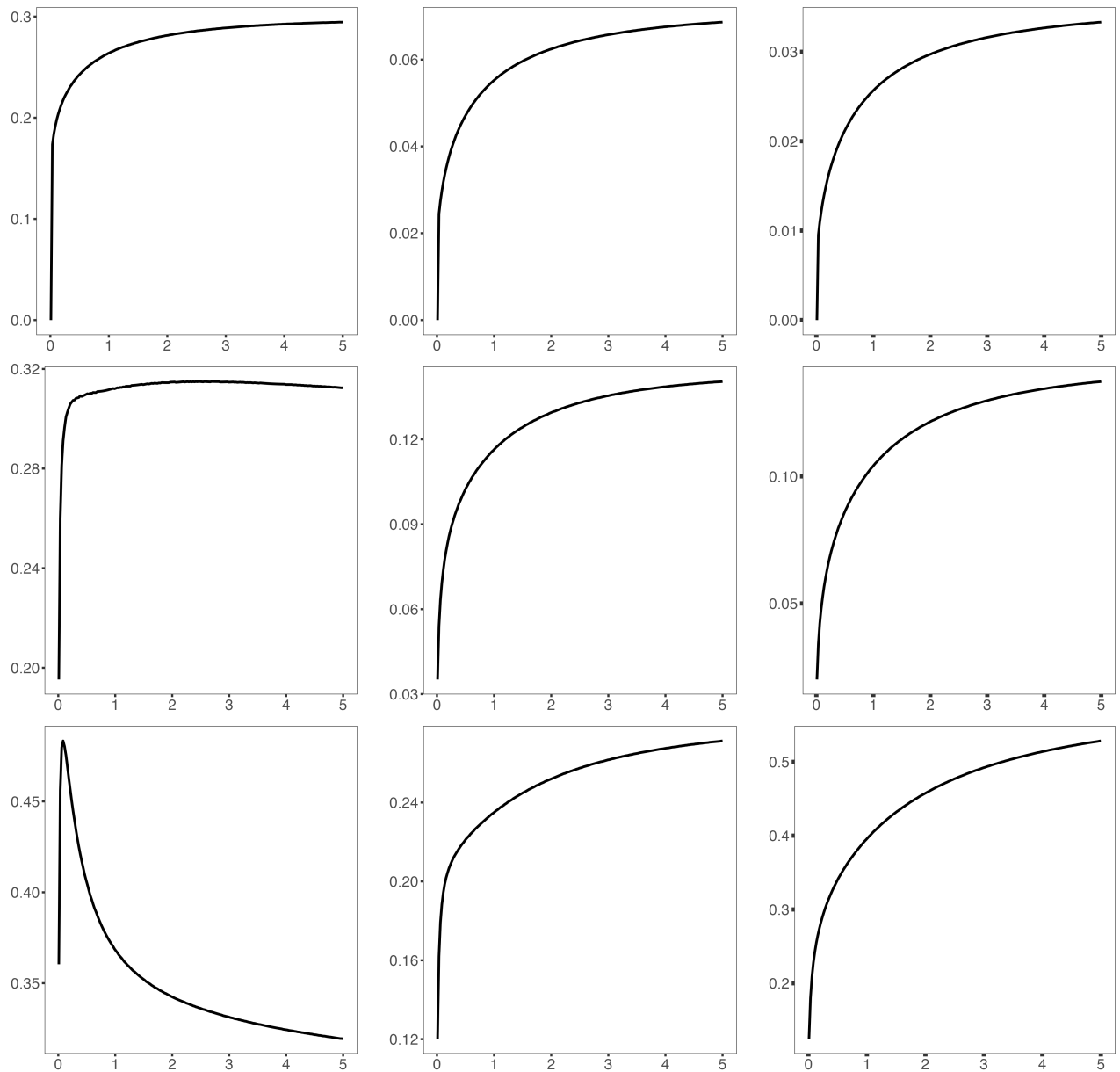


Figure S.2.3:  $\Xi(\lambda)$  against  $\lambda$  when  $A = 0.5$  and  $\gamma_1 = 2$ . Columns (left-to-right):  $D = I_p, \Sigma_p, \Sigma_p^2$ ; Rows (top-to-bottom):  $\gamma_2 = 0.5, 1, 2$ .

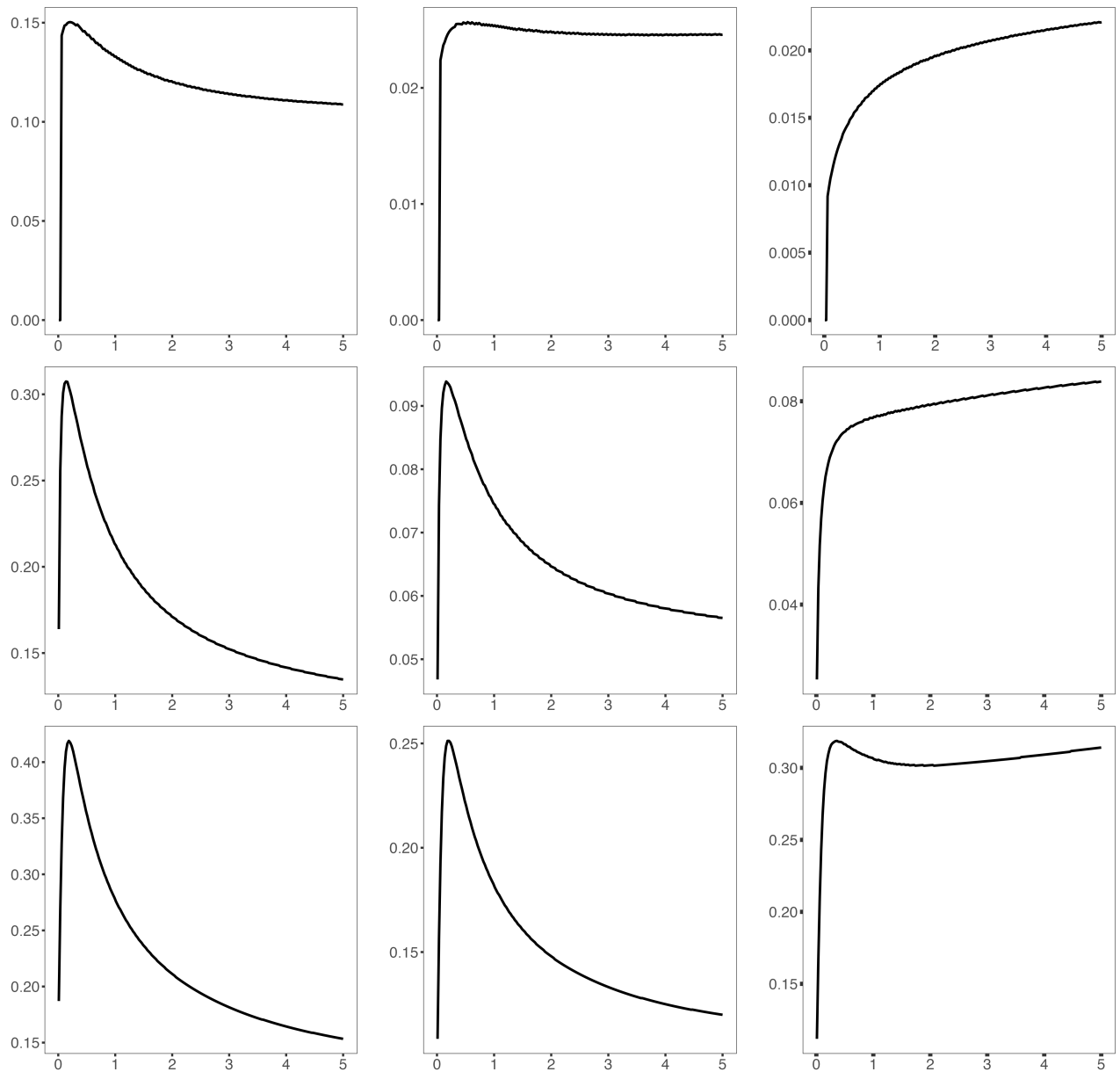


Figure S.2.4:  $\Xi(\lambda)$  against  $\lambda$  when  $A = 0.9$  and  $\gamma_1 = 2$ . Columns (left-to-right):  $D = I_p, \Sigma_p, \Sigma_p^2$ ; Rows (top-to-bottom):  $\gamma_2 = 0.5, 1, 2$ .

### S.3 Simulation study: additional details

#### S.3.1 Estimation accuracy: additional details

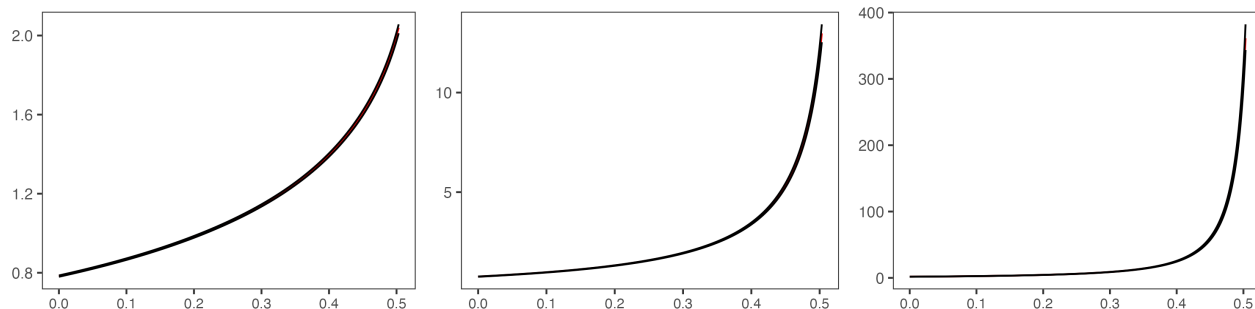


Figure S.3.1: The estimated  $s(x)$ ,  $s'(x)$  and  $s''(x)$  (from left to right) when  $\Sigma_p$  is *Toeplitz*,  $\hat{\gamma}_2 = 0.5$ ,  $\lambda = 0.5$ . Red: the true functions; Black: 5% and 95% pointwise percentile bands of the estimated functions.

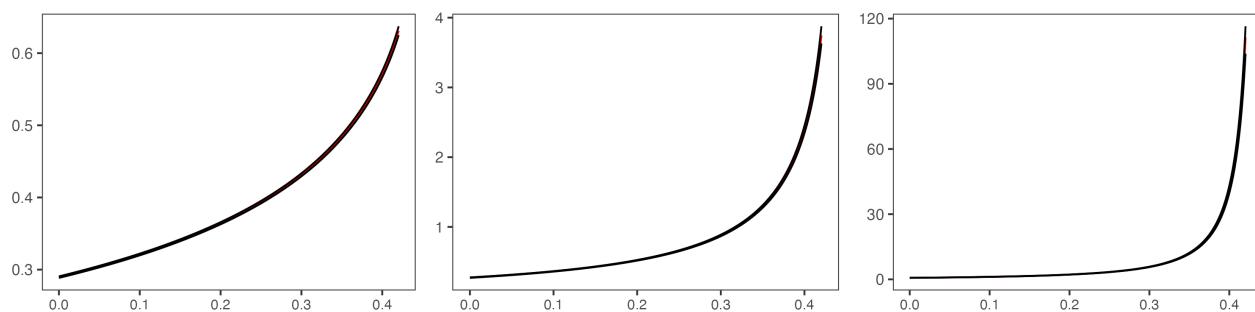


Figure S.3.2: The estimated  $s(x)$ ,  $s'(x)$  and  $s''(x)$  (from left to right) when  $\Sigma_p$  is *Factor-model*,  $\hat{\gamma}_2 = 5$ ,  $\lambda = 1.5$ . Red: the true functions; Black: 5% and 95% pointwise percentile bands of the estimated functions.

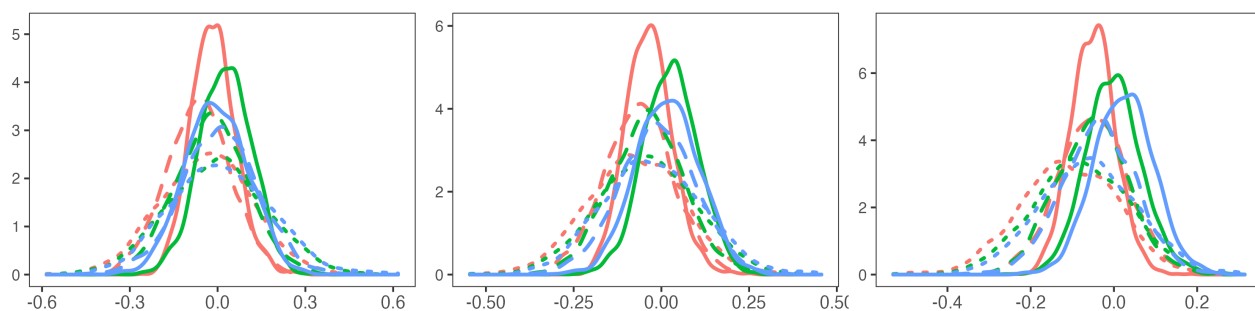


Figure S.3.3: Density of  $p^{2/3}(\hat{\Theta}_1 - \Theta_1)/\Theta_2$  when  $\Sigma_p$  is *Factor-model*. From left to right:  $\hat{\gamma}_1 = \hat{\gamma}_2$ ,  $\hat{\gamma}_1 = 2\hat{\gamma}_2$ ,  $\hat{\gamma}_1 = 5\hat{\gamma}_2$ . Line type:  $\hat{\gamma}_2 = 0.5$  (solid), 2 (dashed), 5 (dotted). Color:  $\lambda = 0.5$  (red), 1 (green), 1.5 (blue).

#### S.3.2 Empirical null distribution: additional details

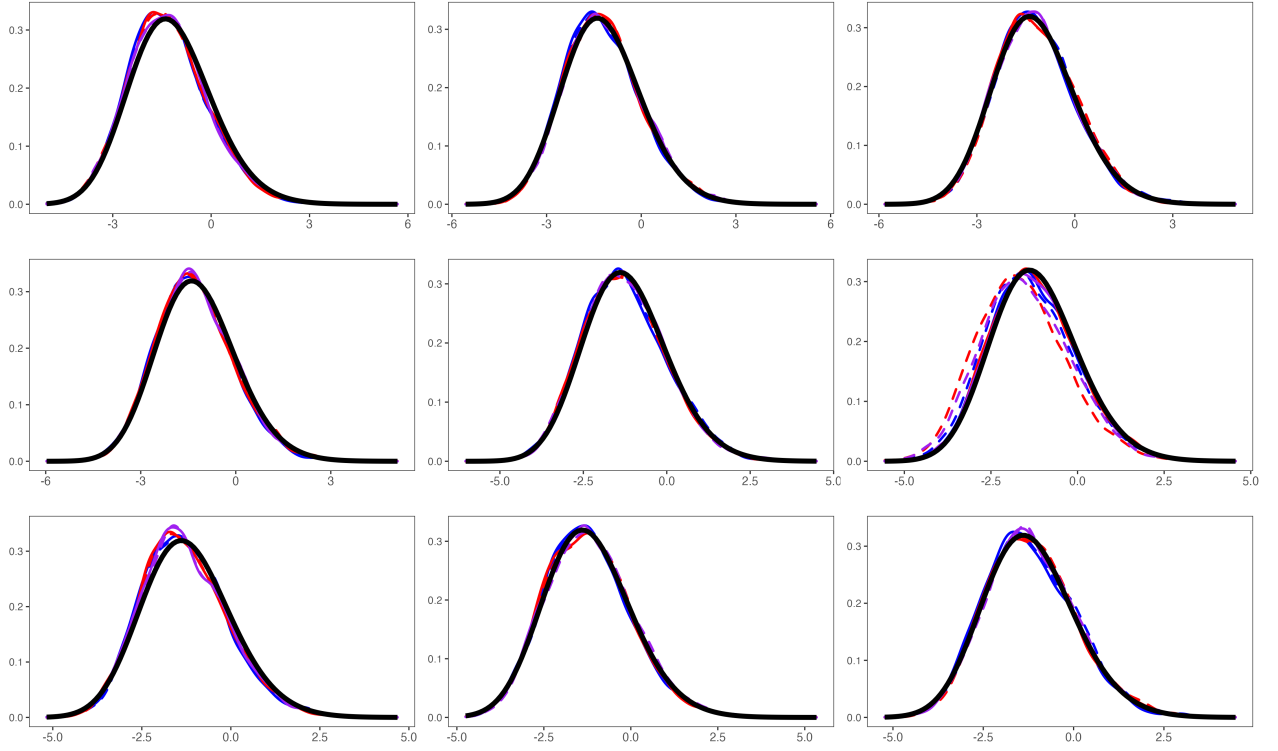


Figure S.3.4: Empirical density of  $\ell_{\max}(\mathbf{F}_\lambda)$  with  $\lambda = 0.5$ . Solid lines use true parameters for normalization; dashed lines use estimated ones. Colors indicate  $n_1$ : blue = 100, red = 250, purple = 500. Columns (left to right) correspond to  $\hat{\gamma}_2 = 0.5, 2, \text{ and } 5$ ; rows (top to bottom) correspond to  $\Sigma_p$  models: Poly-Decay, Toeplitz, and Factor. Black line: PDF of  $\text{TW}_1$  (baseline).

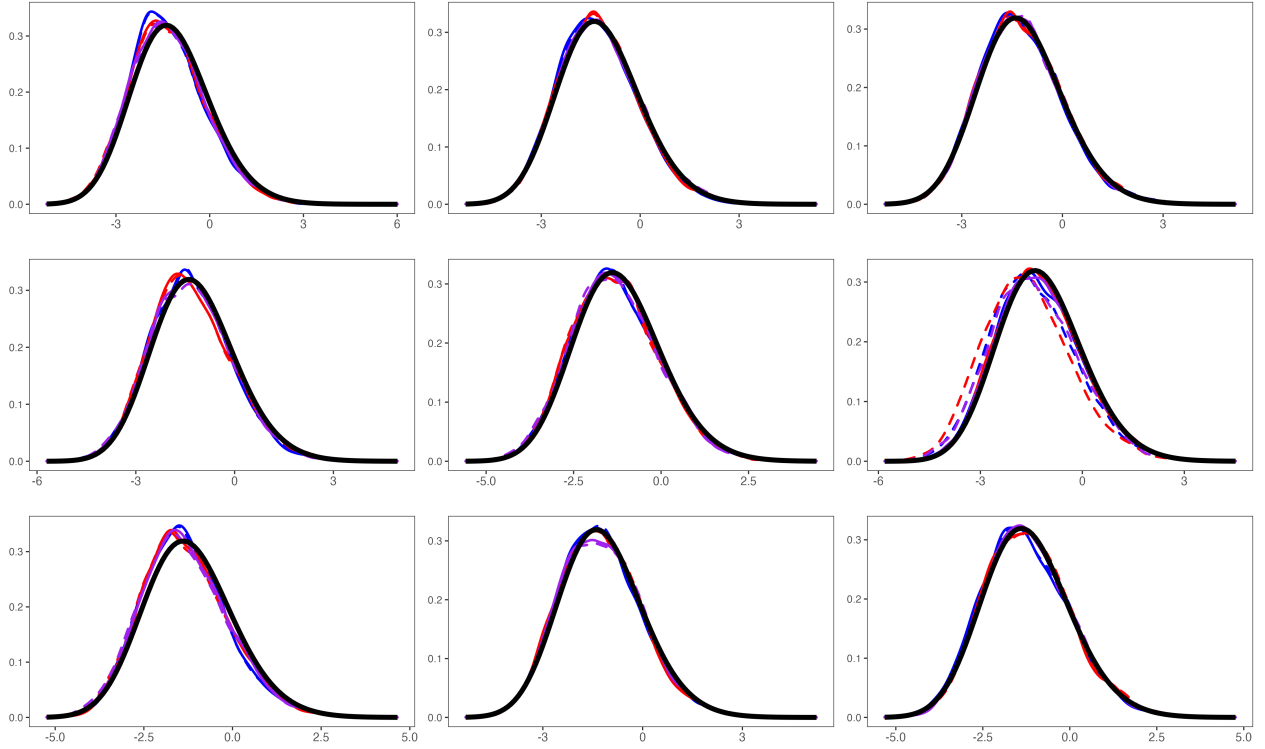


Figure S.3.5: Empirical density of  $\ell_{\max}(\mathbf{F}_\lambda)$  with  $\lambda = 1$ . Solid lines use true parameters for normalization; dashed lines use estimated ones. Colors indicate  $n_1$ : blue = 100, red = 250, purple = 500. Columns (left to right) correspond to  $\hat{\gamma}_2 = 0.5, 2, \text{ and } 5$ ; rows (top to bottom) correspond to  $\Sigma_p$  models: Poly-Decay, Toeplitz, and Factor. Black line: PDF of  $\text{TW}_1$  (baseline).

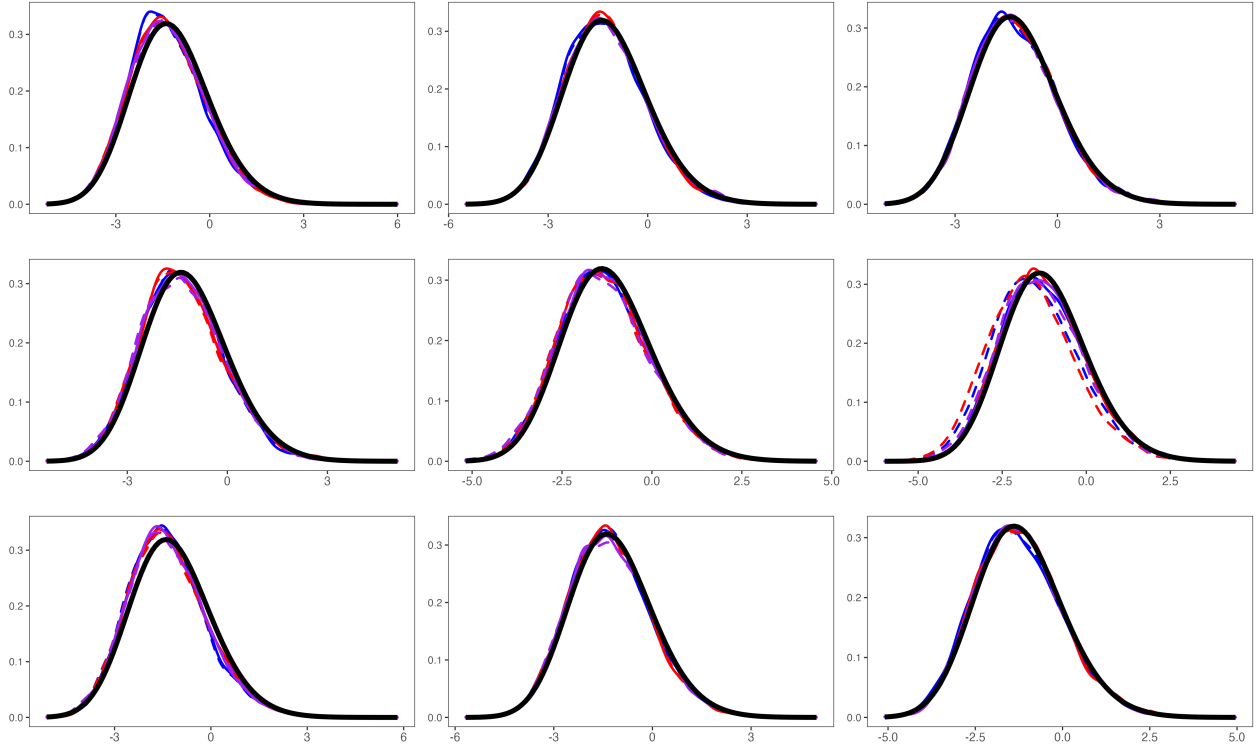


Figure S.3.6: Empirical density of  $\ell_{\max}(\mathbf{F}_\lambda)$  with  $\lambda = 1.5$ . Solid lines use true parameters for normalization; dashed lines use estimated ones. Colors indicate  $n_1$ : blue = 100, red = 250, purple = 500. Columns (left to right) correspond to  $\hat{\gamma}_2 = 0.5, 2, \text{ and } 5$ ; rows (top to bottom) correspond to  $\Sigma_p$  models: Poly-Decay, Toeplitz, and Factor. Black line: PDF of  $\text{TW}_1$  (baseline).

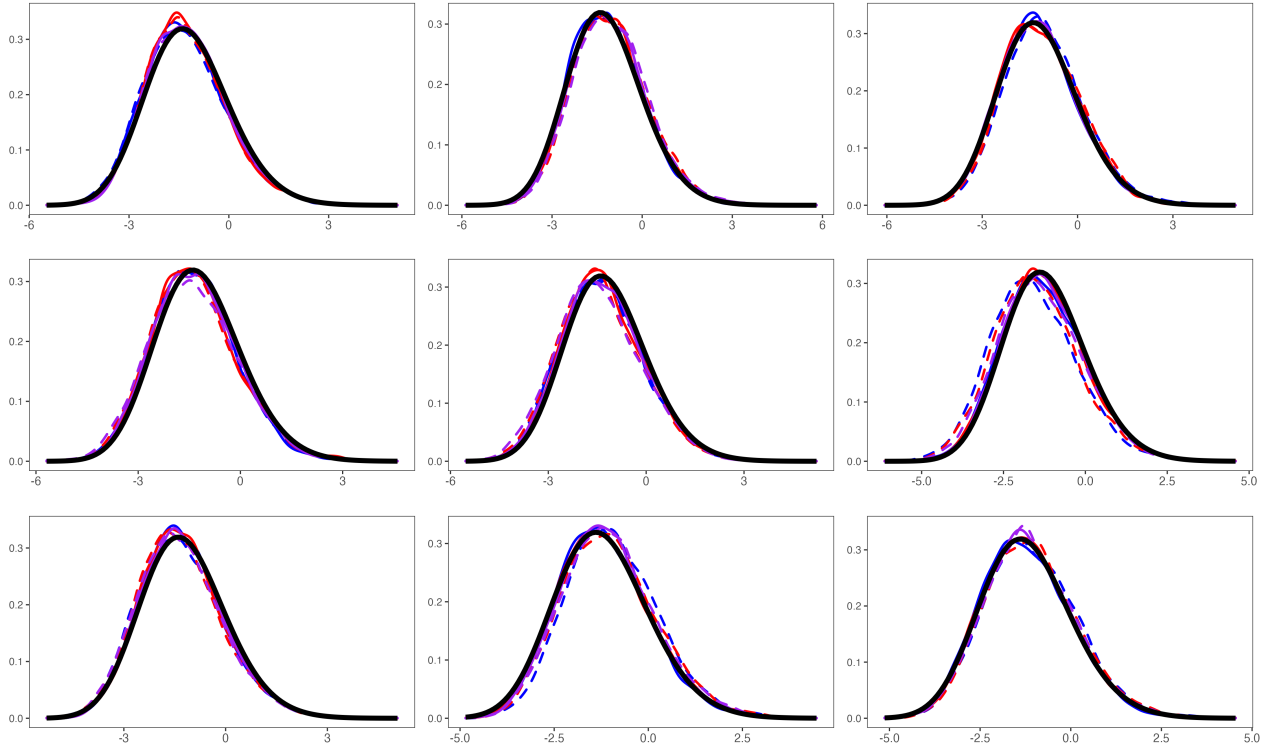


Figure S.3.7: Empirical density of  $\ell_{\max}(\mathbf{F}_\lambda)$  with  $\lambda = \hat{\lambda}_{I_p}$ . Solid lines use true parameters for normalization; dashed lines use estimated ones. Colors indicate  $n_1$ : blue = 100, red = 250, purple = 500. Columns (left to right) correspond to  $\hat{\gamma}_2 = 0.5, 2, \text{ and } 5$ ; rows (top to bottom) correspond to  $\Sigma_p$  models: Poly-Decay, Toeplitz, and Factor. Black line: PDF of  $\text{TW}_1$  (baseline).

### S.3.3 Empirical power: additional details

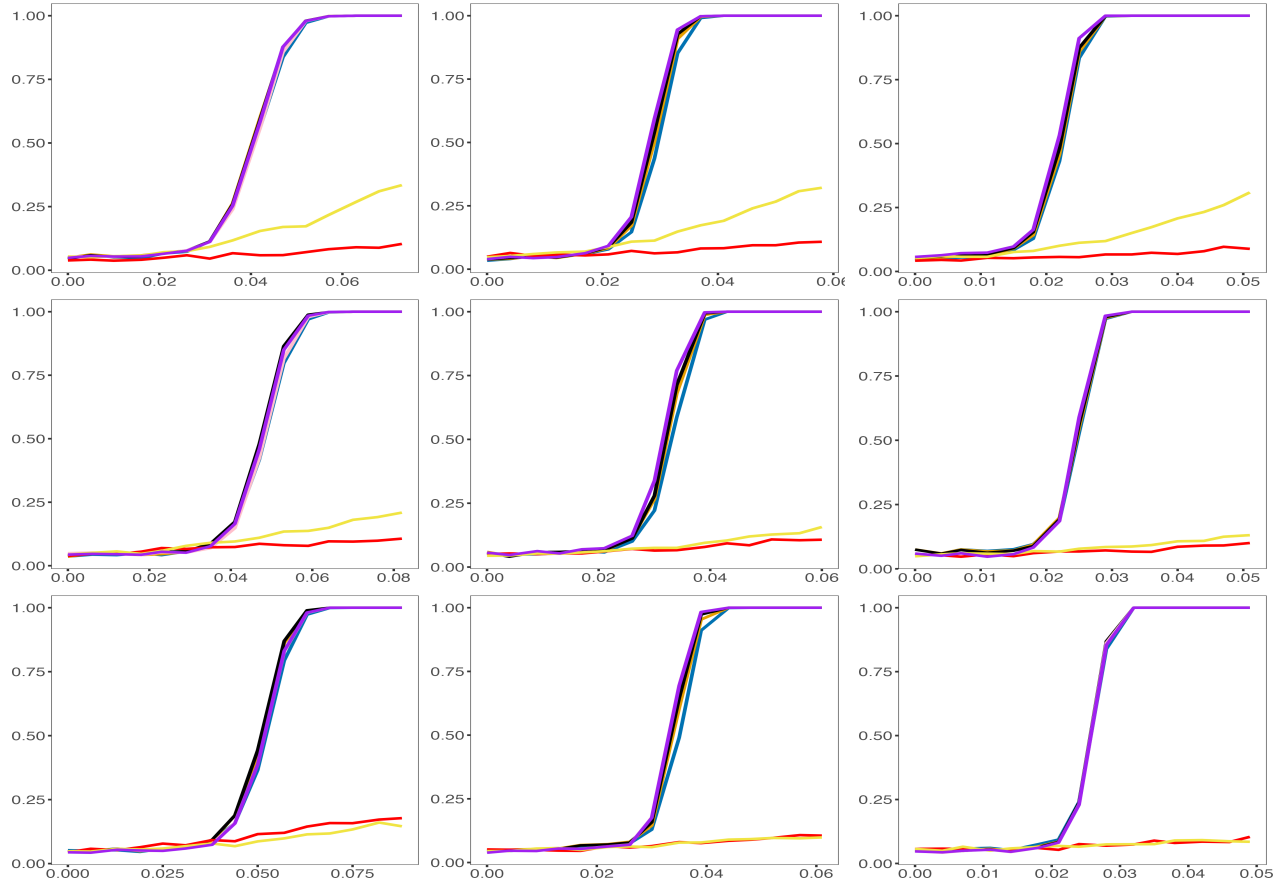


Figure S.3.8: Size-adjusted empirical power when  $\Sigma$  is Toeplitz. Columns (left to right):  $\hat{\gamma}_2 = 0.5, 2, 5$ . Rows (top to bottom):  $n_1 = 100, 250, 500$ . Blue:  $\lambda = 0.5$ ; Orange:  $\lambda = 1$ ; Black:  $\lambda = 1.5$ ; Purple:  $\lambda = \hat{\lambda}_{I_p}$ ; Pink:  $\lambda = \hat{\lambda}_{\Sigma_p}$ ; Red: Proj-LRT; Yellow: Ridge-LRT.

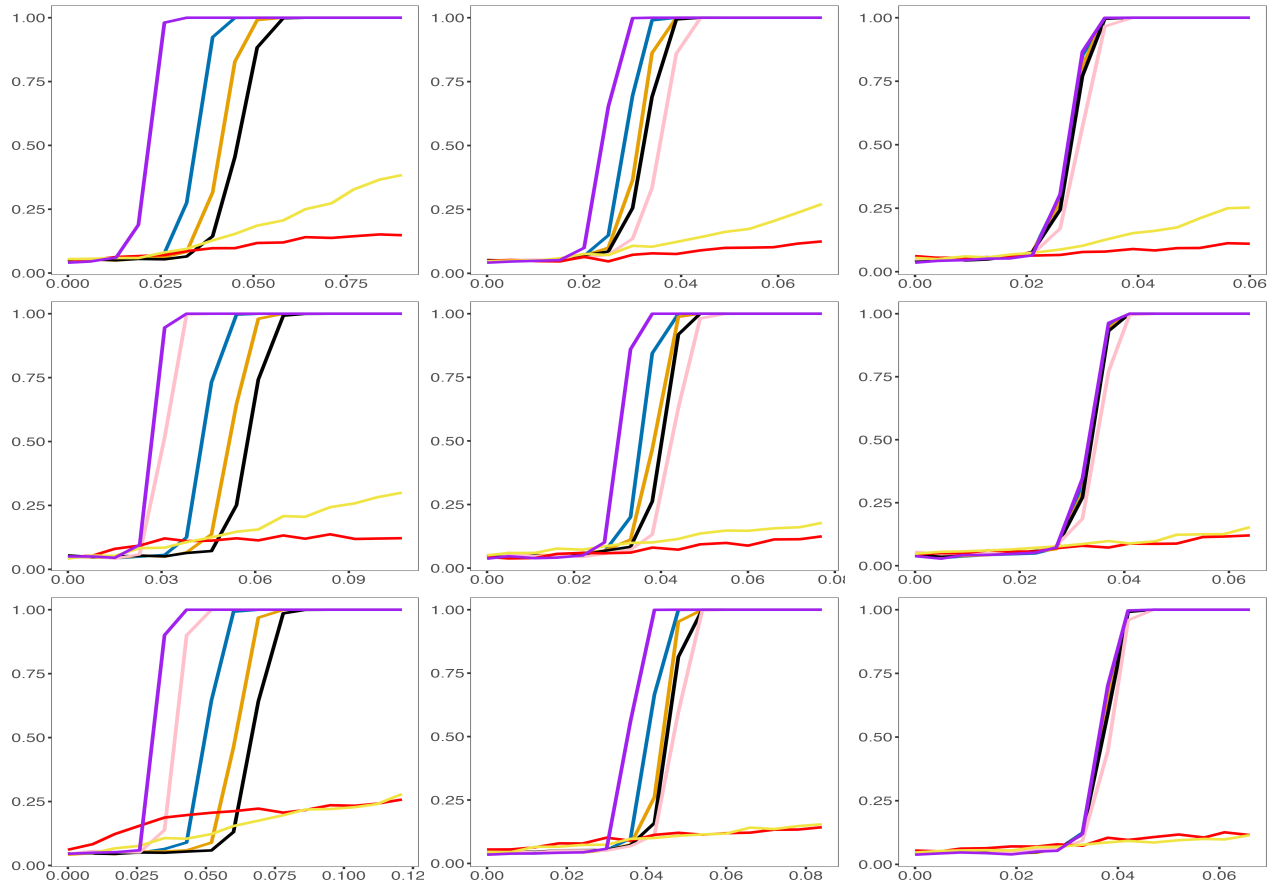


Figure S.3.9: Size-adjusted empirical power when  $\Sigma$  is Factor. Columns (left to right):  $\hat{\gamma}_2 = 0.5, 2, 5$ . Rows (top to bottom):  $n_1 = 100, 250, 500$ . Blue:  $\lambda = 0.5$ ; Orange:  $\lambda = 1$ ; Black:  $\lambda = 1.5$ ; Purple:  $\lambda = \hat{\lambda}_{I_p}$ ; Pink:  $\lambda = \hat{\lambda}_{\Sigma_p}$ ; Red: Proj-LRT; Yellow: Ridge-LRT.

## S.4 Basic Definitions and Additional Properties

In the remaining sections, we present the proofs of all technical results stated in the manuscript. We begin in this section by introducing the necessary notations and definitions. We then provide additional results concerning the properties of the Marčenko–Pastur equation (2.1) and equation (2.3). Throughout this section, we assume Conditions **C1–C6**, which will not be restated explicitly.

### S.4.1 Basic definitions

Throughout, we use  $c$ ,  $c'$ ,  $C$ , or  $C'$  to denote a general constant that may vary from line to line. We always use  $E = E(z)$  and  $\eta = \eta(z)$  to denote the real and imaginary part of a complex value  $z$ . The argument  $z$  is frequently omitted from mathematical expressions.

**Definition S.4.1** (Matrix norms). *Let  $A = (a_{ij})$  be a complex matrix. We define the following norms*

$$\|A\| = \max_{\|x\|=1} \|x^*Ax\|, \quad \|A\|_\infty = \max_{i,j} |a_{ij}|, \quad \|A\|_F = \sqrt{\text{tr}(AA^*)},$$

where  $A^*$  is the conjugate transpose of a matrix  $A$ . If  $A$  is a vector, we write  $|A| = \|A\|$  for simplicity.

The following notion of a high-probability bound has been used in a number of works on random matrix theory. It provides a simple way of systematizing and making precise statements of the form “ $\xi$  is bounded with high probability by  $\zeta$  up to small powers of  $n$ ”.

**Definition S.4.2** (Stochastic domination).

(i) *Consider two families of nonnegative random variables*

$$\xi = \left( \xi^{(n)}(u) : m \in \mathbb{N}, u \in U^{(n)} \right), \quad \zeta = \left( \zeta^{(n)}(u) : n \in \mathbb{N}, u \in U^{(n)} \right),$$

where  $U^{(n)}$  is a possibly  $n$ -dependent parameter set. We say that  $\xi$  is stochastically dominated by  $\zeta$ , uniformly in  $u$ , if for all (small)  $\varepsilon > 0$  and (large)  $D > 0$  we have

$$\sup_{u \in U^{(n)}} \mathbb{P} \left[ \xi^{(n)}(u) > n^\varepsilon \zeta^{(n)}(u) \right] \leq n^{-D}$$

for large enough  $n \geq n_0(\varepsilon, D)$ . Throughout this paper the stochastic domination will always be uniform in all parameters (such as matrix indices, deterministic vectors, and spectral parameters  $z$  in certain domain that are not explicitly fixed). If  $\xi$  is stochastically dominated by  $\zeta$ , uniformly in  $u$ , we use the notation  $\xi < \zeta$ . Moreover, if for some complex family  $\xi$  we have  $|\xi| < \zeta$  we also write  $\xi = O_{<}(\zeta)$ .

(ii) We extend the definition of  $O_{<}(\cdot)$  to matrices in the weak operator sense as follows. Let  $A$  be a family of complex square random matrices and  $\zeta$  a family of nonnegative random variables. Then we use  $A = O_{<}(\zeta)$  to mean  $|\langle \mathbf{v}, A\mathbf{w} \rangle| < \zeta |\mathbf{v}| |\mathbf{w}|$  uniformly for all deterministic vectors  $\mathbf{v}$  and  $\mathbf{w}$ .

(iii) If there exists a positive constant  $C$  such that  $\xi \leq C\zeta$ , then we write  $\xi \lesssim \zeta$ . If further there exists a positive constant  $C'$  such that  $\zeta \leq C'\xi$ , then we write  $\xi \asymp \zeta$ .

**Definition S.4.3.** We say that an event  $\Lambda$  holds with high probability if for any large positive constant  $D$ , there exists  $n_0(D)$  such that

$$\mathbb{P}(\Lambda^c) \leq n^{-D}, \quad \text{for any } n \geq n_0(D).$$

### S.4.2 Additional properties of the Marčenko-Pastur Equation

We present additional properties of the solution to the Marčenko-Pastur Equation (2.1). Applying Lemma 2.1 with the population ESD being  $\mathcal{G}_\lambda(1/\tau)$  (the composition of the inverse operator and  $\mathcal{G}_\lambda$ ) and the dimension-to-sample-size ratio being  $\gamma_1$ , we have that for any  $z \in \mathbb{C}^+$ , there is a unique solution  $q(z)$  in  $\mathbb{C}^+$  to

$$z = -\frac{1}{q} + \gamma_1 \int \frac{d\mathcal{G}_\lambda(\tau)}{\tau + q}. \quad (\text{S.1})$$

Moreover,  $q(z)$  is the Stieltjes transform of a probability measure, denoted to be  $\mathcal{F}_q$ , compactly supported in  $(0, \infty)$ .

Recall the definition of  $\phi(z)$ :  $\mathbb{C}^+ \rightarrow \mathbb{C}^+$  as the Stieltjes transform of  $\mathcal{G}_\lambda$  (See Lemma 2.3). That is,

$$\phi(z) = \int \frac{d\mathcal{G}_\lambda(\tau)}{\tau - z}, \quad z \in \mathbb{C}^+.$$

For convenience, we extend the definition of  $\phi(z)$  to  $z \in \mathbb{C}^- = \{E + i\eta : \eta < 0\}$  by setting  $\phi(z) = \overline{\phi(\bar{z})}$  if  $\eta < 0$ . By doing so, we can concisely write (S.1) as

$$z = -\frac{1}{q(z)} + \gamma_1 \phi(-q(z)).$$

Recall that  $s(x)$  is the extension of  $\phi(z)$  to the real line. Define the function

$$f(q) = -\frac{1}{q} + \gamma_1 s(-q), \quad \text{for } q \in (-\rho, 0).$$

Recall the definition of  $\beta$  and  $\Theta_1$  in Theorem 2.2. The following relationship holds. The critical point of  $f(q)$

is  $-\beta$  since  $f'(-\beta) = 1/\beta^2 - \gamma_1 s'(\beta) = 0$ . Moreover,

$$\Theta_1 = f(-\beta) = \frac{1}{\beta} + \gamma_1 s(\beta).$$

**Lemma S.4.1.** *The following results are known for  $\mathcal{F}_q$  and  $q(z)$ .*

(1) *The rightmost edge of the support of  $\mathcal{F}_q$  is  $\Theta_1$ .*

(2) *Fix any small constant  $a > 0$ . Then, there exists a constant  $C > 0$ , depending on  $a$ , such that*

$$C^{-1} \leq |q(z)| \leq C, \quad \text{and} \quad \Im q(z) \geq C^{-1}\eta,$$

*for all  $z \in \mathbb{C}^+$  satisfying  $a \leq |z| \leq a^{-1}$ .*

(3) *There exists sufficiently small constants  $C > 0$  and  $C' > 0$  such that for all  $z \in \{E + i\eta : |E - \Theta_1| \leq C, 0 < \eta < C^{-1}\}$*

$$\inf_{\tau \in S_{\mathcal{G}_\lambda}} |\tau + q(z)| \geq C',$$

*where  $S_{\mathcal{G}_\lambda}$  is the support of  $\mathcal{G}_\lambda$ . It indicates that the equation (S.1) is non-singular near  $\Theta_1$ .*

(4) *There exists an open ball of  $\Theta_1$  (in  $\mathbb{C}$ ), say  $\mathfrak{N}_{\Theta_1}$  such that when  $z = E + i\eta \in \mathfrak{N}_{\Theta_1} \cap \mathbb{C}^+$ ,*

$$\Im q(z) \asymp \begin{cases} \sqrt{\kappa + \eta} & \text{if } E < \Theta_1, \\ \frac{\eta}{\sqrt{\kappa + \eta}} & \text{if } E > \Theta_1, \end{cases}$$

*where  $\kappa = |E - \Theta_1|$ .*

These results are well-known in the RMT literature. See Silverstein and Choi (1995), Bao et al. (2015), Knowles and Yin (2017) and the references therein.

Next, we are interested in the behavior of Eq. (S.1) when a small perturbation is added to  $z$  and  $z$  is near  $\Theta_1$ . For this purpose, we consider the following domains of  $z$ . For the positive constants  $a$  and  $a'$ , we define

$$D = D(a, a', n_1) := \{z = E + i\eta \in \mathbb{C}^+ : |E - \Theta_1| \leq a, n_1^{-1+a'} \leq \eta \leq 1/a'\}. \quad (\text{S.2})$$

In the subsequent analysis, we shall always choose  $a$  and  $a'$  to be such that Result (3) of Lemma S.4.1 holds for all  $z \in D$ .

The following lemma indicates that if a small perturbation is added to  $z$  when  $z \in D$ , Eq. (S.1) is stable in the sense that  $q(z)$  will only have small changes. The results are a combination of Definition 5.4 and Definition

A.2 of Knowles and Yin (2017). Therefore, the proof is omitted.

**Lemma S.4.2** (Strong stability of Eq. (S.1)). *Eq. (S.1) is strongly stable in the following sense. Suppose that  $\delta : D \rightarrow (0, \infty)$  satisfies  $p^{-2} \leq \delta(z) \leq 1/\log(p)$  for  $z \in D$  and that  $\delta$  is Lipschitz continuous with Lipschitz constant  $p^2$ . Suppose moreover that for each fixed  $z \in D$ , the function  $\eta \rightarrow \delta(E + i\eta)$  is nonincreasing for  $\eta > 0$ . Suppose that  $u : D \rightarrow \mathbb{C}^+$  is the Stieltjes transform of a compactly supported probability measure. Let  $z \in D$  and suppose that*

$$|\tilde{z} - z| \leq \delta(z),$$

where  $\tilde{z} = -1/u(z) + \gamma_2\phi(-u(z))$ . Note that  $z = -1/q(z) + \gamma_2\phi(-q(z))$  and  $u(z) = q(\tilde{z})$ .

If  $\Im z < 1$ , suppose also that

$$|u - q| \leq \frac{C\delta}{\sqrt{\kappa + \eta} + \sqrt{\delta}} \tag{S.3}$$

holds at  $z + ip^{-5}$ . Here,  $\kappa = |E - \Theta_1|$ . Then, Eq. (S.3) holds at  $z$ .

It is worth mentioning that if for some  $z_0 \in D$  with  $\eta(z_0) \geq 1$ ,  $|\tilde{z}_0 - z_0| \leq \delta(z_0)$  is satisfied, then Eq. (S.3) holds for all  $z$  in

$$\left\{ z \mid E(z) = E(z_0), \quad \eta(z_0) - \eta(z) \in p^{-4}\mathbb{N} \right\} \cap D,$$

by induction.

### S.4.3 Additional properties of the generalized Marčenk-Pastur Equation for $\mathbf{G}_\lambda$

In this subsection, we present additional properties of  $\phi(z)$ . These results are analogous to those for  $q(z)$  in Section S.4.2. Recall that as in Lemma 2.3,  $\phi(z)$  is the solution to Eq. (2.3), cited here for the readers' convenience

$$\phi(z) = \int \frac{\tau dF^{\Sigma_\infty}(\tau)}{\tau\{[1 + \gamma_2\phi(z)]^{-1} - z\} + \lambda}.$$

Recall that as explained in Section 2.1, the equation can be reformulated to

$$z = h(z) + \left[ 1 + \gamma_2 \int \frac{\tau dF^{\Sigma_\infty}(\tau)}{-\tau h(z) + \lambda} \right]^{-1},$$

where  $h(z) = z - [1 + \gamma_2\phi(z)]^{-1}$ .

Recall that  $\rho$  is defined to be the leftmost edge of the support of  $\mathcal{G}_\lambda$ . The following basic properties of  $\phi(z)$  follow immediately from the arguments in Section 5 of Li (2024).

**Lemma S.4.3** (Characterization of  $\rho$ ). *(1) If  $F^{\Sigma_\infty}$  is continuous at  $\sigma_{\max}$  and Case (ii) of Definition 2.2 is satisfied, then  $\rho > \lambda/\sigma_{\max}$  and  $\mathcal{G}_\lambda$  is continuous at  $\rho$ . There exists a neighborhood of  $\rho$ , say  $\mathfrak{N}$ , such that*

when  $E \in \mathfrak{N}$  and  $\eta > 0$ ,

$$\Im\phi(z) \asymp \begin{cases} \sqrt{\kappa + \eta} & \text{if } E > \rho, \\ \frac{\eta}{\sqrt{\kappa + \eta}} & \text{if } E < \rho, \end{cases}$$

where  $\kappa = |E - \rho|$ .

(2) If  $F^{\Sigma_\infty}$  is discrete at  $\sigma_{\max}$  as in Case (i) of Definition 2.2 and additionally  $\gamma_2\omega_{\max} < 1$ , then the statements in (1) also hold.

(3) If  $F^{\Sigma_\infty}$  is discrete at  $\sigma_{\max}$  as in Case (i) of Definition 2.2 and additionally  $\gamma_2\omega_{\max} > 1$ , then  $\rho = \lambda/\sigma_{\max}$ . As  $z \rightarrow \rho$ ,  $\Im\phi(z)$  diverges.

The expression of  $\Im\phi(z)$  near  $\rho$  is proved using the argument in the proof of (A.7) of Knowles and Yin (2017) combined with the results in Section 5 of Li (2024). The details are omitted.

We shall focus on Case (1) and Case (2) of Lemma S.4.3 in the rest of this section. For the positive constants  $a$  and  $a'$ , we define the following domains. First, we define a domain around  $\rho$  with the imaginary part at least  $n_2^{-1+a'}$  as

$$Q = Q(a, a', n_2) = \{z \in \mathbb{C}^+ : |E| \leq a^{-1}, \quad E \leq \rho + a, \quad n_2^{-1+a'} \leq \eta \leq 1/a'\}.$$

Secondly, we restrict the real part to be smaller than  $\rho$  and define

$$Q_- = Q_-(a, a', n_2) = \{z \in Q(a, a', n_2) : E \leq \rho\}.$$

Thirdly, we define a domain that is away from the support of  $\mathcal{G}_\lambda$  as

$$Q_{\text{away}} = Q_{\text{away}}(a, a', n_2) = \{z \in \mathbb{C}^+ : a \leq \text{dist}(z, \mathcal{I}) \leq a^{-1}, \eta \geq n_2^{-1+a'}\},$$

where  $\mathcal{I} = [\rho, (1 + \sqrt{\gamma_2})^2 + \lambda/\liminf \ell_{\min}(\Sigma_p)]$ . Here, we are using the fact that the rightmost edge of the support of  $\mathcal{G}_\lambda$  is bounded by  $(1 + \sqrt{\gamma_2})^2 + \lambda/\liminf \ell_{\min}(\Sigma_p)$ .

The following boundedness property of  $\phi(z)$  follow immediately from the arguments in Section 5 of Li (2024).

**Lemma S.4.4** (Boundedness of  $\phi(z)$ ). *Suppose that  $\rho > \lambda/\sigma_{\max}$ . There exists constants  $a, a', C$  and  $C'$  such that for all  $z \in Q$ ,*

$$|\phi(z)| \leq C', \quad \Im\phi(z) \geq C\eta, \quad |1 + \gamma_2\phi(z)| \geq C, \quad \text{and} \quad \inf_{\tau \in \mathcal{S}} |-\tau h(z) + \lambda| \geq C,$$

where  $S$  is the support of  $F^{\Sigma_\infty}$ .

Instead, suppose that  $\rho = \lambda/\sigma_{\max}$ . Then, for all  $z$  such that  $|E| \leq a^{-1}$ ,  $E < \rho - a$ ,  $n_2^{-1+a'} \leq \eta \leq 1/a'$ , the same bounds hold.

In the subsequent analysis, we shall always choose  $a$  and  $a'$  to be such that the boundedness of  $\phi(z)$  in Lemma S.4.4 holds for  $z \in Q$ . It implies that Eq. (2.3) is non-singular when  $z \in Q$ .

The following lemma is analogous to Lemma S.4.2. It indicates that if a small perturbation is added to  $z$  when  $z \in Q$ , then Eq. (2.3) is stable in the sense that  $\phi(z)$  or  $h(z)$  will only have limited changes.

**Lemma S.4.5** (Strong stability of Eq. (2.3)). *Suppose that  $\rho > \lambda/\sigma_{\max}$ . Eq. (2.3) is strongly stable in  $Q$  in the following sense. Suppose that  $\delta : Q \rightarrow (0, \infty)$  satisfies  $p^{-2} \leq \delta(z) \leq 1/\log(p)$  for  $z \in Q$  and that  $\delta$  is Lipschitz continuous with Lipschitz constant  $p^2$ . Suppose moreover that for each fixed  $z \in Q$ , the function  $\eta \rightarrow \delta(E + i\eta)$  is nonincreasing for  $\eta > 0$ . Suppose that  $v(z) = z - [1 + \gamma_2 \varrho(z)]^{-1}$  where  $\varrho(z)$  is the Stieltjes transform of a compactly supported probability measure. Let  $z \in Q$  and suppose that*

$$|\tilde{z} - z| \leq \delta(z),$$

where

$$\tilde{z} = v(z) + \left[ 1 + \gamma_2 \int \frac{\tau dF^{\Sigma_\infty}(\tau)}{-\tau v(z) + \lambda} \right]^{-1}.$$

Note that  $v(z) = h(\tilde{z})$ .

If  $\Im z < 1$ , suppose also that

$$|v - h| \leq \frac{C\delta}{\sqrt{|E - \rho| + \eta} + \sqrt{\delta}} \tag{S.4}$$

holds at  $z + ip^{-5}$ . Then, Eq. (S.4) holds at  $z$ .

Moreover, when  $z$  is away from the support of  $\mathcal{G}_\lambda$ . The bound can be improved. The following lemma holds for both the case  $\rho > \lambda/\sigma_{\max}$  and  $\rho = \lambda/\sigma_{\max}$ .

**Lemma S.4.6.** *Eq. (2.3) is strongly stable in  $Q_{\text{away}}$  in the following sense. Suppose that  $\delta : Q_{\text{away}} \rightarrow (0, \infty)$  satisfies  $\delta(z) \leq 1/\log(p)$  for  $z \in Q_{\text{away}}$ . Suppose that  $v(z) = z - [1 + \gamma_2 \varrho(z)]^{-1}$  where  $\varrho(z)$  is the Stieltjes transform of a compactly supported probability measure. Let  $z \in Q_{\text{away}}$  and suppose that*

$$|\tilde{z} - z| \leq \delta(z),$$

where

$$\tilde{z} = v(z) + \left[ 1 + \gamma_2 \int \frac{\tau dF^{\Sigma_\infty}(\tau)}{-\tau v(z) + \lambda} \right]^{-1}.$$

Then,

$$|v(z) - h(z)| \leq C\delta(z),$$

for any  $z \in Q_{\text{away}}$ .

**Corollary S.4.1.** *It is worth mentioning that if for some  $z_0 \in Q$  with  $\eta(z_0) \geq 1$ ,  $|\tilde{z}_0 - z_0| \leq \delta(z_0)$  is satisfied, then Eq. (S.4) holds for all  $z$  in*

$$\left\{ z \mid E(z) = E(z_0), \quad \eta(z_0) - \eta(z) \in p^{-4}\mathbb{N} \right\} \cap Q.$$

It follows easily by induction.

**Corollary S.4.2.** *Under the conditions of Lemma S.4.5, if Eq. (S.4) holds, then we also have*

$$|\varrho - \phi| \leq \frac{c\delta}{\sqrt{\kappa + \eta} + \sqrt{\delta}}.$$

It is obvious since

$$v - h = \frac{\gamma_2(\phi - \varrho)}{(1 + \gamma_2\varrho)(1 + \gamma_2\phi)}$$

and  $|1 + \gamma_2\phi(z)| \asymp 1$ ,  $|1 + \gamma_2\varrho(z)| \asymp 1$  when  $z \in Q$ .

**Corollary S.4.3.** *Using Lemma S.4.5, we immediately obtain the following result. Suppose that  $\varrho(z)$  satisfies*

$$\varrho(z) = \int \frac{\tau dF^{\Sigma_\infty}(\tau)}{\tau\{[1 + \gamma_2\varrho(z) + \delta_2(z)]^{-1} - z\} + \lambda} + \delta_1(z), \quad z \in Q.$$

Here,  $\delta_1$  and  $\delta_2$  are such that  $|\delta_1|$  and  $|\delta_2|$  satisfy the conditions on  $\delta$  in Lemma S.4.5. If  $\Im z < 1$ , suppose also that

$$|\varrho - \phi| \leq \frac{C|\delta_1| + C|\delta_2|}{\sqrt{\kappa + \eta} + \sqrt{|\delta_1| + |\delta_2|}} \tag{S.5}$$

holds at  $z + ip^{-5}$ . Then, Eq. (S.5) holds at  $z$ .

*Proof of Lemma S.4.5.* Lemma S.4.5 can be shown following very similar arguments to those in the proof of Lemma S.4.2 presented in Section A.2 of Knowles and Yin (2017). Indeed, the key arguments are Lemma A.3 of Knowles and Yin (2017) which states the regular behavior of the derivatives of the function

$$f(q) = -\frac{1}{q} + \gamma_1 s(-q)$$

near its critical points. To prove Lemma S.4.5, we replace the function with

$$f_{\text{new}}(h) = h + \left[ 1 + \gamma_2 \int \frac{\tau dF^{\Sigma_\infty}(\tau)}{-\tau h + \lambda} \right]^{-1},$$

Section 5 of Li (2024) indicates that the function has the same behavior at its critical point  $h_0$  (See Lemma 3.1 for the definition of  $h_0$ ). Moreover, a similar quadratic equation of  $(v - h)$  to Eq. (A.13) of Knowles and Yin (2017) can be easily obtained using Taylor's expansion. The rest arguments in Section A.2 of Knowles and Yin (2017) can be used nearly verbatim on the new definition of  $f_{\text{new}}(\cdot)$ . We therefore omit further details.  $\square$

*Proof of Lemma S.4.6.* When  $z$  is away from the support of  $\mathcal{G}_\lambda$ , as when  $z \in Q_{\text{away}}$ ,  $|h'(\tilde{z})|$  is bounded. Therefore,

$$|v(z) - h(z)| = |h(\tilde{z}) - h(z)| \leq \int_z^{\tilde{z}} |h(\zeta)| |d\zeta| \leq C\delta(z).$$

$\square$

*Proof of Corollary S.4.3.* The result follows from Lemma S.4.5 and Corollary S.4.2 because the specified  $\rho$  is such that

$$\left| \tilde{v}(z) + \left[ 1 + \gamma_2 \int \frac{\tau dF^{\Sigma_\infty}(\tau)}{-\tau \tilde{v}(z) + \lambda} \right]^{-1} - z \right| \leq C(|\delta|_1 + |\delta|_2),$$

where  $\tilde{v}(z) = z - [1 + \gamma_2 \rho(z)]^{-1}$ .  $\square$

## S.5 Properties of $\mathbf{G}_\lambda$ under Gaussianity

In this section, we mainly study the properties of  $\mathbf{G}_\lambda$  under the following additional conditions:

**SC1**  $\mathbf{Z}$  is normally distributed.

**SC2**  $\rho > \lambda/\sigma_{\max}$ .

The main results in this section can be extended to the case when  $\rho = \lambda/\sigma_{\max}$ . The extension is presented in Section S.5.4.

When  $\mathbf{Z}$  is normally distributed,  $\mathbf{G}_\lambda$  has the same distribution as

$$\mathbf{G}_\lambda \stackrel{\text{def}}{=} \tilde{\mathbf{Z}}\tilde{\mathbf{Z}}^T + \lambda\Sigma_p^{-1},$$

where  $\tilde{\mathbf{Z}}$  is  $p \times n_2$  whose entries are iid  $N(0, 1/n_2)$ . Results in this section are expected to hold when  $\mathbf{Z}$  satisfies **C2**. The extension to non-Gaussianity can be completed following the strategy in Sections 7–10 of Knowles and Yin (2017), which is however beyond our scope.

Importantly, under **C5** and **SC2**, for all sufficiently large  $p$ ,

$$(p/n_2)F^{\Sigma_p}(\ell_{\max}(\Sigma_p)) \leq 1 - \epsilon \text{ for some } \epsilon > 0. \quad (\text{S.1})$$

In the subsequent analysis, it is more convenient to consider a finite-sample version of Eq. (2.3). Specifically, let  $\phi_p(z)$  be the unique solution in  $\mathbb{C}^+$  to

$$\phi_p = \int \frac{\tau dF^{\Sigma_p}(\tau)}{\tau\{[1 + (p/n_2)\phi_p]^{-1} - z\} + \lambda}, \quad z \in \mathbb{C}^+. \quad (\text{S.2})$$

Moreover, define

$$x_p(h) = h + \left[ 1 + (p/n_2) \int \frac{\tau dF^{\Sigma_p}(\tau)}{-\tau h + \lambda} \right]^{-1}.$$

Let  $\rho_p$  be the finite-sample version of  $\rho$  when  $(\gamma_2, F^{\Sigma_\infty})$  is replaced by  $(p/n_2, F^{\Sigma_p})$ . That is,  $\rho_p = x_p(h_0^{(p)})$  where  $h_0^{(p)}$  is the unique solution in  $(0, \lambda/\ell_{\max}(\Sigma_p))$  to  $x_p'(h_0^{(p)}) = 0$ . It is a simple matter to verify that  $h_0^{(p)}$  exists and is unique. It is because  $x_p'$  is monotonically decreasing and  $x_p'(h) < 0$  for all  $h$  close to  $\lambda/\ell_{\max}(\Sigma_p)$  when  $p$  is sufficiently large because of Eq. (S.1)..

It is not hard to verify that  $\phi_p(z)$  also satisfies the properties of  $\phi(z)$  presented in Section S.5, when all the parameters are replaced by their finite-sample version. We will later refer to these properties on  $\phi_p(z)$  without any proof.

**Lemma S.5.1.** *Suppose that **C1–C6** and **SC1–SC2** hold. We have*

$$p^{2/3}|h_0^{(p)} - h_0| \rightarrow 0, \quad p^{2/3}|\rho_p - \rho| \rightarrow 0.$$

*Proof of Lemma S.5.1.* Recall that  $\rho = x(h_0)$  where  $x'(h_0) = 0$  and  $h_0 < \lambda/\sigma_{\max}$ . For sufficiently large  $p$ ,  $h_0 < \lambda/\ell_{\max}(\Sigma_p) - \epsilon$  for all sufficiently small  $\epsilon > 0$ . Notice that

$$\rho_p - \rho = x_p(h_0^{(p)}) - x(h_0) = x_p(h_0^{(p)}) - x_p(h_0) + x_p(h_0) - x(h_0) = x_p'(\tilde{h})(h_0^{(p)} - h_0) + (x_p(h_0) - x(h_0)),$$

where  $\tilde{h}$  is a point in between  $h_0$  and  $h_0^{(p)}$ . The second term on the right hand side is clearly  $o(p^{-2/3})$  since under **C6**,  $\|F^{\Sigma_\infty} - F^{\Sigma_p}\| = o(p^{-2/3})$  and  $|p/n_2 - \gamma_2| = o(p^{-2/3})$ .

It remains to show  $|h_0^{(p)} - h_0| = o(p^{-2/3})$ . To this end, observe that for some  $\tilde{\tilde{h}}$  in between  $h_0^{(p)}$  and  $h_0$ ,

$$0 = x_p'(h_0^{(p)}) = x_p'(h_0) + x_p''(\tilde{\tilde{h}})(h_0^{(p)} - h_0).$$

While  $C \leq |x_p''(h)| \leq C^{-1}$  when  $h$  is bounded away from  $\lambda/\ell_{\max}(\Sigma_p)$ , we obtain that  $|h_0^{(p)} - h_0| = O(x_p'(h_0))$ .

While  $x'(h_0) = 0$ ,  $x'_p(h_0) = o(p^{-2/3})$  since  $\|F^{\Sigma_\infty} - F^{\Sigma_p}\| = o(p^{-2/3})$  and  $|p/n_2 - \gamma_2| = o(p^{-2/3})$ . It completes the proof of the lemma.  $\square$

In this section, we aim to establish the following technical results. We first introduce a fundamental control parameter as

$$\Psi(z) = \sqrt{\frac{\Im\phi_p(z)}{n_2\eta}} + \frac{1}{n_2\eta}.$$

Recall the definition of the domain  $Q$ ,  $Q_-$  and  $Q_{\text{away}}$  in Section S.4. We define a finite-sample version of the domains as

$$\begin{aligned} Q^{(p)} &= Q^{(p)}(a, a', n_2) = \{z \in \mathbb{C}^+, \quad |E| \leq a^{-1}, \quad E \leq \rho_p + a, \quad n_2^{-1+a'} \leq \eta \leq 1/a'\}, \\ Q_-^{(p)} &= Q_-^{(p)}(a, a', n_2) = \{z \in Q^{(p)}(a, a', n_2), \quad E \leq \rho_p - n_2^{-2/3+a'}, \quad n_2^{-2/3} \leq \eta \leq 1/a'\}, \\ Q_{\text{away}}^{(p)} &= Q_{\text{away}}^{(p)}(a, a', n_2) = \{z \in \mathbb{C}^+ : a \leq \text{dist}(z, \mathcal{I}) \leq a^{-1}, \quad \eta \geq n_2^{-1+a'}\}, \end{aligned}$$

where  $\mathcal{I} = [\rho_p, (1 + \sqrt{p/n_2})^2 + \lambda/\ell_{\min}(\Sigma_p)]$ .

Call the resolvent of  $\mathbf{G}_\lambda$

$$R(z) = (\mathbf{G}_\lambda - zI_p)^{-1}, \quad z \in \mathbb{C}^+.$$

**Theorem S.5.1** (Strong local law of  $R(z)$ ). *Suppose that **C1–C6** and **SC1–SC2** hold. There exists constants  $a > 0$  such that the following local laws hold for arbitrary  $a' > 0$ .*

(i) *The entrywise local law in  $Q^{(p)}$  holds as*

$$R(z) - (\lambda\Sigma_p^{-1} - m_p(z)I_p)^{-1} = O_{<}(\Psi(z)),$$

*uniformly in  $Q^{(p)}$ , where  $m_p(z) = z - [1 + (p/n_2)\phi_p(z)]^{-1}$ .*

(ii) *The averaged local law in  $Q^{(p)}$  holds as*

$$\hat{\phi}_p(z) - \phi_p(z) = O_{<} \left( \frac{1}{n_2\eta} \right),$$

*where  $\hat{\phi}_p(z) = p^{-1}\text{tr}R(z)$ .*

(iii) *The averaged local law in  $Q_-^{(p)}$  holds as*

$$\hat{\phi}_p(z) - \phi_p(z) = O_{<} \left( \frac{1}{n_2(\kappa + \eta)} \right),$$

*where  $\kappa = |\rho_p - E|$ .*

(iv) The averaged local law in  $Q_{\text{away}}^{(p)}$  holds as

$$\hat{\phi}_p(z) - \phi_p(z) = O_{\prec} \left( \frac{1}{n_2} \right).$$

Once Theorem S.5.1 is ready, it is not hard to deduce the following rigidity of the smallest eigenvalue of  $\mathbf{G}_\lambda$ .

**Theorem S.5.2** (Rigidity of the smallest eigenvalue of  $\mathbf{G}_\lambda$  under Gaussianity). *Under the conditions of Theorem S.5.1, for any fixed  $\epsilon \in (0, 2/3)$ , with high probability, there is no eigenvalue of  $\mathbf{G}_\lambda$  in  $(-\infty, \rho_p - n_2^{-2/3+\epsilon})$ .*

The following theorem shows the convergence of *linear spectral statistics* of  $\mathbf{G}_\lambda$ .

**Theorem S.5.3.** *Suppose the conditions of Theorem S.5.1 hold. Consider the interval*

$$\mathcal{I}_\epsilon = [\rho_p - \epsilon, (1 + \sqrt{p/n_2})^2 + \lambda / \liminf \ell_{\min}(\Sigma_p) + \epsilon],$$

where  $\epsilon$  is any fixed positive constant.

(i) *Then, with high probability, all eigenvalues of  $\mathbf{G}_\lambda$  are contained in  $\mathcal{I}_\epsilon$ . We denote the event as  $\mathfrak{M}$ .*

(ii) *Let  $f$  be any function analytic on an open interval containing the interval  $\mathcal{I}_\epsilon$ . We have*

$$\mathbb{1}_{(\mathfrak{M})} p^{2/3} \left| \frac{1}{p} \sum_{j=1}^p f(\ell_j(\mathbf{G}_\lambda)) - \int f(\tau) d\mathcal{G}_\lambda(\tau) \right| < \frac{1}{n_2}.$$

### S.5.1 Proof of Theorem S.5.1

Throughout the section, we focus on the representation  $\mathbf{G}_\lambda = \tilde{\mathbf{Z}}\tilde{\mathbf{Z}}^T + \lambda\Sigma_p^{-1}$  where  $\tilde{\mathbf{Z}}$  is  $p \times n_2$  whose entries are iid  $N(0, 1/n_2)$ . We shall temporarily assume that  $\Sigma_p$  is diagonal with diagonal elements  $\sigma_1 \geq \sigma_2 \geq \dots \geq \sigma_p$ . The extension to general  $\Sigma_p$  is given in Section S.5.1.5.

In the subsequent analysis, we closely follow the arguments in Sections 4 and 5 of Knowles and Yin (2017). We therefore omit many details and refer to the corresponding arguments in Knowles and Yin (2017). We frequently omit the arguments  $z$  from our notation.

### S.5.1.1 Basic tools

Define the  $(p + n_2) \times (p + n_2)$  block matrix

$$\mathbf{J}(z) = \mathbf{K}(z)^{-1}, \quad \mathbf{K}(z) = \begin{pmatrix} \lambda \Sigma_p^{-1} - z I_p & \tilde{\mathbf{Z}} \\ \tilde{\mathbf{Z}}^T & -I_{n_2} \end{pmatrix}. \quad (\text{S.3})$$

The reason for considering  $\mathbf{J}$  and  $\mathbf{K}$  is that  $\mathbf{J}$  contains the resolvent  $R(z)$  as one of its blocks (see Lemma S.5.2 below).

Call

$$\Omega(z) = \begin{pmatrix} (\lambda \Sigma_p^{-1} - m_p(z) I_p)^{-1} & 0 \\ 0 & (z - m_p(z)) I_{n_2} \end{pmatrix}.$$

We shall later show that  $\mathbf{J} - \Omega = O_{<}(\Psi)$  in  $Q^{(p)}$ . It actually implies the entrywise local law in  $Q^{(p)}$ .

We make the following notation. We use  $A_{st}$  to denote the  $(s, t)$ -th element of a matrix  $A$ . The four blocks of  $\mathbf{J}(z)$  are called  $\mathbf{J}_{(11)}$ ,  $\mathbf{J}_{(12)}$ ,  $\mathbf{J}_{(21)}$  and  $\mathbf{J}_{(22)}$ . For a set of indices, say  $S \subset \{1, 2, \dots, p + n_2\}$ , we define the minors  $\mathbf{K}^{(S)} = (\mathbf{K}_{st}, s, t \notin S)$ . That is,  $\mathbf{K}$  but with the rows and columns whose indices specified in  $S$  deleted. We also write  $\mathbf{J}^{(S)} = (\mathbf{K}^{(S)})^{-1}$ . The block formed by the first  $p$  rows and columns of  $\mathbf{J}^{(S)}$  is called  $\mathbf{J}_{(11)}^{(S)}$ . The block formed by the last  $n_2$  rows and columns of  $\mathbf{J}^{(S)}$  is called  $\mathbf{J}_{(22)}^{(S)}$ . Similar for  $\mathbf{J}_{(12)}^{(S)}$  and  $\mathbf{J}_{(21)}^{(S)}$ . Similar notation is made for the matrix  $\Omega$ .

For  $u = 1, 2, \dots, p$ , call the  $u$ -th row of  $\tilde{\mathbf{Z}}$  to be  $\tilde{\mathbf{Z}}_{u\cdot}$ . For  $i = p + 1, \dots, p + n_2$ , we use  $\tilde{\mathbf{Z}}_{\cdot i}$  to denote the  $(i - p)$ -th column of  $\tilde{\mathbf{Z}}$ . Moreover, if  $u \in \{1, \dots, p\}$ , let  $e_u$  denote the standard unit vector of dimension  $p$  in the coordinate direction  $u$ . If  $i \in \{p + 1, \dots, p + n_2\}$ , let  $e_i$  denote the standard unit vector of dimension  $n_2$  in the coordinate direction  $(i - p)$ .

The following lemma is a variant of Lemma 4.4 in Knowles and Yin (2017). These results follow directly from the Schur complement formula and resolvent identities that have been previously derived in Knowles and Yin (2017) and the references therein. The proof is therefore omitted.

**Lemma S.5.2** (Resolvent Identities). *Suppose that  $\Sigma_p$  is diagonal with diagonal elements  $\sigma_1, \dots, \sigma_p$ .*

(i) *We have*

$$\mathbf{J} = \begin{pmatrix} \mathbf{J}_{(11)} & \mathbf{J}_{(12)} \\ \mathbf{J}_{(21)} & \mathbf{J}_{(22)} \end{pmatrix} = \begin{pmatrix} R & R\tilde{\mathbf{Z}} \\ \tilde{\mathbf{Z}}^T R & \tilde{\mathbf{Z}}^T R\tilde{\mathbf{Z}} - I_{n_2} \end{pmatrix}.$$

(ii) *For  $u \in \{1, 2, \dots, p\}$ , we have*

$$\frac{1}{\mathbf{J}_{uu}} = \lambda/\sigma_u - z - \tilde{\mathbf{Z}}_{u\cdot} \mathbf{J}_{(22)}^{(u)} \tilde{\mathbf{Z}}_{\cdot u}^T.$$

For  $u \neq v \in \{1, 2, \dots, p\}$ ,

$$\mathbf{J}_{uv} = -\mathbf{J}_{uu} \tilde{\mathbf{Z}}_u \mathbf{J}_{(22)}^{(u)} e_v = -\mathbf{J}_{vv} e_u^T \mathbf{J}_{(22)}^{(v)} \tilde{\mathbf{Z}}_v^T = \mathbf{J}_{uu} \mathbf{J}_{vv}^{(u)} \tilde{\mathbf{Z}}_u \mathbf{J}_{(22)}^{(uv)} \tilde{\mathbf{Z}}_v^T.$$

(iii) For  $i \in \{p+1, \dots, p+n_2\}$ , we have

$$\frac{1}{\mathbf{J}_{ii}} = -1 - \tilde{\mathbf{Z}}_i^T \mathbf{J}_{(11)}^{(i)} \tilde{\mathbf{Z}}_i.$$

For  $i \neq j \in \{p+1, \dots, p+n_2\}$ , we have

$$\mathbf{J}_{ij} = -\mathbf{J}_{ii} \tilde{\mathbf{Z}}_i^T \mathbf{J}_{(11)}^{(i)} e_j = -\mathbf{J}_{jj} e_i^T \mathbf{J}_{(11)}^{(j)} \tilde{\mathbf{Z}}_j = \mathbf{J}_{ii} \mathbf{J}_{jj}^{(i)} \tilde{\mathbf{Z}}_i^T \mathbf{J}_{(11)}^{(ij)} \tilde{\mathbf{Z}}_j.$$

(iv) For  $u \in \{1, 2, \dots, p\}$  and  $i \in \{p+1, \dots, p+n_2\}$ ,

$$\mathbf{J}_{ui} = -\mathbf{J}_{ii} e_u^T \mathbf{J}_{(11)}^{(i)} \tilde{\mathbf{Z}}_i.$$

(v) If  $i, j, k \notin S$  and  $i, j \neq k$ ,

$$\mathbf{J}_{ij}^{(S)} = \mathbf{J}_{ij}^{(S \cup \{k\})} + \frac{\mathbf{J}_{ik}^{(S)} \mathbf{J}_{kj}^{(S)}}{\mathbf{J}_{kk}^{(S)}}.$$

The following result is our fundamental tool for estimating entries of  $\mathbf{J}$ .

**Lemma S.5.3.** Fix  $a > 0$ . Then, the following estimates hold for any  $z \in Q^{(p)}$ . We have

$$\|\mathbf{J}\| \leq \frac{C}{\eta^3}, \quad \|\partial z \mathbf{J}\| \leq \frac{C}{\eta^6}.$$

Furthermore, let  $\mathbf{w} \in \mathbb{R}^p$  and  $\mathbf{v} \in \mathbb{R}^{n_2}$ . Then, we have the bounds

$$\begin{aligned} \sum_{u=1}^p |\mathbf{w}^T \mathbf{J}_{(11)} e_u|^2 &= \frac{\Im \mathbf{w}^T \mathbf{J}_{(11)} \mathbf{w}}{\eta}, \\ \sum_{i=p+1}^{p+n_2} |\mathbf{v}^T \mathbf{J}_{(22)} e_i|^2 &\leq \frac{C \|\tilde{\mathbf{Z}} \tilde{\mathbf{Z}}^T\|}{\eta} \Im \mathbf{v}^T \mathbf{J}_{(22)} \mathbf{v} + C \mathbf{v}^T \mathbf{v}, \\ \sum_{u=1}^p |\mathbf{v}^T \mathbf{J}_{(21)} e_u|^2 &= \frac{\Im \mathbf{v}^T \mathbf{J}_{(22)} \mathbf{v}}{\eta}, \\ \sum_{i=p+1}^{p+n_2} |\mathbf{w}^T \mathbf{J}_{(12)} e_i|^2 &\leq C \|\tilde{\mathbf{Z}} \tilde{\mathbf{Z}}^T\| \sum_{u=1}^p |\mathbf{w}^T \mathbf{J}_{(11)} e_u|^2. \end{aligned}$$

The estimates remain true for  $\mathbf{J}^{(S)}$  instead of  $\mathbf{J}$  if  $S \subset \{1, \dots, p\}$  or  $S \subset \{p+1, \dots, p+n_2\}$ .

*Proof.* First, consider the bound on the operator norm of  $\mathbf{J}$ .

$$\|\mathbf{J}\| \leq \left\| \begin{pmatrix} (\lambda\Sigma_p^{-1} - zI_p)^{-1} & 0 \\ 0 & I \end{pmatrix} \right\| \left\| \begin{pmatrix} I & (\lambda\Sigma_p^{-1} - zI)^{-1/2}\tilde{\mathbf{Z}} \\ \tilde{\mathbf{Z}}^T(\lambda\Sigma_p^{-1} - zI)^{-1/2} & -I \end{pmatrix}^{-1} \right\| = \|J_1\| \|J_2\|, \text{ say.}$$

For  $J_1$ , we clearly have  $\|J_1\| \leq C/(|E - \lambda/\sigma_1| + \eta) \leq C/\eta$ , for  $z \in Q^{(p)}$ . The eigen structure of a matrix of the form  $J_2$  is analyzed in (4.12-4.15) of Knowles and Yin (2017). Based on their arguments,

$$\begin{aligned} \|J_2\| &\leq C(1 + \max_u \frac{|s_u| + 1}{|s_u - 1|}) \leq C(1 + \max_u \frac{(C/\eta)\|\tilde{\mathbf{Z}}\tilde{\mathbf{Z}}^T\| + 1}{|s_u - 1|}) \\ &\leq C + (C/\eta)\|\tilde{\mathbf{Z}}\tilde{\mathbf{Z}}^T\|\|\lambda\Sigma_p^{-1} - zI\| \|(\tilde{\mathbf{Z}}\tilde{\mathbf{Z}}^T - (\lambda\Sigma_p^{-1} - zI))^{-1}\| \leq C + \frac{C}{\eta^2}, \end{aligned}$$

where  $s_k$ 's are the eigenvalues of  $(\lambda\Sigma_p^{-1} - zI)^{-1/2}\tilde{\mathbf{Z}}\tilde{\mathbf{Z}}^T(\lambda\Sigma_p^{-1} - zI)^{-1/2}$ . The bound on  $\|\mathbf{J}\|$  follows.

The bound on the operator norm of  $\partial_z \mathbf{J}$  follows from the fact that  $\|\partial_z \mathbf{J}\| = \|\mathbf{J}(\partial_z \mathbf{K})\mathbf{J}\| \leq \frac{C}{\eta^6}$ .

Next, using Result (i) of Lemma S.5.2,

$$\sum_{u=1}^p |\mathbf{w}^T \mathbf{J}_{(11)} e_u|^2 = \sum_{u=1}^p \mathbf{w}^T \mathbf{J}_{(11)} e_u e_u^T \bar{\mathbf{J}}_{(11)} \mathbf{w} = \mathbf{w}^T \mathbf{J}_{(11)} \bar{\mathbf{J}}_{(11)} \mathbf{w} = \mathbf{w}^T \frac{\Im \mathbf{J}_{(11)}}{\eta} \mathbf{w}.$$

Moreover,

$$\begin{aligned} \sum_{i=p+1}^{p+n_2} |\mathbf{v}^T \mathbf{J}_{(22)} e_i|^2 &= \sum_{i=p+1}^{p+n_2} |\mathbf{v}^T \tilde{\mathbf{Z}}^T R \tilde{\mathbf{Z}} e_i - \mathbf{v}^T e_i|^2 \leq 2\mathbf{v}^T \tilde{\mathbf{Z}}^T \mathbf{J}_{(11)} \tilde{\mathbf{Z}} \tilde{\mathbf{Z}}^T \bar{\mathbf{J}}_{(11)} \tilde{\mathbf{Z}} \mathbf{v} + 2\mathbf{v}^T \mathbf{v} \\ &\leq C \|\tilde{\mathbf{Z}}\tilde{\mathbf{Z}}^T\| \|\mathbf{v}^T \tilde{\mathbf{Z}}^T \mathbf{J}_{(11)} \bar{\mathbf{J}}_{(11)} \tilde{\mathbf{Z}} \mathbf{v}\| + C \mathbf{v}^T \mathbf{v} \leq C \|\tilde{\mathbf{Z}}\tilde{\mathbf{Z}}^T\| \frac{\Im \mathbf{v}^T \mathbf{J}_{(22)} \mathbf{v}}{\eta} + C \mathbf{v}^T \mathbf{v}. \end{aligned}$$

The rest two results on  $\mathbf{J}_{(12)}$  and  $\mathbf{J}_{(21)}$  can be proved similarly using Result (i) of Lemma S.5.2. We omit the details.  $\square$

**Lemma S.5.4.** *Under C1,  $\|\tilde{\mathbf{Z}}\tilde{\mathbf{Z}}^T\| \leq (1 + \sqrt{p/n_2})^2 + \epsilon$  with high probability, for any fixed  $\epsilon > 0$ .*

The lemma follows from Theorem 2.10 of Alex Bloemendal et al. (2014).

### S.5.1.2 Weak entrywise law

We first show a weak entrywise local law of  $\mathbf{J}$  in  $Q^{(p)}$ .

**Proposition S.5.1.** *Suppose that the assumptions of Theorem S.5.1 hold. Define*

$$\Lambda = \max_{1 \leq s, t \leq p+n_2} |(\mathbf{J} - \Omega)_{st}| \quad \text{and} \quad \Lambda_o = \max_{s \neq t} |(\mathbf{J} - \Omega)_{st}|.$$

Then,  $\Lambda < (n_2\eta)^{-1/4}$  uniformly in  $z \in Q^{(p)} \cup Q_{\text{away}}^{(p)}$ .

Define the averaged control parameter

$$\mathfrak{B} = \mathfrak{B}_p + \mathfrak{B}_n, \quad \mathfrak{B}_p = \left| \frac{1}{p} \sum_{i=u}^p (\mathbf{J}_{uu} - \Omega_{uu}) \right|, \quad \mathfrak{B}_n = \left| \frac{1}{n_2} \sum_{i=p+1}^{p+n_2} (\mathbf{J}_{ii} - \Omega_{ii}) \right|.$$

Note that  $\mathfrak{B}_p = |\hat{\phi}_p - \phi_p|$ . We have the trivial bound  $\mathfrak{B} \leq C\Lambda$ .

For  $s \in \{1, 2, \dots, p + n_2\}$ , we introduce the conditional expectation

$$\mathbb{E}_s[\cdot] = \mathbb{E}[\cdot | \mathbf{K}^{(s)}].$$

Using Lemma S.5.2, we get that, for  $u \in \{1, \dots, p\}$ ,

$$\frac{1}{\mathbf{J}_{uu}} = \lambda/\sigma_u - z - \frac{1}{n_2} \text{tr} \mathbf{J}_{(22)}^{(u)} - W_u, \quad W_u = (1 - \mathbb{E}_u)(\tilde{\mathbf{Z}}_u \mathbf{J}_{(22)}^{(u)} \tilde{\mathbf{Z}}_u^T). \quad (\text{S.4})$$

For  $i \in \{p + 1, \dots, p + n_2\}$ ,

$$\frac{1}{\mathbf{J}_{ii}} = -1 - \frac{1}{n_2} \text{tr} \mathbf{J}_{(11)}^{(i)} - W_i, \quad W_i = (1 - \mathbb{E}_i)(\tilde{\mathbf{Z}}_i^T \mathbf{J}_{(11)}^{(i)} \tilde{\mathbf{Z}}_i). \quad (\text{S.5})$$

We define the  $z$ -dependent event  $\Xi = \{\Lambda \leq 1/(\log n_2)\}$  and the control parameter

$$\Psi_{\mathfrak{B}} = \sqrt{\frac{\Im \phi_p + \mathfrak{B}}{n_2\eta}}.$$

The following estimate is analogous to Lemma 5.2 of Knowles and Yin (2017).

**Lemma S.5.5.** *Suppose that the assumptions of Theorem S.5.1 hold. Then, uniformly for  $s \in \{1, \dots, p + n_2\}$  and  $z \in Q^{(p)} \cup Q_{\text{away}}^{(p)}$ , we have*

$$\mathbb{1}(\Xi)(|W_s| + \Lambda_o) < \Psi_{\mathfrak{B}},$$

$$\mathbb{1}(\eta \geq 1)(|W_s| + \Lambda_o) < \Psi_{\mathfrak{B}}.$$

*Proof of Lemma S.5.5.* The proof relies on the identities from Lemma S.5.2 and large deviation estimates like Lemma 3.1 of Alex Bloemendal et al. (2014). The arguments in the proof are similar to those in Lemma 5.2 of Knowles and Yin (2017).

From (1) of Lemma S.4.4, when  $z \in Q^{(p)} \cup Q_{\text{away}}^{(p)}$ ,  $|\Omega_{ss}| \asymp 1$ . Therefore,

$$\mathbb{1}(\Xi)\mathbf{J}_{ss} \asymp 1.$$

Using Result (v) of Lemma S.5.2 and a simple induction argument, it is not hard to conclude that

$$\mathbb{1}(\Xi)\mathbf{J}_{ss}^{(S)} \asymp 1,$$

for any  $S \subset \{1, \dots, p+n_2\}$  and  $s \notin S$ , satisfying  $|S| \leq C$ .

Let us first estimate  $\Lambda_o$ . When  $u \neq v \in \{1, \dots, p\}$ , using Result (ii) of Lemma S.5.2 and a large deviation estimation (Lemma 3.1 of Alex Bloemendal et al. (2014)),

$$\mathbb{1}(\Xi)|\mathbf{J}_{uv}| \leq \mathbb{1}(\Xi)|\mathbf{J}_{uu}\mathbf{J}_{vv}^{(u)}| \left| \sum_{i,j=p+1}^{p+n_2} \tilde{Z}_{ui}\tilde{Z}_{vj}\mathbf{J}_{i,j}^{(uv)} \right| < \mathbb{1}(\Xi)C \left( \frac{1}{n_2^2} \sum_{i,j=p+1}^{p+n_2} |\mathbf{J}_{ij}^{(uv)}|^2 \right)^{1/2}. \quad (\text{S.6})$$

The term in parentheses is

$$\begin{aligned} \mathbb{1}(\Xi) \frac{1}{n_2^2} \sum_{i,j=p+1}^{p+n_2} |\mathbf{J}_{ij}^{(uv)}|^2 &= \mathbb{1}(\Xi) \frac{1}{n_2^2} \sum_{i,j=p+1}^{p+n_2} |e_i^T \mathbf{J}_{22}^{(uv)} e_j|^2 < \mathbb{1}(\Xi) \frac{1}{n_2^2 \eta} \|\tilde{Z}\tilde{Z}^T\| \sum_{i=p+1}^{p+n_2} \Im \mathbf{J}_{ii}^{(uv)} + \mathbb{1}(\Xi) \frac{1}{n_2} \\ &< \mathbb{1}(\Xi) \frac{1}{n_2^2 \eta} \|\tilde{Z}\tilde{Z}^T\| \sum_{i=p+1}^{p+n_2} \Im \mathbf{J}_{ii} + \mathbb{1}(\Xi) \frac{\Lambda_o^2}{n_2 \eta} + \mathbb{1}(\Xi) \frac{1}{n_2} < \frac{\Im \phi_p + \mathfrak{B} + \Lambda_o^2}{n_2 \eta} + \frac{1}{n_2} < \frac{\Im \phi_p + \mathfrak{B} + \Lambda_o^2}{n_2 \eta}. \end{aligned}$$

Here, we are using Result (v) of Lemma S.5.2, Lemma S.5.4 and Lemma S.5.3. The last step is due to the fact that  $1 < \Im \phi_p / \eta$ .

A similar result for  $\mathbf{J}_{ij}$ ,  $\mathbf{J}_{ui}$ , and  $\mathbf{J}_{iu}$ ,  $i \in \{p+1, p+n_2\}$  and  $u \in \{1, p\}$  can be obtained using Result (iii) and (iv) of Lemma S.5.2 and a large deviation estimation. We omit the details as the arguments are very similar.

All together, we conclude that

$$\mathbb{1}(\Xi)\Lambda_o < \mathbb{1}(\Xi) \sqrt{\frac{\Im \phi_p + \mathfrak{B} + \Lambda_o^2}{n_2 \eta}}.$$

Since  $1/\sqrt{n_2 \eta} \rightarrow 0$  when  $z \in Q^{(p)}$ , it is easy to deduce that  $\mathbb{1}(\Xi)\Lambda_o < \Psi_{\mathfrak{B}}$ .

An analogous argument for  $|W_s|$  (see e.g. Lemma 5.2 of Erdős et al. (2013)) completes the proof of the statement in Proposition S.5.1 when  $\Xi$  holds.

As for the case when  $\eta \geq 1$ , we proceed similarly. For  $\eta \geq 1$ , we proceed as above to get  $|W_s| < n_2^{-1/2}$ ,

where we used that  $\|\mathbf{J}\| \leq C/\eta \leq C$  by Lemma S.5.3. Similarly, as in Eq. (S.6), we get

$$\mathbf{J}_{uv} \leq |\mathbf{J}_{uu}\mathbf{J}_{vv}^{(u)}| \left| \sum_{i,j=p+1}^{p+n_2} \tilde{Z}_{ui}\tilde{Z}_{vj}\mathbf{J}_{i,j}^{(uv)} \right| < |\mathbf{J}_{uu}\mathbf{J}_{vv}^{(u)}| \frac{1}{\sqrt{n_2}},$$

where in the last step we used that  $|\Im\mathbf{J}_{ii}^{(uv)}| \leq C$  because  $\|\mathbf{J}\| \leq C$ . Moreover,  $|\mathbf{J}_{uu}\mathbf{J}_{vv}^{(u)}| \leq C$ . This completes the proof of Lemma S.5.5.  $\square$

In the following, we aim to show that  $\hat{\phi}_p$  satisfies a perturbed version of Eq. (S.2) when  $\Xi$  holds or when  $\eta \geq 1$ . From Eq. (S.4), Eq. (S.5), Lemma S.5.5, Result (v) of Lemma S.5.2, we get that uniformly for  $u \in \{1, \dots, p\}$ ,  $i \in \{p+1, \dots, p+n_2\}$ ,  $z \in Q^{(p)} \cup Q_{\text{away}}^{(p)}$ ,

$$\mathbb{1}(\Xi) \frac{1}{\mathbf{J}_{uu}} = \mathbb{1}(\Xi) \left( \lambda/\sigma_u - z - \frac{1}{n_2} \sum_{i=p+1}^{p+n_2} \mathbf{J}_{ii} - W_u + O_{<}(\Psi_{\mathfrak{B}}^2) \right), \quad (\text{S.7})$$

$$-\mathbb{1}(\Xi) \frac{1}{\mathbf{J}_{ii}} = \mathbb{1}(\Xi) \left( 1 + \frac{1}{n_2} \sum_{u=1}^p \mathbf{J}_{uu} + W_i + O_{<}(\Psi_{\mathfrak{B}}^2) \right). \quad (\text{S.8})$$

Invert Eq. (S.8), get the Taylor's expansion of the right-hand side to the order of  $W_i^2$ , and average the equation over  $i = p+1, \dots, p+n_2$ . We obtain

$$-\mathbb{1}(\Xi) \frac{1}{n_2} \sum_{i=p+1}^{p+n_2} \mathbf{J}_{ii} = \mathbb{1}(\Xi) \frac{1}{1 + \frac{1}{n_2} \sum_{u=1}^p \mathbf{J}_{uu}} + \mathbb{1}(\Xi) \delta_1, \quad (\text{S.9})$$

where the residual  $\delta_1$  is

$$\mathbb{1}(\Xi) \delta_1 = \mathbb{1}(\Xi) [W]_n + \mathbb{1}(\Xi) \frac{1}{n_2} \sum_{i=p+1}^{p+n_2} O_{<}(|W_i|^2) + \mathbb{1}(\Xi) O_{<}(\Psi_{\mathfrak{B}}^2) = \mathbb{1}(\Xi) [W]_n + O_{<}(\Psi_{\mathfrak{B}}^2),$$

$$[W]_n = \frac{1}{(1 + \frac{1}{n_2} \sum_{u=1}^p \mathbf{J}_{uu})^2} \frac{1}{n_2} \sum_{i=p+1}^{p+n_2} W_i.$$

Here, we are using Lemma S.5.5.

Similarly, from Eq. (S.7),

$$\mathbb{1}(\Xi) \frac{1}{p} \sum_{u=1}^p \mathbf{J}_{uu} = \mathbb{1}(\Xi) \frac{1}{p} \sum_{u=1}^p \frac{1}{\lambda/\sigma_u - z - \frac{1}{n_2} \sum_{i=p+1}^{p+n_2} \mathbf{J}_{ii}} + \delta_2,$$

where

$$\mathbb{1}(\Xi) \delta_2 = \mathbb{1}(\Xi) [W]_p + \mathbb{1}(\Xi) \frac{1}{p} \sum_{u=1}^p O_{<}(|W_u|^2) + \mathbb{1}(\Xi) O_{<}(\Psi_{\mathfrak{B}}^2) = \mathbb{1}(\Xi) [W]_p + O_{<}(\Psi_{\mathfrak{B}}^2),$$

$$[W]_p = \frac{1}{p} \sum_{u=1}^p \frac{-1}{(\lambda/\sigma_u - z - \frac{1}{n_2} \sum_{i=p+1}^{p+n_2} \mathbf{J}_{ii})^2} W_u.$$

All together, we obtain

$$\mathbb{1}(\Xi) \hat{\phi}_p = \mathbb{1}(\Xi) \int \frac{dF^{\Sigma_p}(\tau)}{\lambda/\tau - z - \frac{1}{1 + (p/n_2) \hat{\phi}_p}} + \mathbb{1}(\Xi) \delta_2,$$

which is a perturbed version of Eq. (S.2). Note that Lemma S.5.5 guarantees that  $\mathbb{1}(\Xi) \delta_1 < \Psi_{\mathfrak{B}}$  and  $\mathbb{1}(\Xi) \delta_2 < \Psi_{\mathfrak{B}}$ . This estimate is actually not tight. We shall later improve the estimate to  $O_{<}(\Psi_{\mathfrak{B}}^2)$ .

On the other hand, it is not hard to identify that the derivation actually only relies on fact that  $\mathbb{1}(\Xi)(|W|_s + \Lambda_o) < \Psi_{\mathfrak{B}}$  from Lemma S.5.5. Since the same control holds when  $\eta \geq 1$ . We obtain that

$$\mathbb{1}(\eta \geq 1) \hat{\phi}_p = \mathbb{1}(\eta \geq 1) \int \frac{dF^{\Sigma_p}(\tau)}{\lambda/\tau - z - \frac{1}{1 + (p/n_2) \hat{\phi}_p}} + \mathbb{1}(\eta \geq 1) \delta_2,$$

and  $\mathbb{1}(\eta \geq 1) \delta_1 < \Psi_{\mathfrak{B}}$ ,  $\mathbb{1}(\Xi) \delta_2 < \Psi_{\mathfrak{B}}$ .

We apply Lemma S.4.5, Lemma S.4.6, and Corollary S.4.3 to control the difference between  $\hat{\phi}_p$  and  $\phi_p$  when  $\eta \geq 1$ . In particular, we have the following results.

**Lemma S.5.6.** *Suppose that the conditions of Theorem S.5.2 hold. Then, we have  $\Lambda < n_2^{-1/2}$  uniformly in  $z \in Q^{(p)} \cup Q_{\text{away}}^{(p)}$  satisfying  $\eta \geq 1$ .*

*Proof.* Applying Lemma S.5.5,  $\Lambda_o < \Psi_{\mathfrak{B}} < n_2^{-1/2}$ . Here, we are using the fact that  $\Im \phi_p + \mathfrak{B} = O(1)$ , when  $\eta \geq 1$ . We only need to show the diagonal elements are such that

$$\begin{aligned} \mathbf{J}_{uu} - \frac{1}{\lambda/\sigma_u - m_p} &< n_2^{-1/2}, \quad u = 1, 2, \dots, p, \\ -\mathbf{J}_{ii} - \frac{1}{1 + p/n_2 \phi_p} &< n_2^{-1/2}, \quad i = p+1, p+2, \dots, p+n_2. \end{aligned}$$

Applying Lemma S.4.6 or Corollary S.4.3, when  $\eta \geq 1$ ,

$$|\hat{\phi}_p - \phi_p| \leq C(|\delta_1| + |\delta_2|) < \Psi_{\mathfrak{B}} < n_2^{-1/2}.$$

Then, by Eq. (S.8)

$$-\frac{1}{\mathbf{J}_{ii}} = 1 + \phi_p + (\hat{\phi}_p - \phi_p) + W_i + O_{<}(\Psi_{\mathfrak{B}}^2) = 1 + \phi_p + O_{<}(n_2^{-1/2}).$$

Therefore,  $-\mathbf{J}_{ii} - \frac{1}{1 + \phi_p} < n_2^{-1/2}$ . The estimate of  $\mathbf{J}_{uu}$  is obtained similarly.  $\square$

To show Proposition S.5.1, we apply the stochastic continuity argument, exactly as Section 4 of Alex Bloemendal et al. (2014). The argument allows us to propagate smallness of  $\Lambda$  from  $\eta \geq 1$  to the whole domain  $Q^{(p)} \cup Q_{\text{away}}^{(p)}$ . Note that in the domain,  $\eta \geq n_2^{-1+a'}$ . We choose  $\varepsilon < a'/4$  and an arbitrary  $D > 0$ . Let

$$L(z) = \{z\} \cup \{s \in Q^{(p)} \cup Q_{\text{away}}^{(p)} : \Re s = \Re z, \quad \Im s \in [\Im z, 1] \cap [n_2^{-5}\mathbb{N}]\}.$$

We introduce the random function

$$v(z) := \max_{s \in L(z)} \Lambda(s)(n_2 \Im s)^{1/4}$$

Our goal is to prove that with high probability there is a gap in the range of  $v$ , i.e.

$$\mathbb{P} \left( v(z) \leq n_2^\varepsilon, \quad v(z) > n_2^{\varepsilon/2} \right) \leq N^{-D+5} \quad (\text{S.10})$$

for all  $z \in Q^{(p)} \cup Q_{\text{away}}^{(p)}$  and large enough  $n_2$ . This equation says that with high probability the range of  $v$  has a gap: it cannot take values in the interval  $(n_2^{\varepsilon/2}, n_2^\varepsilon]$ .

Since we are dealing with random variables, one has to keep track of probabilities of exceptional events. To that end, we only work on a discrete set of values of  $\eta$ , which allows us to control the exceptional probabilities by a simple union bound.

Next, we prove Eq. (S.10). First, Lemma S.5.5 yields  $\mathbb{1}(\Xi)(|\delta_1| + |\delta_2|) < \Psi_{\mathfrak{B}} \leq (n_2 \eta)^{-1/2}$ . Since  $\{v(z) \leq n_2^\varepsilon\} \subset \Xi(z) \cap \Xi(s)$  for all  $z \in Q^{(p)} \cup Q_{\text{away}}^{(p)}$  and  $s \in L(z)$ , we find that for all  $z \in Q^{(p)} \cup Q_{\text{away}}^{(p)}$  and  $s \in L(z)$  that

$$\mathbb{P} \left( v(z) \leq n_2^\varepsilon, \quad (|\delta_1(s)| + |\delta_2(s)|)(n_2 \Im s)^{1/2} > n_2^{\varepsilon/2} \right) \leq n_2^{-D}$$

for large enough  $n_2$  (independent of  $z$  and  $w$ ). Using a union bound, we therefore get

$$\mathbb{P} \left( v(z) \leq n_2^\varepsilon, \quad \max_{s \in L(z)} (|\delta_1| + |\delta_2|)(n_2 \Im s)^{1/2} > n_2^{\varepsilon/2} \right) \leq n_2^{-D+5}$$

Next, applying Lemma S.4.5 and Lemma S.4.6 with the perturbation  $n_2^{\varepsilon/2}(n_2 \Im s)^{-1/2}$ , we get

$$\mathbb{P} \left( v(z) \leq n_2^\varepsilon, \quad \max_{s \in L(z)} \mathfrak{B}_p(s)(n_2 \Im s)^{1/4} > n_2^{\varepsilon/4} \right) \leq n_2^{-D+5}.$$

Moreover, since  $-\mathbf{J}_{ii} - (1 + (p/n_2)\phi_p)^{-1} = O_{<}(\mathfrak{B}_p) + O_{<}(\Psi_{\mathfrak{B}})$ , we have

$$\mathbb{P} \left( v(z) \leq n_2^\varepsilon, \quad \max_{s \in L(z)} \mathfrak{B}(s)(n_2 \Im s)^{1/4} > 2n_2^{\varepsilon/4} \right) \leq n_2^{-D+5}.$$

Then, Eq. (S.10) follows from the bound

$$\begin{aligned}
& \mathbb{P}\left(v(z) \leq n_2^\varepsilon, v(s) \geq n_2^{\varepsilon/2}\right) \\
& \leq \mathbb{P}\left(v(z) \leq n_2^\varepsilon, \max_{s \in L(z)} \Lambda(s)(n_2 \Im s)^{1/4} \geq n_2^{\varepsilon/2}\right) \\
& \leq \mathbb{P}\left(v(z) \leq n_2^\varepsilon, \max_{s \in L(z)} \Psi_{\mathfrak{B}}(n_2 \Im s)^{1/4} \geq n_2^{\varepsilon/2}\right) \\
& \leq \mathbb{P}\left(v(z) \leq n_2^\varepsilon, \max_{s \in L(z)} \mathfrak{B}(n \Im s)^{-1}(n_2 \Im s)^{1/2} \geq (1/2)n_2^\varepsilon\right) + n^{-D+5} \\
& \leq \mathbb{P}\left(v(z) \leq n_2^\varepsilon, \max_{s \in L(z)} \mathfrak{B}(n_2 \Im s)^{1/4} \geq n_2^\varepsilon(n_2 \Im s)^{3/4}/2\right) + n^{-D+5} \\
& \leq \mathbb{P}\left(v(z) \leq n_2^\varepsilon, \max_{s \in L(z)} \mathfrak{B}(n_2 \Im s)^{1/4} \geq n_2^\varepsilon(n_2)^{3a'/4}/2\right) + n^{-D+5} \\
& \leq 2n_2^{-D+5}.
\end{aligned}$$

Here, we are using the fact that for all  $s \in L(z)$

$$\frac{\Im \phi_p(s)}{n_2 \Im s} (n_2 \Im s)^{1/2} = \frac{\Im \phi_p(s)}{\sqrt{n_2 \Im s}} < 1.$$

Therefore,

$$\mathbb{P}\left(v(z) \leq n_2^\varepsilon, \max_{s \in L(z)} \Im \phi_p(s)(n \Im s)^{-1}(n_2 \Im s)^{1/2} \geq (1/2)n_2^\varepsilon\right) \leq n_2^{-D+5}.$$

We conclude the proof of Proposition S.5.1 by combining Eq. (S.10) and Lemma (S.5.6) with a continuity argument. We choose a lattice  $\Delta \subset Q^{(p)} \cup Q_{\text{away}}^{(p)}$  such that  $|\Delta| \leq n_2^{10}$  and for each  $z \in Q^{(p)} \cup Q_{\text{away}}^{(p)}$  there exists a  $s \in \Delta$  satisfying  $|z - s| \leq N^{-4}$ . Then, Eq. (S.10) combined with a union bound yields

$$\mathbb{P}\left(\exists s \in \Delta : v(s) \in \left(n_2^{\varepsilon/2}, n_2^\varepsilon\right]\right) \leq n_2^{-D+15}$$

From the definitions of  $\Lambda$  and  $Q^{(p)} \cup Q_{\text{away}}^{(p)}$ , we find that  $v$  is Lipschitz continuous, with Lipschitz constant  $n_2^2$ .

$$\mathbb{P}\left(\exists z \in Q^{(p)} \cup Q_{\text{away}}^{(p)} : v(z) \in \left(2n_2^{\varepsilon/2}, n_2^\varepsilon\right]\right) \leq n_2^{-D+15}$$

By Lemma S.5.6, we have

$$\mathbb{P}\left(v(z) > n_2^{\varepsilon/2}\right) \leq n_2^{-D+15}$$

for any  $z \in Q^{(p)} \cup Q_{\text{away}}^{(p)}$  with  $\eta \geq 1$ . Therefore,

$$\mathbb{P}\left(\max_{z \in Q^{(p)} \cup Q_{\text{away}}^{(p)}} v(z) > 2n_2^{\varepsilon/2}\right) \leq 2n_2^{-D+15}.$$

It completes the proof of Proposition S.5.1.

### S.5.1.3 The averaged local law

We use Proposition S.5.1 and improved estimates for the averaged quantities  $[W]_p$  and  $[W]_n$  to deduce the averaged local laws in  $Q^{(p)}$ ,  $Q_-^{(p)}$ , and  $Q_{\text{away}}^{(p)}$ , as in Theorem S.5.1. Indeed, we shall show that

$$\mathbb{1}(\Xi)[W]_p < \Psi_{\mathfrak{B}}^2 \quad \text{and} \quad \mathbb{1}(\Xi)[W]_n < \Psi_{\mathfrak{B}}^2.$$

If so, the estimate of  $\delta_1$  and  $\delta_2$  is improved to  $\mathbb{1}(\Xi)|\delta_1| < \Psi_{\mathfrak{B}}^2$  and  $\mathbb{1}(\Xi)|\delta_2| < \Psi_{\mathfrak{B}}^2$ .

**Lemma S.5.7** (Fluctuation averaging). *Suppose that the assumptions of Theorem S.5.1 hold. Suppose that  $\Upsilon$  is a positive,  $n_2$ -dependent, deterministic function on  $Q^{(p)} \cup Q_{\text{away}}^{(p)}$  satisfying  $n_2^{-1/2} \leq \Upsilon \leq n_2^{-c}$  for some constant  $c > 0$ . Suppose moreover that  $\Lambda < n_2^{-c}$  and  $\Lambda_o < \Upsilon$  on  $Q^{(p)} \cup Q_{\text{away}}^{(p)}$ . Then on  $Q^{(p)} \cup Q_{\text{away}}^{(p)}$  we have*

$$\frac{1}{p} \sum_{u=1}^p \frac{1}{(\lambda/\sigma_u - z - \frac{1}{n_2} \sum_{i=p+1}^{p+n_2} \mathbf{J}_{ii})^2} (1 - \mathbb{E}_u) \frac{1}{\mathbf{J}_{uu}} = O_{<}(\Upsilon^2)$$

and

$$\frac{1}{n_2} \sum_{i=p+1}^{p+n_2} (1 - \mathbb{E}_i) \frac{1}{\mathbf{J}_{ii}} = O_{<}(\Upsilon^2).$$

Th results are an extension of Lemma 5.6 of Knowles and Yin (2017), Lemma 4.9 of Alex Bloemendal et al. (2014), Theorem 4.7 of Erdős et al. (2013). They can be proved using exactly the same method. We therefore omit the details. The readers may refer to the proof of Theorem 4.7 of Erdős et al. (2013) for details.

Note that Proposition S.5.1 implies that  $1 - \mathbb{1}(\Xi) < 0$ , that is  $\Xi$  holds with high probability. In the following analysis, we shall always assume  $\Xi$  holds. Combining with Lemma S.5.5, we have

$$\Lambda < \frac{1}{(n_2 \eta)^{1/4}}, \quad \Lambda_o < \Psi_{\mathfrak{B}},$$

on  $Q^{(p)} \cup Q_{\text{away}}^{(p)}$ . Therefore, the condition of Lemma S.5.7 is satisfied and we obtain

$$|[W]_p| + |[W]_n| < \Psi_{\mathfrak{B}}^2,$$

on  $Q^{(p)} \cup Q_{\text{away}}^{(p)}$ . Recall that  $\delta_1 = [W]_n + O_{<}(\Psi_{\mathfrak{B}}^2)$  and  $\delta_2 = [W]_p + O_{<}(\Psi_{\mathfrak{B}}^2)$ . We immediately get

$$(|\delta_1| + |\delta_2|) < \Psi_{\mathfrak{B}}^2,$$

uniformly in  $Q^{(p)} \cup Q_{\text{away}}^{(p)}$ .

The following lemma holds immediately from the definition of  $\Psi_{\mathfrak{B}}$ .

**Lemma S.5.8.** *Let  $c > 0$  and suppose that we have  $\mathfrak{B} < (n_2\eta)^{-c}$  uniformly in  $z \in Q^{(p)} \cup Q_{\text{away}}^{(p)}$ . Then, we have*

$$|\delta_1| + |\delta_2| < \frac{\Im\phi_p + (n_2\eta)^{-c}}{n_2\eta}$$

uniformly in  $z \in Q^{(p)} \cup Q_{\text{away}}^{(p)}$ .

We first consider the averaged local law in  $Q^{(p)}$ . Suppose  $\mathfrak{B} < (n_2\eta)^{-c}$ . Then, uniformly in  $z \in Q^{(p)}$ ,

$$|\delta_1| + |\delta_2| < \frac{\Im\phi_p + (n_2\eta)^{-c}}{n_2\eta}.$$

We invoke Lemma S.4.5 to get

$$\begin{aligned} \mathfrak{B}_p = |\hat{\phi}_p - \phi_p| &< \frac{\frac{\Im\phi_p + (n_2\eta)^{-c}}{n_2\eta}}{\sqrt{\kappa + \eta} + \sqrt{\frac{\Im\phi_p + (n_2\eta)^{-c}}{n_2\eta}}} \leq \frac{\Im\phi_p}{n_2\eta} \frac{1}{\sqrt{\kappa + \eta}} + \sqrt{\frac{(n_2\eta)^{-c}}{n_2\eta}} \\ &\leq \frac{C}{n_2\eta} + (n_2\eta)^{-1/2-c/2} < (n_2\eta)^{-1/2-c/2}. \end{aligned} \quad (\text{S.11})$$

In the fourth step, we are using the expression of  $\Im\phi_p$  as shown in Lemma S.4.3. As for  $\mathfrak{B}_n$ , plugging the estimate of  $\hat{\phi}_p$  back to Eq. (S.9), we also have

$$\mathfrak{B}_n < \mathfrak{B}_p + \Psi_{\mathfrak{B}}^2 < (n_2\eta)^{-1/2-c/2} + \frac{\Im\phi_p + (n_2\eta)^{-c}}{n_2\eta} < (n_2\eta)^{-1/2-c/2}.$$

All together, we have shown that

$$\mathfrak{B} < (n_2\eta)^{-c} \quad \implies \quad \mathfrak{B} < (n_2\eta)^{-1/2-c/2}. \quad (\text{S.12})$$

From Proposition S.5.1, we know that  $\mathfrak{B} \leq C\Lambda < (n_2\eta)^{-1/4}$ . Therefore, for any  $\varepsilon > 0$ , we iterate Eq. (S.12) finite number of times to get,

$$\mathfrak{B} < (n_2\eta)^{-1+\varepsilon}.$$

It completes the proof of the averaged local law in  $Q^{(p)}$  in Theorem S.5.1 under the additional assumption that  $\Sigma_p$  is diagonal.

Next, we consider the averaged local law in  $Q_-^{(p)}$ . This follows exactly from the same arguments but with the specific form of  $\Im\phi_p$  when  $E \leq \rho - n^{-2/3+a'}$ . When  $E$  is restricted to  $E \leq \rho - n_2^{-2/3+a'}$  and  $\eta \geq n_2^{-2/3}$ , we

have

$$\Im\phi_p \asymp \frac{\eta}{\sqrt{\kappa + \eta}},$$

where  $\kappa = \rho - E$ . Assume that  $\mathfrak{B} < (n_2\eta)^{-c}$ . When  $z \in Q_-^{(p)}$ , Eq. (S.11) can be improved to

$$\mathfrak{B}_p < \frac{\Im\phi_p}{n_2\eta\sqrt{\kappa + \eta}} + \frac{1}{(n_2\eta)^c} \frac{1}{n_2\eta\sqrt{\kappa + \eta}} = \frac{1}{n_2(\kappa + \eta)} + \frac{1}{(n_2\eta)^c} \frac{1}{n_2\eta\sqrt{\kappa + \eta}} < \frac{1}{n_2(\kappa + \eta)} + \frac{1}{(n_2\eta)^{c+a'/2}}.$$

plugging the estimate of  $\hat{\phi}_p$  back to Eq. (S.9), we also have

$$\mathfrak{B}_n < \mathfrak{B}_p + \frac{\Im\phi_p + (n_2\eta)^{-c}}{n_2\eta} < \frac{1}{n_2(\kappa + \eta)} + \frac{1}{(n_2\eta)^{c+a'/2}}.$$

All together, we get

$$\mathfrak{B} < \frac{1}{(n_2\eta)^c} \implies \mathfrak{B} < \frac{1}{n_2(\kappa + \eta)} + \frac{1}{(n_2\eta)^{c+a'/2}}.$$

Again, from Propostion S.5.1,  $\mathfrak{B} < (n_2\eta)^{-1/4}$ . We iterate the equation finite number of times to get,

$$\mathfrak{B} < \frac{1}{n_2(\kappa + \eta)},$$

uniformly on  $Q_-^{(p)}$ . It completes the proof of the averaged local law in  $Q_-^{(p)}$  in Theorem S.5.1 under the additional assumption that  $\Sigma_p$  is diagonal.

Lastly, we consider the averaged local law in  $Q_{\text{away}}^{(p)}$ . It follows from similar arguments as the previous two cases. On  $Q_{\text{away}}^{(p)}$ , we invoke Lemma S.4.6 to control  $|\hat{\phi}_p - \phi_p|$ . Assuming  $\mathfrak{B} < (n_2\eta)^{-c}$ , then

$$\mathfrak{B}_p = |\hat{\phi}_p - \phi_p| \leq C|\delta_1| + C|\delta_2| < \frac{\Im\phi_p + (n_2\eta)^{-c}}{n_2\eta} < \frac{1}{n_2} + (n_2\eta)^{-c-1} < \frac{1}{n_2} + (n_2\eta)^{-c-1}.$$

Here, we are using the fact that  $\Im\phi_p/\eta \asymp 1$  when  $z$  is away from the support of  $\mathcal{G}_\lambda$ . The rest arguments are very similar to those in the previous two cases. We omit further details.

We completed the proof of the averaged local laws when  $\Sigma_p$  is diagonal. The diagonal assumption will be removed in Section S.5.1.5.

#### S.5.1.4 The entrywise local law

It remains to prove the entrywise local law. Using Eq. (S.4), Result (v) of Lemma S.5.2, Lemma S.5.5 and the averaged local law, we obtain

$$\mathbf{J}_{uu} - \frac{1}{\lambda/\sigma_u - z + \phi_p} < \Psi_{\mathfrak{B}} < \Psi,$$

uniformly for  $u = 1, \dots, p$  and  $z \in Q^{(p)}$ . Similarly, using Eq. (S.5),

$$\mathbf{J}_{ii} + \frac{1}{1 + (p/n_2)\phi_p} < \Psi,$$

uniformly for  $i = p + 1, \dots, p + n_2$  and  $z \in Q^{(p)}$ . Moreover, since  $\Lambda_o < \Psi_{\mathfrak{B}} < \Psi$ , the entrywise local law follows.

### S.5.1.5 Extension to non-diagonal $\Sigma_p$

In this section, we show that Theorem S.5.1 and Theorem S.5.2 when the population covariance matrix is non-diagonal. In order to utilize the notation in the previous sections, we denote the population covariance as  $\tilde{\Sigma}_p$  and continue to use  $\Sigma_p$  to denote the diagonal matrix containing the eigenvalues of  $\tilde{\Sigma}_p$ . The eigendecomposition of  $\tilde{\Sigma}_p$  is denoted as

$$\tilde{\Sigma}_p = H\Sigma_p H^T,$$

where  $H$  is the eigenvector matrix of  $\tilde{\Sigma}_p$ . In this section, we show that if Theorem S.5.1 holds with  $\Sigma_p$ , it also holds with  $\tilde{\Sigma}_p$ . All definitions in Section S.5.1.1 are kept.

Define

$$\begin{aligned} \tilde{\mathbf{K}} &= \begin{pmatrix} H & 0 \\ 0 & I_{n_2} \end{pmatrix} \mathbf{K} \begin{pmatrix} H^T & 0 \\ 0 & I_{n_2} \end{pmatrix}, \\ \tilde{\mathbf{J}} &= \begin{pmatrix} H & 0 \\ 0 & I_{n_2} \end{pmatrix} \mathbf{J} \begin{pmatrix} H^T & 0 \\ 0 & I_{n_2} \end{pmatrix}, \\ \tilde{\Omega} &= \begin{pmatrix} H & 0 \\ 0 & I_{n_2} \end{pmatrix} \Omega \begin{pmatrix} H^T & 0 \\ 0 & I_{n_2} \end{pmatrix}. \end{aligned}$$

Then,  $\tilde{\mathbf{K}}$ ,  $\tilde{\mathbf{J}}$  and  $\tilde{\Omega}$  are equal to  $\mathbf{K}$ ,  $\mathbf{J}$  and  $\Omega$  when  $\Sigma_p$  is replaced by  $\tilde{\Sigma}_p$ .

The averaged local laws in  $Q^{(p)}$ ,  $Q_-^{(p)}$  and  $Q_{\text{away}}^{(p)}$  still hold when  $\mathbf{J}$  and  $\Omega$  are replaced by  $\tilde{\mathbf{J}}$  and  $\tilde{\Omega}$ , since

$$\frac{1}{p} \sum_{u=1}^p \tilde{\mathbf{J}}_{uu} = \frac{1}{p} \text{tr}(\tilde{\mathbf{J}}_{(11)}) = \frac{1}{p} \text{tr}(\mathbf{J}_{(11)} H^T H) = \hat{\phi}_p.$$

It remains to show the entrywise local law. We shall actually show

$$H(\mathbf{J}_{(11)} - \Omega_{(11)})H^T = O_{<}(\Psi),$$

uniformly in  $Q^{(p)}$ . In components, this reads

$$\left| \sum_{u,v=1}^p H_{iu} \left( \mathbf{J}_{uv} - \mathbb{1}(u=v) \frac{1}{\lambda/\sigma_u - m_p} \right) H_{vj} \right| < \Psi,$$

for all  $i, j \in \{1, 2, \dots, p\}$ .

The proof is based on the polynomialization method developed in Section 5 of Alex Bloemendal et al. (2014). The argument is very similar to that of Alex Bloemendal et al. (2014), and we only outline the differences.

By the assumption

$$\mathbf{J}_{(11)} - (\lambda \Sigma_p^{-1} - m_p I_p)^{-1} = O_{<}(\Psi)$$

and orthogonality of  $H$ , we have

$$\sum_{u,v=1}^p H_{iu} \left( \mathbf{J}_{uv} - \mathbb{1}(u=v) \frac{1}{\lambda/\sigma_u - m_p} \right) H_{vj} = \sum_{u=1}^p H_{iu} \left( \mathbf{J}_{uu} - \frac{1}{\lambda/\sigma_u - m_p} \right) H_{uj} + \sum_{u \neq v} H_{iu} \mathbf{J}_{uv} H_{vj} = O_{<}(\Psi) + \mathcal{Z}$$

where we defined  $\mathcal{Z} := \sum_{u \neq v} H_{iu} \mathbf{J}_{uv} H_{vj}$ . We need to prove that  $|\mathcal{Z}| < \Psi$ , which, following Section 5 of Alex Bloemendal et al. (2014) we do by estimating the moment  $\mathbb{E}|\mathcal{Z}|^k$  for fixed  $k \in 2\mathbb{N}$ . The argument from Section 5 of Alex Bloemendal et al. (2014) may be taken over with minor changes.

Use Result (ii) and (v) of Lemma S.5.2,

$$\sum_{u \neq v \notin S} H_{iu} \mathbf{J}_{uv}^{(S)} H_{vj} = \sum_{u \neq v \notin S} H_{iu} H_{vj} \mathbf{J}_{uu}^{(S)} \mathbf{J}_{vv}^{(S \cup \{u\})} \left( \tilde{\mathbf{Z}}_u \cdot \mathbf{J}_{(22)}^{(S \cup \{uv\})} \tilde{\mathbf{Z}}_v^T \right)$$

for any  $S \subset \{1, 2, \dots, p\}$  and

$$\begin{aligned} \mathbf{J}_{uu}^{(S)} &= \frac{1}{\lambda/\sigma_u - z - \tilde{\mathbf{Z}}_u \cdot \mathbf{J}_{(22)}^{(S \cup \{u\})} \tilde{\mathbf{Z}}_u^T} \\ &= \sum_{\ell=0}^{L-1} \frac{1}{(\lambda/\sigma_u - z + [1 + (p/n_2)\phi_p]^{-1})^{\ell+1}} \left( \left( \tilde{\mathbf{Z}}_u \cdot \mathbf{J}_{(22)}^{(S \cup \{u\})} \tilde{\mathbf{Z}}_u^T \right) - \frac{1}{1 + (p/n_2)\phi_p} \right)^\ell + O_{<}(\Psi^L). \end{aligned}$$

We omit further details.

## S.5.2 Proof of Theorem S.5.2

The rigidity of the smallest eigenvalue of  $\mathbf{G}_\lambda$  can be proved using the averaged local law in  $Q_-^{(p)}$  as in Theorem S.5.1. In the following,  $\epsilon \in (0, 2/3)$  is fixed. Notice that  $|\rho_p - \rho| = o(p^{-2/3})$ . We only need to show that with high probability there is no eigenvalue in  $(-\infty, \rho_p - n_2^{-2/3+\epsilon})$ . Indeed, it suffices to consider the interval  $[\lambda/\ell_{\max}(\Sigma_p), \rho_p - n_2^{-2/3+\epsilon}]$ , since  $\mathbf{G}_\lambda = \tilde{\mathbf{Z}} \tilde{\mathbf{Z}}^T + \lambda \Sigma_p^{-1}$ .

Recall the definition of  $Q^{(p)}$  and  $Q_-^{(p)}$ . We consider  $a$  and  $a'$  to be sufficiently small so that  $\{z : E \in \lambda/\ell_{\max}(\Sigma_p), \rho_p - n_2^{-2/3+\epsilon}], n_2^{-2/3} \leq \eta \leq 1\}$  is contained in  $Q_-^{(p)}$ . Consider the set  $Q^* = Q_-^{(p)} \cap \{z \mid \eta = n_2^{-1/2-\epsilon/4}|E - \rho|^{1/4}\}$ .

To show that there is no eigenvalue in  $[\lambda/\ell_{\max}(\Sigma_p), \rho - n_2^{-2/3+\epsilon}]$ , we only need to show that uniformly in  $Q^*$

$$\Im \hat{\phi}_p(z) < n_2^{-\epsilon/2}(n_2\eta)^{-1}.$$

It is because that  $\hat{\phi}_p$  is the Stieltjes transform of  $\mathbf{G}_\lambda$ . When  $z = \ell(\mathbf{G}_\lambda) + i\eta$  where  $\ell(\mathbf{G}_\lambda)$  is an eigenvalue of  $\mathbf{G}_\lambda$ ,  $\Im \hat{\phi}_p(z) \asymp \frac{1}{n_2\eta}$ .

Recall that in Lemma S.4.3 for  $z \in Q^*$ ,

$$\Im \phi_p \asymp \eta(|E - \rho| + \eta)^{-1/2}.$$

We conclude that it suffices to prove

$$|\hat{\phi}_p - \phi_p| < \frac{1}{n_2(|E - \rho| + \eta)},$$

which is ensured by the averaged local law in  $Q_-^{(p)}$  in Theorem S.5.1.

### S.5.3 Proof of Theorem S.5.3

Theorem S.5.2 indicates that the smallest eigenvalue of  $\mathbf{G}_\lambda$  is larger than  $\rho - \epsilon$  with high probability. Lemma S.5.4 indicates that the largest eigenvalue of  $\mathbf{G}_\lambda$  is smaller than  $x_{\text{right}} = (1 + \sqrt{\gamma_2})^2 + \lambda/\liminf \ell_{\min}(\Sigma_p) + \epsilon$ . Therefore, the statement in (i) of Theorem S.5.3 holds.

The convergence of  $p^{-1} \sum_{j=1}^p f(\ell_j(\mathbf{G}_\lambda))$  can be proved using the strategy of Bai and Silverstein (2004). We consider a contour in the complex plane that encloses the interval  $[\rho - \epsilon, (1 + \sqrt{\gamma_2})^2 + \lambda/\liminf \ell_{\min}(\Sigma_p) + \epsilon]$ . Without loss of generality, we choose the rectangle, denoted to be  $\mathcal{R}$ , with the four vertices

$$z_1 = \rho - 2\epsilon + \epsilon'i, \quad z_2 = \rho - 2\epsilon - \epsilon'i, \quad z_3 = x_{\text{right}} + \epsilon + \epsilon'i, \quad z_4 = x_{\text{right}} + \epsilon - \epsilon'i.$$

In the following, we choose  $\epsilon$  and  $\epsilon'$  to be sufficiently small so that the function  $f$  is analytic on the rectangle.

Clearly, with high probability the rectangle encloses all eigenvalues of  $\mathbf{G}_\lambda$ . When it is true,

$$\frac{1}{p} \sum_{j=1}^p f(\ell_j(\mathbf{G}_\lambda)) = \int f(\tau) dF^{\mathbf{G}_\lambda}(\tau) = \frac{1}{2\pi i} \oint_{\mathcal{R}} f(z) \hat{\phi}_p(z) dz.$$

Here, the contour integral is taken over the rectangle in the positive direction in the complex plane. In the integral, we extend the definition of  $\hat{\phi}_p$  to  $\mathbb{C}^-$  by setting  $\hat{\phi}_p(z) = \overline{\hat{\phi}_p(\bar{z})}$  if  $\eta(z) < 0$ .

Fix any  $c \in (0, 1)$ . We truncate  $\mathcal{R}$  at  $\eta = n_2^{-1+c/2}$ . Specifically, we define  $\hat{\mathcal{R}} = \mathcal{R} \cap \{z : \eta \geq n_2^{-1+c/2}\}$ . Then,

$$n_2^{1-c} \mathbb{1}(\mathfrak{M}) \left| \oint_{\mathcal{R} \setminus \hat{\mathcal{R}}} f(z) \hat{\phi}_p(z) dz \right| \leq C n_2^{1-c} n_2^{-1+c/2} \rightarrow 0.$$

It follows

$$\left| \oint_{\mathcal{R} \setminus \hat{\mathcal{R}}} f(z) \hat{\phi}_p(z) dz \right| < \frac{1}{n_2}.$$

Therefore, to show

$$\left| \frac{1}{p} \sum_{j=1}^p f(\ell_j(\mathbf{G}_\lambda)) - \int f(\tau) d\mathcal{G}_\lambda(\tau) \right| < \frac{1}{n_2},$$

it suffices to show

$$\oint_{\hat{\mathcal{R}}} |f(z)| \left| \hat{\phi}_p(z) - \phi_p(z) \right| dz < \frac{1}{n_2}.$$

It is a direct consequence from the averaged local law on  $Q_{\text{away}}^{(p)}$  in Theorem S.5.1. It completes the proof.

#### S.5.4 Discrete case

In Theorem S.5.1, Theorem S.5.2, Theorem S.5.3, we focus on the case when  $\rho > \lambda/\sigma_{\max}$  as in **SC2**. In this section, we consider the case when  $\rho = \lambda/\sigma_{\max}$ . We show analogous results as Theorem S.5.1, Theorem S.5.2 and Theorem S.5.3.

**Theorem S.5.4.** *Suppose that C1–C6 and SC1 hold. Suppose  $\rho = \lambda/\sigma_{\max}$ . Then, with probability 1, the smallest eigenvalue of  $\mathbf{G}_\lambda$  is  $\lambda/\ell_{\max}(\Sigma_p)$ .*

**Theorem S.5.5.** *Suppose the conditions in Theorem S.5.4 hold. Then, uniformly in  $Q_{\text{away}}^{(p)}$*

$$\hat{\phi}_p(z) - \phi_p(z) = O_{<} \left( \frac{1}{n_2} \right).$$

**Theorem S.5.6.** *Suppose the conditions in Theorem S.5.4 hold. The results in Theorem S.5.3 still hold.*

*Proof of Theorem S.5.4.* Under Definition 2.2, for all sufficiently large  $p$ , we have

$$pF^{\Sigma_p}(\{\ell_{\max}(\Sigma_p)\}) > n_2.$$

Note that  $pF^{\Sigma_p}(\{\ell_{\max}(\Sigma_p)\})$  is the rank of the eigen-subspace associated with the smallest eigenvalue of  $\lambda\Sigma_p^{-1}$ ,

that is  $\ell_{\max}(\Sigma_p)$ . The rank of  $\tilde{\mathbf{Z}}\tilde{\mathbf{Z}}^T$  is  $n_2$  with probability 1, since the condition implies that  $p > n_2$ . Therefore, using Wey's inequality, we obtain that there are at least 1 eigenvalue of  $\tilde{\mathbf{Z}}\tilde{\mathbf{Z}}^T$  less or equal to  $\lambda/\ell_{\max}(\Sigma_p)$ , which is the smallest one since  $\ell_{\min}(\tilde{\mathbf{Z}}\tilde{\mathbf{Z}}^T + \lambda\Sigma_p^{-1}) \geq \lambda/\ell_{\max}(\Sigma_p)$ . Therefore,  $\ell_{\min} = \lambda/\ell_{\max}(\Sigma_p)$ .  $\square$

*Proof of Theorem S.5.5.* The proof of Theorem S.5.5 follows from the same arguments as those in the proof of Theorem S.5.1. We only need to replace the bound in Lemma S.4.5 by that in Lemma S.4.6.  $\square$

*Proof.* The proof of Theorem S.5.6 follows from the same arguments as those in the proof of Theorem S.5.3. In the last step, the bound on  $|\hat{\phi}_p - \phi_p|$  is given by Theorem S.5.5.  $\square$

## S.6 Proof of Theorem 2.2

We start the proof by formulating the resolvent  $(U_1^T \mathbf{Z}^T \mathbf{G}_\lambda^{-1} \mathbf{Z} U_1 - z I_{n_1})^{-1}$  of  $\tilde{\mathbf{F}}_\lambda$ , for  $z \in \mathbb{C}^+$ . Following the strategy in Knowles and Yin (2017) and Han et al. (2018), we construct a linearizing block matrix as

$$\mathbf{H}(z) = \mathbf{H}(z, \mathbf{Z}) = \begin{pmatrix} -z I_{n_1} & U_1^T \mathbf{Z}^T & 0 \\ \mathbf{Z} U_1 & -\lambda \Sigma_p^{-1} & \mathbf{Z} U_2 \\ 0 & U_2^T \mathbf{Z}^T & I_{n_2} \end{pmatrix}.$$

By the Schur complement formula, it turns out that the upper-left block of the  $3 \times 3$  block matrix  $\mathbf{H}^{-1}(z)$ , called  $\mathbf{L}(z)$ , is the resolvent of  $\tilde{\mathbf{F}}_\lambda$ , that is

$$\mathbf{L}(z) = \Delta^T \mathbf{H}^{-1}(z) \Delta = (U_1^T \mathbf{Z}^T \mathbf{G}_\lambda^{-1} \mathbf{Z} U_1 - z I_{n_1})^{-1}, \quad \text{where } \Delta = \begin{bmatrix} I_{n_1} \\ 0_{(p+n_2) \times n_1} \end{bmatrix}.$$

It then suffices to focus on  $\mathbf{H}^{-1}(z)$  instead of  $\tilde{\mathbf{F}}_\lambda$  directly. The reason is that  $\mathbf{H}(z)$  is linear in  $\mathbf{Z}$ .

Recall that  $\Theta_1$  is the right most edge of the support of  $F_q$  as in Lemma S.4.1. We introduce the fundamental control parameter

$$\Phi(z) = \sqrt{\frac{\Im q(z)}{n_1 \eta}} + \frac{1}{n_1 \eta}.$$

Recall the definition of the domain  $D$  in Eq. (S.2) that is around  $\Theta_1$  as

$$D = D(a, a', n_1) := \{z = E + i\eta \in \mathbb{C}^+ : |E - \Theta_1| \leq a, n_1^{-1+a'} \leq \eta \leq 1/a'\}.$$

The core of the proof is to build the following strong local law of the resolvent  $\mathbf{L}(z)$  in  $D$ .

**Theorem S.6.1.** *Suppose that C1-C6 hold, Then, there exists a  $> 0$  such that the following results hold for arbitrary  $a' > 0$ .*

(i) *The entrywise local law holds as*

$$\mathbf{L}(z) - q(z) I_{n_1} = O_{<}(\Phi(z)),$$

*uniformly  $z \in D$ .*

(ii) *The averaged local law holds as*

$$|\bar{L}(z) - q(z)| < \frac{1}{n_1 \eta},$$

uniformly  $z \in D$ . Here,

$$\bar{L}(z) = \frac{1}{n_1} \sum_{i=1}^{n_1} \mathbf{L}_{ii}(z)$$

and  $\mathbf{L}_{ij}(z)$  is the  $(i, j)$ -th element of  $\mathbf{L}(z)$ .

Once Theorem S.5.1 is ready, we can show the edge universality of  $\tilde{\mathbf{F}}_\lambda$ , which means that the limiting distribution of

$$\frac{p^{2/3}}{\Theta_2} (\ell_{\max}(\tilde{\mathbf{F}}_\lambda) - \Theta_1)$$

is not affected by the distribution of  $\mathbf{Z}$  as long as Condition **C2** is satisfied. Similar to Theorem 6.3 of Erdős et al. (2012), to show the edge universality, it suffices to show the following Green function comparison theorem.

**Theorem S.6.2.** *Let  $\epsilon > 0$ ,  $\eta = n^{-2/3-\epsilon}$ ,  $E_1, E_2 \in \mathbb{R}$  satisfy  $E_1 < E_2$  and*

$$|E_1 - \Theta_1|, |E_2 - \Theta_1| \leq n^{-2/3+\epsilon}$$

Set  $K : \mathbb{R} \rightarrow \mathbb{R}$  to be a smooth function such that

$$\max_x |K^{(l)}(x)| \leq C, \quad l = 1, 2, 3, 4, 5$$

for some constant  $C$ . Then there exists a constant  $c > 0$  such that for large enough  $n$  and small enough  $\epsilon$ , we have

$$\left| \mathbb{E}K \left( n \int_{E_1}^{E_2} \Im \bar{L}_{\mathbf{Z}}(x + i\eta) dx \right) - \mathbb{E}K \left( n \int_{E_1}^{E_2} \Im \bar{L}_{\mathbf{Z}^0}(x + i\eta) dx \right) \right| \leq n^{-c},$$

where  $\bar{L}_{\mathbf{Z}}(z)$  is  $(1/n_1) \sum_{i=1}^{n_1} \mathbf{L}_{ii}(z)$  when  $\mathbf{Z}$  satisfies the moment condition **C2** and  $\bar{L}_{\mathbf{Z}^0}(z)$  is similar to  $\bar{L}_{\mathbf{Z}}(z)$  but with  $\mathbf{Z}$  replaced by a Gaussian matrix  $\mathbf{Z}^0$ .

It is a standard procedure in RMT to connect Theorem S.6.2 to the edge universality of  $\tilde{\mathbf{F}}_\lambda$ . In particular, we can fix  $E^* < p^{-2/3}$  such that  $\ell_{\max}(\tilde{\mathbf{F}}_\lambda) \leq \Theta_1 + E^*$  with high probability. Choosing  $|E - \Theta_1| < p^{-2/3}$ ,  $\eta = n_1^{-2/3-9\epsilon}$  and  $l = \frac{1}{2}n_1^{-2/3-\epsilon}$ , then for some sufficiently small constant  $\epsilon$  and sufficiently large constant  $M$ , there exists a constant  $n_0(\epsilon, M)$  such that

$$\begin{aligned} \mathbb{E}K \left( \frac{n_1}{\pi} \int_{E-l}^{\Theta_1+E^*} \Im \bar{L}_{\mathbf{Z}}(x + i\eta) dx \right) &\leq \mathbb{P} \left( \ell_{\max}(\tilde{\mathbf{F}}_\lambda) \leq E \right) \leq \mathbb{E}K \left( \frac{n_1}{\pi} \int_{E+l}^{\Theta_1+E^*} \Im \bar{L}_{\mathbf{Z}}(x + i\eta) dx \right) + n_1^{-M}, \quad (\text{S.1}) \\ \mathbb{E}K \left( \frac{n_1}{\pi} \int_{E-l}^{\Theta_1+E^*} \Im \bar{L}_{\mathbf{Z}^0}(x + i\eta) dx \right) &\leq \mathbb{P} \left( \ell_{\max}(\tilde{\mathbf{F}}_\lambda^0) \leq E \right) \leq \mathbb{E}K \left( \frac{n_1}{\pi} \int_{E+l}^{\Theta_1+E^*} \Im \bar{L}_{\mathbf{Z}^0}(x + i\eta) dx \right) + n_1^{-M}, \end{aligned} \quad (\text{S.2})$$

where  $\tilde{\mathbf{F}}_\lambda^0$  is as  $\tilde{\mathbf{F}}_\lambda$  but when  $\mathbf{Z}$  is additionally Gaussian,  $n_1 \geq n_0(\epsilon, M)$ , and  $K$  is a smooth cutoff function

satisfying the condition in Theorem S.6.2. We omit the proof of (S.1) and (S.2) because it is a standard procedure in RMT. Similar works include Corollary 5.1 of Lemma 6.1 of Erdős et al. (2012), Bao et al. (2014), and Lemma 4.1 of Pillai and Yin (2014).

Following (S.1), (S.2) and Theorem S.6.2, we can show

$$\mathbb{P}(\ell_{\max}(\tilde{\mathbf{F}}_\lambda) \leq E) \geq \mathbb{P}(\ell_{\max}(\tilde{\mathbf{F}}_\lambda^0) \leq E - 2l) - n_1^{-M},$$

$$\mathbb{P}(\ell_{\max}(\tilde{\mathbf{F}}_\lambda) \leq E) \leq \mathbb{P}(\ell_{\max}(\tilde{\mathbf{F}}_\lambda^0) \leq E + 2l) + n_1^{-M}.$$

It then follows that

$$\mathbb{P}\left(\frac{p^{2/3}}{\Theta_2}(\ell_{\max}(\tilde{\mathbf{F}}_\lambda) - \Theta_1) \leq s\right) - \mathbb{P}\left(\frac{p^{2/3}}{\Theta_2}(\ell_{\max}(\tilde{\mathbf{F}}_\lambda^0) - \Theta_1) \leq s\right) \longrightarrow 0. \quad (\text{S.3})$$

The remaining tasks are as follows.

**Step 1:** Prove Theorem S.6.1 under Gaussianity.

**Step 2:** Prove the asymptotic Tracy-Widom distribution of the normalized largest root as in Theorem 2.2 under Gaussianity. That is, to prove

$$\mathbb{P}\left(\frac{p^{2/3}}{\Theta_2}(\ell_{\max}(\tilde{\mathbf{F}}_\lambda^0) - \Theta_1) \leq s\right) \rightarrow \text{TW}_1(s),$$

for any  $s \in \mathbb{R}$ .

**Step 3:** Prove Theorem S.6.1 under the general condition **C2**.

**Step 4:** Establish edge universality by proving Theorem S.6.2 under the general condition **C2**. It then follows from **Step 2** and Eq. (S.3) that the asymptotic Tracy-Widom distribution of the normalized largest root holds under the general condition.

The technical arguments in the remaining proof are routine in the literature on “local laws” of random matrices. Similar works include Alex Bloemendal et al. (2014), Knowles and Yin (2017), Han et al. (2016), and Han et al. (2018). Indeed, most arguments in the proof are variants of those in these prior works with limited changes. Accordingly, in the following sections, we provide an outline of the proof and refer to these prior works for detailed arguments.

## Step 1: Proof of Theorem S.6.1 under Gaussianity

We first show that Theorem S.6.1 holds under the additional assumption that  $\mathbf{Z}$  is Gaussian. Note that  $\mathbf{Z}U_1$  and  $\mathbf{Z}U_2$  are independent under Gaussianity. We can equivalently consider the matrix

$$\tilde{\mathbf{Z}}_1^T \mathbf{G}_\lambda^{-1} \tilde{\mathbf{Z}}_1, \quad \text{and} \quad \mathbf{G}_\lambda = \tilde{\mathbf{Z}}_2 \tilde{\mathbf{Z}}_2^T + \lambda \Sigma_p^{-1},$$

where  $\tilde{\mathbf{Z}}_1$  is a  $p \times n_1$  matrix whose entries are iid  $N(0, 1/n_1)$ ,  $\tilde{\mathbf{Z}}_2$  is a  $p \times n_2$  matrix whose entries are iid  $N(0, 1/n_2)$ , and  $\tilde{\mathbf{Z}}_1$  and  $\tilde{\mathbf{Z}}_2$  are independent.

The main strategy in the proof is as follows. Fixing  $\mathbf{G}_\lambda$ , Theorem 3.14 of Knowles and Yin (2017) can be applied to  $\tilde{\mathbf{Z}}^T \mathbf{G}_\lambda^{-1} \tilde{\mathbf{Z}}$  with  $\mathbf{G}_\lambda^{-1}$  be regarded as “ $\Sigma$ ” in their work. The local laws of  $\tilde{\mathbf{F}}_\lambda$  is then obtained as in Theorem S.6.1 but with  $q(z)$  replaced by a finite-sample version. In particular, we fix  $\mathbf{G}_\lambda$  and define a finite-sample version of Eq. (S.1) as

$$z = \hat{f}(q), \quad \hat{f}(q) = -\frac{1}{q} + \frac{1}{n_1} \sum_{j=1}^p \frac{1}{g_j + q},$$

where  $g_1 \geq g_2 \geq \dots \geq g_p \geq \lambda/\sigma_{\max} > 0$  are eigenvalues of  $\mathbf{G}_\lambda$ . Again, applying Lemma 2.1, for any  $z \in \mathbb{C}^+$ , there exists a unique solution  $\hat{q}_p(z) \in \mathbb{C}^+$  to the above equation. Secondly, we apply the results in Section S.5 to show that  $\hat{q}_p$  converges uniformly to  $q(z)$  in the domain  $D$ .

Let  $\hat{\beta}_p \in (0, g_p)$  be such that  $\hat{f}'(-\hat{\beta}_p) = 0$ . That is,

$$\hat{f}'(-\hat{\beta}_p) = \frac{1}{\hat{\beta}_p^2} - \frac{1}{n_1} \sum_{j=1}^p \frac{1}{(g_j - \hat{\beta}_p)^2} = 0.$$

Clearly, for any fixed discrete points  $g_j$ 's such that  $g_p > 0$ ,  $\hat{\beta}_p$  exists and is unique. Let  $\hat{\Theta}_{p1} = \hat{f}(-\hat{\beta}_p)$  and

$$\hat{\Phi}(z) = \sqrt{\frac{\Im \hat{q}_p(z)}{n_1 \eta}} + \frac{1}{n_1 \eta}.$$

Define the following domain

$$\hat{D} = \hat{D}(a, a', n_1) := \{z = E + i\eta \in \mathbb{C}^+ : |E - \hat{\Theta}_{p1}| \leq a, \quad n_1^{-1+a'} \leq \eta \leq 1/a'\}.$$

The following results hold by applying Theorem 3.14 of Knowles and Yin (2017).

**Theorem S.6.3.** *Suppose that C1–C6 hold. Fix  $\mathbf{G}_\lambda$  and let  $\mathbf{L}(z)$  be the resolvent of  $\tilde{\mathbf{Z}}_1^T \mathbf{G}_\lambda^{-1} \tilde{\mathbf{Z}}_1$  at  $z$ . Moreover, suppose that*

$$|\hat{\beta}_p - g_p| > c, \tag{S.4}$$

for all sufficiently large  $p$  and a sufficiently small constant  $c$ . Then, there exists constants  $a, a' > 0$  such that the following local laws hold.

(i) The entrywise local law in  $\hat{D}$  holds as

$$\mathbf{L}(z) - \hat{q}_p(z)I_{n_1} = O_{\prec}(\hat{\Phi}(z)),$$

uniformly in  $\hat{D}(a, a', n_1)$ .

(ii) The averaged local law in  $\hat{D}$  holds as

$$|\bar{L}(z) - \hat{q}_p(z)| < \frac{1}{n_1\eta},$$

uniformly in  $\hat{D}(a, a', n_1)$ .

Given Theorem S.6.3, to show Theorem S.6.1, it suffices to show the following theorem.

**Theorem S.6.4.** *Suppose that C1–C6 hold.  $\mathbf{G}_\lambda$  satisfies the following properties.*

(i) There exists  $c > 0$  such that Eq. (S.4) holds with high probability;

(ii)  $|\hat{\Theta}_{p1} - \Theta_1| < n_2^{-1}$ ;

(iii) There exists  $a > 0$  such that for arbitrary  $a' > 0$ ,

$$|\hat{q}_p(z) - q(z)| < \frac{1}{n_1\eta},$$

uniformly in  $\hat{D}(a, a', n_1)$ .

The rest of this subsection is devoted to the proof of Theorem S.6.4. We separately consider two cases:  $\rho > \lambda/\sigma_{\max}$  and  $\rho = \lambda/\sigma_{\max}$ . For both cases, since  $s'(x) \rightarrow \infty$  as  $x \rightarrow \rho$ , we have that  $\beta < \rho$ . Recall the definition of  $f(q)$  and the relationship between  $\beta$ ,  $\Theta_1$  and  $f(q)$  as introduced in Section S.4.2.

We first consider the case when  $\rho > \lambda/\sigma_{\max}$ . Theorem S.5.2 in Section S.5 indicates that

$$|g_p - \rho| < n_2^{-2/3}.$$

In order to show  $|\hat{\beta}_p - g_p| \geq c$  with high probability for some constant  $c$ , it suffices to show that  $|\hat{\beta}_p - \beta| < n_2^{-1}$  in probability. For  $q \in \mathbb{C}^+ \cup (-\rho, 0)$ , we consider  $f'(q)$ ,  $f''(q)$ , and  $\hat{f}'(q)$

$$f'(q) = \frac{1}{q^2} - \gamma_1 \int \frac{d\mathcal{G}_\lambda(\tau)}{(\tau + q)^2},$$

$$f''(q) = -\frac{2}{q^3} + 2\gamma_1 \int \frac{d\mathcal{G}_\lambda(\tau)}{(\tau + q)^3},$$

$$\hat{f}'(q) = \frac{1}{q^2} - \frac{1}{n_1} \sum_{j=1}^p \frac{1}{(g_p + q)^2}.$$

Since  $\beta \in (0, \rho)$ , there exists a domain  $\mathfrak{D}_q = \{z : |E + \beta| \leq C, 0 \leq \eta \leq C'\}$  for some  $C, C' > 0$  such that

$$|f''(q)| \asymp 1, \quad q \in \mathfrak{D}_q.$$

We notice that in  $(-g_p, 0)$ ,  $\hat{f}''(q) > 0$ . Therefore, there exists at most one critical point of  $\hat{f}'(q)$  on  $(-g_p, 0)$ . To show that  $|\hat{\beta}_p - \beta| < n_2^{-1}$ , we only need to show that for arbitrary small  $\epsilon > 0$ , there exists a root to  $\hat{f}(q) = 0$  in  $(-\beta - n_1^{-1+\epsilon}, -\beta + n_1^{-1+\epsilon})$  with high probability. Clearly,

$$\Re f'(-\beta \pm n_2^{-1+\epsilon} + in_2^{-1+\epsilon/2}) \asymp \pm n_2^{-1+\epsilon},$$

$$\Im f'(-\beta \pm n_2^{-1+\epsilon} + in_2^{-1+\epsilon/2}) \asymp n_2^{-1+\epsilon/2},$$

Due to the analyticity of the function  $f'(q)$  and  $\hat{f}'(q)$  when  $q \in \mathfrak{D}_q$ , Theorem S.5.3 suggests that

$$\mathbb{1}(g_p \geq (\rho + \beta)/2) \left| \hat{f}(-\beta \pm n_2^{-1+\epsilon} + in_2^{-1+\epsilon/2}) - f(-\beta \pm n_2^{-1+\epsilon} + in_2^{-1+\epsilon/2}) \right| < \frac{1}{n_2}.$$

It follows that when  $g_p \geq (\rho + \beta)/2$ , with high probability

$$\Re \hat{f}'(-\beta \pm n_2^{-1+\epsilon} + in_2^{-1+\epsilon/2}) \asymp \pm n_2^{-1+\epsilon},$$

$$\Im \hat{f}'(-\beta \pm n_2^{-1+\epsilon} + in_2^{-1+\epsilon/2}) \asymp \pm n_2^{-1+\epsilon/2}.$$

Moreover, since  $g_p \geq (\rho + \beta)/2$ ,  $|\hat{f}''(q)| \asymp 1$  when  $q \in \mathfrak{D}_q$ , we conclude that with high probability

$$\hat{f}'(-\beta \pm n_2^{-1+\epsilon}) \asymp \pm n_2^{-1+\epsilon}.$$

It implies that there exists a critical point of  $\hat{f}'(q)$  in between  $-\beta \pm n_2^{-1+\epsilon}$  with high probability. It completes the proof of Result (i).

It follows immediately that when  $g_p \geq (\rho + \beta)/2$ ,

$$\hat{\Theta}_{p1} - \Theta_1 = \hat{f}(-\hat{\beta}_p) - f(-\beta) = (\hat{f}(-\hat{\beta}_p) - \hat{f}(-\beta)) + (\hat{f}(-\beta) - f(-\beta)).$$

The first term is such that

$$\hat{f}(-\hat{\beta}_p) - \hat{f}(-\beta) = O_{<}(\hat{\beta}_p - \beta) = O_{<}(\frac{1}{n_2}).$$

Here, we are using the fact that  $\hat{f}'(q)$  is bounded within  $\mathfrak{D}_q$ . For the second term, for arbitrary  $\epsilon > 0$

$$\hat{f}(-\beta) - f(-\beta) = \hat{f}(-\beta + in_2^{-1+\epsilon/2}) - f(-\beta + in_2^{-1+\epsilon/2}) + O_{<}(n_2^{-1+\epsilon/2}) = O_{<}(1/n_2) + O_{<}(n_2^{-1+\epsilon/2}).$$

Here, we are using Theorem S.5.3 and the fact that  $f'(q) \asymp$  and  $\hat{f}(q) \asymp 1$  when  $g_p \geq (\rho + \beta)/2$ . It follows that  $|\hat{\Theta}_{p1} - \Theta_1| < 1/n_2$ .

Lastly, we show  $|\hat{q}_p(z) - q(z)| < \frac{1}{n_1\eta}$  uniformly in  $\hat{D}(a, a', n_1)$ . Recall that

$$z = -\frac{1}{\hat{q}_p(z)} + (p/n_1) \int \frac{dF^{\mathbf{G}_\lambda}(\tau)}{\tau + \hat{q}_p(z)}.$$

In the following, we always assume the all eigenvalues of  $\mathbf{G}_\lambda$  are contained in  $\mathcal{I}_\epsilon$  for some  $\epsilon > 0$  (See Theorem S.5.3 for the definition of  $\mathcal{I}_\epsilon$ ). Fix  $z = E + i\eta$  such that  $\eta \geq 1$ . Applying Lemma S.4.1, we obtain that

$$\Im \hat{q}_p(z) \geq C,$$

for some constant  $C > 0$ . The constant  $C$  only depends on  $F^{\Sigma_\infty}$ ,  $\gamma_1$  and  $\gamma_2$ . Therefore,  $-\hat{q}_p(z)$  is away from the support of  $\mathcal{G}_\lambda$ . Applying S.5.3,

$$\left| \int \frac{dF^{\mathbf{G}_\lambda}(\tau)}{\tau + \hat{q}_p(z)} - \int \frac{d\mathcal{G}_\lambda(\tau)}{\tau + \hat{q}_p(z)} \right| < \frac{1}{n_2}.$$

It follows that

$$z + O_{<}(n_1^{-1}) = -\frac{1}{\hat{q}_p(z)} + (p/n_1) \int \frac{d\mathcal{G}_\lambda(\tau)}{\tau + \hat{q}_p(z)}.$$

Applying Lemma S.4.2, we obtain

$$|\hat{q}_p(z) - q(z)| < \frac{1}{n_2}.$$

We then use a stochastic continuity argument and Lemma S.4.2 to propagate the smallness of  $|\hat{q}_p(z) - q(z)|$  from  $\eta \geq 1$  to all  $z \in \hat{D}$ . The argument is very similar to those in the proof of Proposition S.5.1. We therefore omit the details. All together, we conclude that

$$|\hat{q}_p(z) - q(z)| < \frac{1}{n_2\eta}.$$

As for the case when  $\rho = \lambda/\sigma_{\max}$ , from Theorem S.5.4, Result (i) clearly holds. Result (ii) and (iii) follow

from the same arguments as in the case of  $\rho = \lambda/\sigma_{\max}$ . We only need to replace Theorem S.5.3 with Theorem S.5.6.

The proof of Theorem S.6.4 is completed.

## Step 2: Asymptotic Tracy-Widom distribution under Gaussianity

The asymptotic Tracy-Widom law of the normalized largest root follows directly from Theorem 2.4 of Lee and Schnelli (2016). Indeed, applying their results, we have

**Theorem S.6.5.** *Suppose that C1–C6 hold. Fix  $\mathbf{G}_\lambda$ . Suppose that  $\mathbf{G}_\lambda$  is such that Eq. (S.4) holds for all sufficiently large  $p$ . Then,*

$$\frac{p^{2/3}}{\hat{\Theta}_{p2}} \left( \ell_{\max}(\tilde{F}_\lambda) - \hat{\Theta}_{p1} \right) \Longrightarrow \text{TW}_1,$$

where  $\hat{\Theta}_{p1}$  is defined in Step 1 and  $\hat{\Theta}_{p2}$  is

$$\hat{\Theta}_{p2} = \left[ (p/n_1)^3 \int \frac{dF^{\mathbf{G}_\lambda}(\tau)}{(\tau - \hat{\beta}_p)^3} + \frac{(p/n_1)^2}{\hat{\beta}_p^3} \right]^{1/3}.$$

In Theorem S.6.4, we showed that Eq. (S.4) holds with high probability and  $|\hat{\Theta}_{p1} - \Theta_1| < n_1^{-1}$ . Following similar arguments, it is not hard to show  $\hat{\Theta}_{p2} - \Theta_2 \rightarrow 0$  in probability. Therefore, the asymptotic Tracy-Widom law of the normalized largest root

$$\frac{p^{2/3}}{\Theta_2} \left( \ell_{\max}(\tilde{F}_\lambda) - \Theta_1 \right) \Longrightarrow \text{TW}_1,$$

follows directly from the Slutsky's theorem.

## Step 3: Proof of Theorem S.6.1 under general condition C2

Theorem S.6.1 holds under the moments condition C2. It can shown by closely following the arguments in Sections 9.1, 9.2 and 10 of Han et al. (2018), originally developed by Knowles and Yin (2017). Only minor changes are needed. We only give an outline of the arguments and highlight the difference from those in Han et al. (2018).

Consider the entrywise local law. It suffices to show that for any orthogonal  $n_1 \times n_1$  matrix  $\mathbf{B}_1$  and  $\mathbf{B}_2$ ,

$$\|\mathbf{B}_1(\mathbf{L} - q(z)I_{n_1})\mathbf{B}_2^*\|_\infty < \Phi(z), \tag{S.5}$$

for all  $z \in S$ , where  $S$  is an  $\epsilon$ -net of  $D$  with  $\epsilon = n_1^{-10}$ . Here,  $\mathbf{B}_2^*$  is the conjugate transpose of  $\mathbf{B}_2$ . Setting  $\delta$  to be a sufficiently small positive constant such that  $n_1^{24\delta}\Phi \ll 1$ , for any given  $\eta \geq \frac{1}{n_1}$ , we define a serial numbers

$\eta_0 \leq \eta_1 \leq \eta_2 \leq \dots \leq \eta_L$ , based on  $\eta$  where

$$L := L(\eta) = \max\{L \in \mathbb{N} : \eta n_1^{l\delta} < n_1^{-\delta}\}.$$

So

$$\eta_l := \eta n_1^{l\delta}, \quad (l = 0, 1, \dots, L-1), \quad \eta_L := 1.$$

We work on the net  $S$  satisfying the condition that  $E + i\eta_l \in S$ ,  $l = 0, \dots, L$ , from now on. We define  $S_m := \{z \in S : \Im z \geq n_1^{-\delta m}\}$  corresponding to the following events:

$$A_m = \{\|\mathbf{B}_1(\mathbf{L}(z) - q(z)I_{n_1})\mathbf{B}_2^* \mathcal{T}_p(\mathbf{Z})\|_\infty < 1, \text{ for any } z \in S_m\} \quad (\text{S.6})$$

and

$$C_m = \{\|\mathbf{B}_1(\mathbf{L}(z) - q(z)I_{n_1})\mathbf{B}_2^* \mathcal{T}_p(\mathbf{Z})\|_\infty < \Phi, \text{ for any } z \in S_m\}. \quad (\text{S.7})$$

Here,

$$\mathcal{T}_p(\mathbf{Z}) = \begin{cases} 1 & \text{if } \|\mathbf{Z}\mathbf{Z}^T\|_F \leq C_0, \\ 0 & \text{otherwise.} \end{cases}$$

Note that there exists sufficiently large  $C_0$  such that  $\mathcal{T}_p(\mathbf{Z}) = 1$  with high probability due to Lemma S.5.4. In the following, we select  $C_0$  to be such a constant.

We start the induction by considering the event  $A_0$  first. In fact, it is not hard to prove that event  $A_0$  holds. By the assumption that  $n_1^{24\delta}\Phi \ll 1$ , it is easy to see that the event  $C_m$  implies the event  $A_m$ . We will prove the event  $(A_{m-1})$  implies the event  $(C_m)$  for all  $1 \leq m \leq \delta^{-1}$  in the sequel, which ensures that Eq. (S.5) holds on the set  $S$  uniformly.

Define

$$F_{st}(\mathbf{Z}, z) = ((\mathbf{B}_1 \mathbf{L}(z) \mathbf{B}_2^*)_{st} - q(z) (\mathbf{B}_1 \mathbf{B}_2^*)_{st}) \mathcal{T}_p(\mathbf{Z}), \quad s, t \in \{1, \dots, n_1\}.$$

By Markov's inequality, it suffices to calculate the upper bound of the higher moments of  $F_{st}(\mathbf{Z}, z)$ . Indeed, we only need to prove the following lemma.

**Lemma S.6.1.** *Let  $k$  be an positive even constant and  $m \leq \delta^{-1}$ . Suppose Eq. (S.6) for all  $z \in S_{m-1}$ . Then we have*

$$\mathbb{E} |F_{st}^k(\mathbf{Z}, z)| < (n_1^{24\delta}\Phi)^k$$

for all  $1 \leq s, t \leq n_1$  and  $z \in S_m$ .

The proof of Lemma S.6.1 closely follows that of Lemma 3 in Han et al. (2018). Similar results can be

found in Lemma 7.5 of Knowles and Yin (2017) and Lemma 5 of Han et al. (2016). In fact, when  $\lambda = 0$ , the central block of  $\mathbf{H}(z)$  becomes zero, reducing  $\mathbf{H}(z)$  to the linearizing block matrix used in Han et al. (2018) (also denoted as  $\mathbf{H}$ ). It is straightforward to verify that all arguments in the proof of Lemma 3 in Han et al. (2018) do not depend on the central block. Specifically, the proof holds for any general matrix  $\mathbf{H}$  where all blocks are linear in  $\mathbf{Z}$  and satisfy certain operator norm bounds.

The proof strategy involves controlling the difference between  $\mathbb{E}|F_{st}^k(\mathbf{Z}, z)|$  and  $\mathbb{E}|F_{st}^k(\mathbf{Z}^{\text{Gauss}}, z)|$ , where  $\mathbf{Z}^{\text{Gauss}}$  has the same structure as  $\mathbf{Z}$  but with Gaussian elements. In Step 1, we established that:

$$\mathbb{E}|F_{st}^k(\mathbf{Z}^{\text{Gauss}}, z)| < (n_1^{24\delta}\Phi)^k.$$

Knowles and Yin (2017) introduced an interpolation method to control this difference. The arguments were later summarized and simplified by Han et al. (2018) in Sections 9.1.1, 9.1.2, and 9.2 of their paper. These arguments can be applied almost verbatim, with only minor modifications needed to adjust the mathematical expressions to their counterparts in our paper.

A minor adaptation is required in the arguments presented in Section 9.2 of Han et al. (2018). While their focus was on controlling all blocks of  $\mathbf{H}^{-1}$ , our context requires consideration of only the upper left corner,  $\mathbf{L} = \Delta^T \mathbf{H}^{-1} \Delta$ . Thus, the arguments concerning the remaining blocks can be omitted. Further details are omitted for brevity.

Regarding the averaged local law, it can be established using the arguments in Section 10 of Han et al. (2018), with notation adjustments to align with our framework.

#### **Step 4: Proof of the Green function comparison theorem**

The theorem can be proved following the same arguments as Section 12 of Han et al. (2018) with notation adjustments to align with our framework.

## S.7 Proof of Theorem 3.2, Lemma 3.3, and Lemma 3.4

First, consider the proof of Theorem 3.2. Let  $F_{(p)}^{\Sigma_\infty}$  be the discretization of  $F^{\Sigma_\infty}$  onto the points in  $R_p$ . Specifically, we assume that  $F_{(p)}^{\Sigma_\infty}$  is the distribution that places masses  $F^{\Sigma_\infty}((\sigma_{p,j-1}, \sigma_{pj}])$  at the point  $\sigma_{pj}$ ,  $j = 1, 2, \dots$ , and  $\sigma_{p0} = -\infty$ . Since  $\text{size}(R_p) = o(p^{-2/3})$ , clearly

$$\mathcal{D}_W(F_{(p)}^{\Sigma_\infty}, F^{\Sigma_\infty}) = o(p^{-2/3}).$$

Recall the errors in Algorithm 1 as

$$e_{ij} = \frac{\hat{Q}_j(z_i)}{|\hat{Q}_j(z_i)|} - \frac{1}{|\hat{Q}_j(z_i)|} \sum_{k=1}^K \frac{\sigma_k^j w_k}{(\sigma_k \lambda \hat{\varphi}(z_i) + \lambda)^j}.$$

Using Lemma 2.1, uniformly for  $y \in J_p$ ,  $\hat{\varphi}(y) - \varphi(y) = o_P(n^{-2/3})$  and  $\hat{\varphi}'(y) - \varphi'(y) = o_P(n^{-2/3})$ . Therefore, together with Marčenko-Pastur equation (2.1),

$$\sup_{y \in J_p} \left| \frac{\hat{Q}(y)}{|\hat{Q}(y)|} - \frac{1}{|\hat{Q}(y)|} \int \frac{\tau dF^{\Sigma_\infty}(\tau)}{\tau \lambda \hat{\varphi}(y) + \lambda} \right| = o_P(p^{-2/3}).$$

It follows then

$$\sup_{y \in J_p} \left| \frac{\hat{Q}(y)}{|\hat{Q}(y)|} - \frac{1}{|\hat{Q}(y)|} \int \frac{\tau dF_{(p)}^{\Sigma_\infty}(\tau)}{\tau \lambda \hat{\varphi}(y) + \lambda} \right| = o_P(p^{-2/3}).$$

Then, we can conclude that the estimated measure  $\hat{F}_p$  is such that

$$\sup_{y \in J_p} \left| \int \frac{\tau d\hat{F}_p(\tau)}{\tau \varphi(y) + 1} - \int \frac{\tau dF^{\Sigma_\infty}(\tau)}{\tau \varphi(y) + 1} \right| = o_P(p^{-2/3}).$$

Under the assumption  $\{\varphi(y), y \in J_p\}$  is dense in  $D(\nu)$ . Therefore,

$$\sup_{z \in D(\nu)} \left| \int \frac{\tau d\hat{F}_p(\tau)}{\tau z + 1} - \int \frac{\tau dF^{\Sigma_\infty}(\tau)}{\tau z + 1} \right| = o_P(p^{-2/3}). \quad (\text{S.1})$$

Similarly, we can get

$$\sup_{z \in D(\nu)} \left| \int \frac{\tau^2 d\hat{F}_p(\tau)}{(\tau z + 1)^2} - \int \frac{\tau^2 dF^{\Sigma_\infty}(\tau)}{(\tau z + 1)^2} \right| = o_P(p^{-2/3}). \quad (\text{S.2})$$

Notice that the functions are analytic in  $z$ . Consider the power series expansion

$$\begin{aligned} \int \frac{\tau d\hat{F}_p(\tau)}{\tau z + 1} - \int \frac{\tau dF^{\Sigma_\infty}(\tau)}{\tau z + 1} &= \sum_{m=0}^{\infty} (-1)^m z^m \left( \int \tau^{m+1} (d\hat{F}_p(\tau) - dF^{\Sigma_\infty}(\tau)) \right) \\ &= \sum_{m=0}^{\infty} (-1)^m z^m (\mu_{m+1}(\hat{F}_p) - \mu_{m+1}(F^{\Sigma_\infty})). \end{aligned}$$

Here,  $\mu_m(\cdot)$  is the  $m$ th moment of a distribution. Using the Cauchy's estimates on the power series coefficients, we have

$$\delta_p = \sup_{m \geq 1} p^{2/3} \nu^m |\mu_m(\hat{F}_p) - \mu_m(F^{\Sigma_\infty})| = o_P(1).$$

Then, it follows that the characteristic functions of  $\hat{F}_p$  and  $F^{\Sigma_\infty}$  are such that for  $t \in \mathbb{R}$ ,

$$\left| \frac{\mathbb{E}_{\hat{F}_p} e^{itX} - \mathbb{E}_{F^{\Sigma_\infty}} e^{itX}}{t} \right| \leq C \nu^{-1} \delta_p p^{-2/3} e^{t/\nu},$$

$$\left| \frac{d}{dt} \frac{\mathbb{E}_{\hat{F}_p} e^{itX} - \mathbb{E}_{F^{\Sigma_\infty}} e^{itX}}{t} \right| \leq C \nu^{-2} \delta_p p^{-2/3} e^{t/\nu}.$$

Following from Corollary 8.3 of Bobkov (2016), for all  $T \geq 3$

$$\mathcal{D}_W(\hat{F}_p, F^{\Sigma_\infty}) \leq \left( \int_{-T}^T \left| \frac{\mathbb{E}_{\hat{F}_p} e^{itX} - \mathbb{E}_{F^{\Sigma_\infty}} e^{itX}}{t} \right|^2 dt \right)^{1/2} + \left( \left| \frac{d}{dt} \frac{\mathbb{E}_{\hat{F}_p} e^{itX} - \mathbb{E}_{F^{\Sigma_\infty}} e^{itX}}{t} \right|^2 dt \right)^{1/2} + \frac{C}{T}.$$

It follows then

$$\mathcal{D}_W(\hat{F}_p, F^{\Sigma_\infty}) \leq \frac{C(1+\nu)}{\nu^2} p^{-2/3} \exp(T) \delta_p + \frac{C}{T}.$$

Note that setting  $T = \log(p^{1/3})$ , we have

$$\mathcal{D}_W(\hat{F}_p, F^{\Sigma_\infty}) = o_P(1).$$

Next, we consider the scenario when  $J_p$  is such that  $\{\varphi(y) : y \in J_p\}$  eventually covers  $[-h_\beta/\lambda - \varepsilon, -h_\beta/\lambda + \varepsilon]$ . Again, due to the fact that uniformly for  $y \in J_p$ ,  $\hat{\varphi}(y_p) - \varphi(y_p) = o_P(p^{-2/3})$ ,  $\hat{\varphi}'(y_p) - \varphi'(y_p) = o_P(p^{-2/3})$ , Eq. (S.1) and Eq. (S.2),

$$\sup_{h \in [h_\beta - \lambda\varepsilon, h_\beta + \lambda\varepsilon]} \left| \int \frac{\tau d\hat{F}_p(\tau)}{-h\tau + \lambda} - \int \frac{\tau dF^{\Sigma_\infty}(\tau)}{-h\tau + \lambda} \right| = o_P(p^{-2/3}).$$

$$\sup_{h \in [h_\beta - \lambda\varepsilon, h_\beta + \lambda\varepsilon]} \left| \int \frac{\tau^2 d\hat{F}_p(\tau)}{(-h\tau + \lambda)^2} - \int \frac{\tau^2 dF^{\Sigma_\infty}(\tau)}{(-h\tau + \lambda)^2} \right| = o_P(p^{-2/3}).$$

It indicates that uniformly in  $h \in [h_\beta - \lambda\varepsilon, h_\beta + \lambda\varepsilon]$ ,

$$\hat{\mathcal{H}}_1(h) - \mathcal{H}_1(h) = o_P(p^{-2/3}), \quad \hat{\mathcal{H}}_2(h) - \mathcal{H}_2(h) = o_P(p^{-2/3}) \quad \text{and} \quad \hat{\mathcal{H}}_3(h) - \mathcal{H}_3(h) = o_P(1).$$

Here, the bound on  $\hat{\mathcal{H}}_3(h) - \mathcal{H}_3(h)$  is due to  $\mathcal{D}_W(\hat{F}_p, F^{\Sigma_\infty})$ . As  $x$ ,  $s(x)$ ,  $s'(x)$ , and  $s''(x)$  are smooth in  $\mathcal{H}_j(h)$ ,

$j = 1, 2, 3$  as shown in Theorem 3.1, we get

$$\hat{\beta} - \beta = o_P(p^{-2/3}), \quad \hat{s}(\hat{\beta}) - s(\beta) = o_P(p^{-2/3}), \quad \hat{s}'(\hat{\beta}) - s'(\beta) = o_P(p^{-2/3}), \quad \hat{s}''(\hat{\beta}) - s''(\beta) = o_P(1).$$

Consequently,  $\hat{\Theta}_1 - \Theta_1 = o_P(p^{-2/3})$  and  $\hat{\Theta}_2 - \Theta_2 = o_P(1)$ .

As for Lemma 3.3, recall that  $\varphi(z)$  is the Stieltjes transform of  $\mathcal{W}$  (Lemma 2.1). Then,

$$\varphi(z) = \int \frac{d\mathcal{W}}{\tau - z}.$$

It follows that  $\{\varphi(z) : z \in \mathbb{C}^+ \text{ and } \text{dist}(z, \text{supp}(\mathcal{W})) \geq c\}$  contains the half disk  $\mathcal{D}(\nu)$  for some  $\nu > 0$ . We can then select  $J_p$  such that  $\varphi(y)$  is dense in  $\mathcal{D}(\nu)$  when  $y \in J_p$ .

As for Lemma 3.4, as  $\gamma_1 \rightarrow \infty$ ,  $\beta \rightarrow 0$  and  $h_\beta/\lambda \rightarrow -\varphi(-\lambda)$ . Therefore, select  $J_p$  to be a grid containing a subsequence dense in  $[-3/2\lambda, -\lambda/2]$ . Then,  $\{\varphi(y) : y \in J_p\}$  will eventually covers a neighborhood of  $-h_\beta/\lambda$ .

## S.8 Proof of Lemma 4.1, Corollary 4.1, Lemma 4.2 and Corollary

### 4.2

First of all, under  $H_a : BC \neq 0$ , we can decompose  $\mathbf{F}_\lambda$  as

$$\mathbf{F}_\lambda = \mathbf{F}_\lambda^{(0)} + \frac{1}{n_1} BC(C^T(XX^T)^{-1}C)^{-1}C^T B^T (\mathbf{W}_2 + \lambda I_p)^{-1} + \frac{1}{n_1} \left( BX P_1 Z^T \Sigma_p^{1/2} + \Sigma_p^{1/2} Z P_1 X^T B^T \right) (\mathbf{W}_2 + \lambda I_p)^{-1},$$

where  $\mathbf{F}_\lambda^{(0)}$  is the regularized  $F$ -matrix under the null hypothesis  $H_0 : BC = 0$ .

Under  $\mathbf{DA}$ ,

$$\frac{1}{p^s} \mathbf{F}_\lambda = \frac{1}{p^s} \mathbf{F}_\lambda^{(0)} + d_p q_p q_p^T (\mathbf{W}_2 + \lambda I_p)^{-1} + \frac{1}{n_1 p^s} \left( BX P_1 Z^T \Sigma_p^{1/2} + \Sigma_p^{1/2} Z P_1 X^T B^T \right) (\mathbf{W}_2 + \lambda I_p)^{-1}.$$

Since  $\ell_{\max}(\mathbf{F}_\lambda^{(0)}) = O_P(1)$  as indicated by Theorem 2.2 and

$$\frac{1}{p^{s/2} n_1} \|BX P_1\|_2 \|Z^T\| \|\Sigma_p^{1/2}\| \|(\mathbf{W}_2 + \lambda I_p)^{-1}\| = O_P(1),$$

we have

$$\frac{1}{p^s} \ell_{\max}(\mathbf{F}_\lambda) = d_p q_p^T (\mathbf{W}_2 + \lambda I_p)^{-1} q_p + o_P(1).$$

Using the main results of El Karoui and Kösters (2011), we can show that

$$q_p^T (\mathbf{W}_2 + \lambda I_p)^{-1} q_p = q_p^T (\lambda \varphi(-\lambda) \Sigma_p + \lambda I_p)^{-1} q_p + o_P(1).$$

The result of Lemma 4.1 follow.

As for Corollary 4.1, under the assumed conditions,  $\tilde{\ell}(\lambda) \rightarrow \infty$ . Therefore,

$$\mathbb{P}\left(\tilde{\ell}(\lambda) > \mathbb{T}\mathbb{W}_1(1 - \alpha) \mid BC\right) \longrightarrow 1.$$

Under **PA**, similarly, we get  $p^{-s} \ell_{\max}(\mathbf{F}_\lambda)$  is dominated by the following term

$$\frac{1}{p^s} \ell_{\max}(\mathbf{F}_\lambda) = \frac{1}{p} \nu^T D^{1/2} (\mathbf{W}_2 + \lambda I_p)^{-1} D^{1/2} \nu + o_P(1).$$

Using Lemma 2.7 of Bai and Silverstein (1998), conditional on  $\mathbf{W}_2$ ,

$$\frac{1}{p} \nu^T D^{1/2} (\mathbf{W}_2 + \lambda I_p)^{-1} D^{1/2} \nu = \frac{1}{p} \text{tr}\left[(\mathbf{W}_2 + \lambda I_p)^{-1} D\right] + o_P(1).$$

Here, the residual  $o_P(1)$  is with respect to  $\mathbb{P}_{BC}$  and the convergence is uniform with respect to  $\mathbf{W}_2$  since  $\|(\mathbf{W}_2 + \lambda)^{-1}\|_2 \leq 1/\lambda$  for any  $\mathbf{W}_2$ .

Again, using the main results of El Karoui and Kösters (2011),

$$\frac{1}{p} \text{tr}\left[(\mathbf{W}_2 + \lambda I_p)^{-1} D\right] = \frac{1}{p} \text{tr}\left[(\lambda \varphi(-\lambda) \Sigma_p + \lambda I_p)^{-1} D\right] + o_P(1).$$

The results of Lemma 4.2 follow.

As for Corollary 4.2, under the assumed conditions,  $\tilde{\ell}(\lambda) \rightarrow \infty$ . Therefore,

$$\mathbb{P}\left(\tilde{\ell}(\lambda) > \mathbb{T}\mathbb{W}_1(1 - \alpha) \mid BC\right) \xrightarrow{\mathbb{P}_{BC}} 1.$$

## S.9 Proof of other technical results

Lemma 2.5, Lemma 3.1 and Corollary 3.1 can be proved using Theorem 3.2, Theorem 4.1, and Theorem 5.1 of Li (2024). Specifically, consider first the case when  $F^{\Sigma_\infty}$  is discrete at  $\sigma_{\max}$  and  $\omega_{\max} \gamma_2 > 1$ . Using Theorem 3.2 of Li (2024),  $\mathcal{G}_\lambda$  is discrete at  $\rho$ . Therefore,

$$s'(x) = \frac{C}{(\rho - x)^2} + C \int_{\tau > \rho} \frac{d\mathcal{G}_\lambda(\tau)}{\tau - x} \rightarrow \infty, \quad \text{as } x \uparrow \rho.$$

When  $\omega_{\max}\gamma_2 < 1$ , it is straightforward to verify that there exists a  $c > 0$  such that  $x'(h) < 0$  when  $h \in [\lambda/\sigma_{\max} - c, \lambda/\sigma_{\max})$ . On the other, as  $h \rightarrow -\infty$ ,  $x'(h) \rightarrow 1$ . Therefore, there exists  $h_0 < \lambda/\sigma_{\max}$  such that  $x'(h_0) = 0$ . Using Theorem 4.1 of Li (2024),  $\rho = x(h_0)$ . Using Theorem 5.1 of Li (2024), there exists constants  $C_1, C_2$  and  $\epsilon$  such that

$$C_1\sqrt{x-\rho} \leq f_{\mathcal{G}_\lambda}(x) \leq C_2\sqrt{x-\rho}, \quad x \in (\rho, \rho + \epsilon)$$

where  $f_{\mathcal{G}_\lambda}$  is the density function of  $\mathcal{G}_\lambda$ . It follows that

$$s'(x) \geq \int_{\rho}^{\rho+\epsilon} \frac{f_{\mathcal{G}_\lambda}(\tau)d\tau}{(\tau-x)^2} \rightarrow \infty, \quad \text{as } x \uparrow \rho.$$

When  $F^{\Sigma_\infty}$  is continuous at  $\sigma_{\max}$  and (ii) of Definition 2.2 holds, Theorem 5.1 of Li (2024) indicates that the square-root behavior of  $f_{\mathcal{G}_\lambda}(x)$  still holds. Therefore,  $s'(x) \rightarrow \infty$  as  $x \uparrow \rho$  due to the same arguments.

Lemma 3.2 follows from the fact that  $x''(h) < 0$  on  $(-\infty, \lambda/\sigma_{\max})$ , which can be verified by direct differentiation.

For the proof of Theorem 3.1, Eq. (3.1) follows directly from an application of Theorem 4.1 of Li (2024). Eq. (3.2) is obtained by differentiating both sides of Eq. (3.1) with respect to  $x_0$ .